U.S. Department
of Transportation
**Federal Railroad
Administration**

Puncture Resistance of Scale Model Aluminum Tank Car Heads

Office of Research and
Development
Washington, D.C. 20590

M. A. Lishaa
C. C. Dai
M. Giltrud
J. C. S. Yang

Advanced Technology and Research, Inc.
3933 Sandy Spring Road
Burtonsville, Maryland 20866

DOT/FRA/ORD-87/06

June, 1987
Final Report

NOTICE

This document is disseminated under the sponsorship of the Department of Transportation in the interest of information exchange. The United States Government assumes no liability for its contents or use thereof.

NOTICE

The United States Government does not endorse products or manufacturers. Trade or manufacturers' names appear herein solely because they are considered essential to the object of this report.

Technical Report Documentation Page

1. Report No.	2. Government Accession No.	3. Recipient's Catalog No.
FRA/ORD-87/06		

4. Title and Subtitle	5. Report Date
Puncture Resistance of Scale Model Aluminum Tank Car Heads	June 1987
	6. Performing Organization Code
	8. Performing Organization Report No.
7. Author(s) M. A. Lishaa, C. C. Dia, M. Gultrud, J. C. S. Yang	
9. Performing Organization Name and Address ... Research, Incorporated	10. Work Unit No. (TRAIS)
	11. Contract or Grant No. DTFR53-84-C-00029
	Type of Report and Period Covered FINAL September 1984 - June 1986
	Sponsoring Agency Code

Report FRA/ORD-87/06 PB87 200069/AS

6/15/87 2 cys - Dave Dancer
1 cy - Mike Coltman
1 cy - Mark White
6/16 1 cy - Doug Dabble, TC
6/25 1 cy - Ed P.
7/24 1 cy - Peter Conlon AAR
10/9 1 cy - TSC library
10/26 - 2 cys - Dave (DTSB, ESPA)

y experience impacts that eliable small scale testing impact situations. In this ied: (1) to assess the ium tank car heads puncture e on the threshold puncture the validity of the scaling on the vulnerability of the situation. A small scale nerability of model tank car 1/10- and 1/5 scale model d. Head protection devices n of steel face plates with ences were found in terms of . The test results indicate elocities of the two scaled on-dimensional analysis of the ulnerability of model tank car re effective than the center inite element model with some the model and full-scale tank

atement
available to the public
National Technical Information
ringfield, Virginia 22161

	21. No. of Pages	22. Price
	97	

rized

METRIC CONVERSION FACTORS

Approximate Conversions to Metric Measures

Symbol	When You Know	Multiply by	To Find	Symbol
		LENGTH		
in	inches	*2.5	centimeters	cm
ft	feet	30	centimeters	cm
yd	yards	0.9	meters	m
mi	miles	1.6	kilometers	km
		AREA		
in^2	square inches	6.5	square centimeters	cm^2
ft^2	square feet	0.09	square meters	m^2
yd^2	square yards	0.8	square meters	m^2
mi^2	square miles	2.6	square kilometers	km^2
	acres	0.4	hectares	ha
		MASS (weight)		
oz	ounces	28	grams	g
lb	pounds	0.45	kilograms	kg
	short tons (2000 lb)	0.9	tonnes	t
		VOLUME		
tsp	teaspoons	5	milliliters	ml
Tbsp	tablespoons	15	milliliters	ml
fl oz	fluid ounces	30	milliliters	ml
c	cups	0.24	liters	l
pt	pints	0.47	liters	l
qt	quarts	0.95	liters	l
gal	gallons	3.8	liters	l
ft^3	cubic feet	0.03	cubic meters	m^3
yd^3	cubic yards	0.76	cubic meters	m^3
		TEMPERATURE (exact)		
°F	Fahrenheit temperature	5/9 (after subtracting 32)	Celsius temperature	°C

*1 in. = 2.54 cm (exactly). For other exact conversions and more detail tables see NBS Misc. Publ. 286, Units of Weight and Measures. Price $2.25 SD Catalog No. C13 10 286.

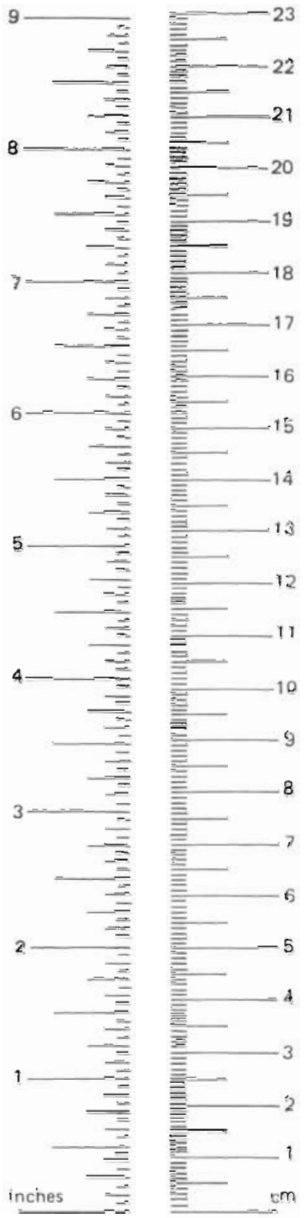

Approximate Conversions from Metric Measures

Symbol	When You Know	Multiply by	To Find	Symbol
		LENGTH		
mm	millimeters	0.04	inches	in
cm	centimeters	0.4	inches	in
m	meters	3.3	feet	ft
m	meters	1.1	yards	yd
km	kilometers	0.6	miles	mi
		AREA		
cm^2	square centimeters	0.16	square inches	in^2
m^2	square meters	1.2	square yards	yd^2
km^2	square kilometers	0.4	square miles	mi^2
ha	hectares (10,000 m^2)	2.5	acres	
		MASS (weight)		
g	grams	0.035	ounces	oz
kg	kilograms	2.2	pounds	lb
t	tonnes (1000 kg)	1.1	short tons	
		VOLUME		
ml	milliliters	0.03	fluid ounces	fl oz
l	liters	2.1	pints	pt
l	liters	1.06	quarts	qt
l	liters	0.26	gallons	gal
m^3	cubic meters	36	cubic feet	ft^3
m^3	cubic meters	1.3	cubic yards	yd^3
		TEMPERATURE (exact)		
°C	Celsius temperature	9/5 (then add 32)	Fahrenheit temperature	°F

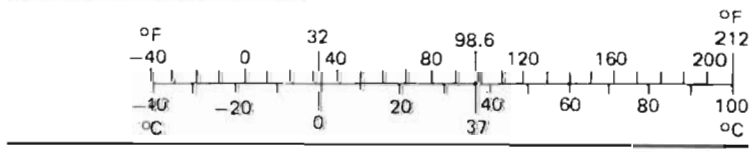

TABLE OF CONTENTS

Table of Contents
(Con't)

LIST OF ILLUSTRATIONS

List of Illustrations (Con't)

List of Illustrations (Con't)

LIST OF TABLES

SUMMARY

In the study of the coupler-tank car head impact phenomena in derailment and switchyard operations, different test conditions have to be considered. In order to correlate the threshold puncture velocity with these conditions, many impact tests need to be performed to obtain the required information. For these studies, a small-scale model testing program is certainly more desirable over the full-scale testing as far as the cost is concerned. It is imperative, however, that the small-scale model impact tests will provide reliable information as to the real full-scale impact phenomena. Therefore, several attempts were made in this study with small-scale impact testing to investigate different tank car head protection devices with different impact conditions. An attempt was made with center impact testing on model aluminum tank car heads: (1) to assess the effectiveness of mitigating materials on increasing the puncture resistance of model aluminum tank car heads; (2) to evaluate the effect of low temperature on the threshold puncture energy of model aluminum tank car heads; (3) to test the validity of the scaling laws adopted on model aluminum tank car heads; and (4) to study the influence of lading on the threshold puncture velocity of model aluminum tank car heads in horizontal impact situations. Two additional attempts were made with off-center impact testing on model aluminum and high-alloy steel tank car heads to assess the vulnerability of model tank car heads under off-center impacts. A number of 1/10- and 1/5-scale model aluminum and high-alloy steel tank car heads were used in this study. Also a Finite Element Model was developed for the prediction of the puncture resistance of scale-model aluminum and high-alloy steel tank car heads.

The small-scale impact testing program includes vertical impact tests (drop-weight) and horizontal impact tests (pendulum). These tests were performed on the scale-model tank car bareheads and heads that were covered by high-alloy steel head shields or steel face plates combined with different kinds of mitigating materials. These materials were used as protective devices to increase the puncture resistance of the scale-model aluminum and high-alloy steel tank car heads in the center and off-center impact tests. Several kinds of mitigating materials were selected and examined in preliminary dynamic impact tests to determine the most suitable material-combination with the most energy absorbing capacity which can be used in impact situations. Beside the high-alloy steel head shield (thick steel plate), two different kinds of mitigating materials combined with steel face plates (thin steel plates) were chosen and used in the center impact tests, while only one of the two mitigating materials combined with steel face-plates was used in the off-center impact tests. This mitigating material was formed from several layers of aluminum honeycomb combined with thin sheets of high-alloy steel; the second material was formed from a single plate of Hytrel Polyester Elastomer "Tecspak" combined with a single thin sheet of high-alloy steel.

The test results indicate that all the protective devices provide good protection to the scale model tank car heads against impact puncture as compared with the barehead impact situation. However, some differences in terms of protection capability between these protective devices in each scale were found. The results of the 1/10-scale drop-weight center impact tests

indicate that the high-alloy steel head shields provided the most protection to the test specimens followed by the steel face plate-aluminum honeycomb materials and then the steel face plate-Tecspak materials. This was changed in the 1/5-scale test results where the honeycomb materials provided the most protection to the test specimens followed by the head shields and then the "Tecspak" plates. The test results also indicate no significant effect of low temperature on the vulnerability of the scale-model aluminum tank car heads.

An examination of the scaling laws adopted revealed that the effect of the strain rate on the accuracy of these laws is negligible when applied to the 1/10- and 1/5-scales. Based on this finding, the threshold puncture velocity of the 1/10-scale model is expected to be higher than the velocity of the 1/5-scale model by 1.0 percent. In comparing the impact test results of the model aluminum tank car heads between these two scales, it shows a good agreement of the effect of the strain rate on the threshold puncture velocity with 3.0 percent in the barehead impact tests. However, it shows 16.0 percent and 21.0 percent differences in the threshold puncture velocities in the other cases where high-alloy steel head shields and steel face plate combined with Tecspak material were used as protective devices, respectively. Also it shows no difference in the case where steel face plates combined with several layers of aluminum honeycomb material was used in the impact tests.

The horizontal impact test results show the effect of lading on increasing the vulnerability of the model aluminum tank car heads to impact puncture. Also it shows that the model aluminum and high-alloy steel tank car bareheads are more vulnerable to impact puncture with off-center horizontal impacts as well as vertical impacts. However, these results indicate the contrary in the case where high-alloy steel head shields or steel face plates combined with aluminum honeycomb material were used as protective devices in the off-center impact.

1. INTRODUCTION

In derailment and switchyard operations, railroad tank cars carrying hazardous materials frequently experience coupler-tank head impacts that result in impairment of the structural integrity of the tank cars. Because of the catastrophic consequences involved in such accidents, which may cause the evacuation of cities, personal deaths and injuries, and property losses totalling millions of dollars, tank car head puncture phenomena have been widely studied (References 1-6) and different protective means have been devised.

In order to increase the resistance of the tank car heads against impact puncture when a coupler or an adjacent car rams into it, steel head shields have been required on all DOT specifications 112A/114A hazardous material railroad tank cars since 1977 and certain newly built DOT specification 105 tank cars. Previous studies (References 2-3) showed that the steel head shield is an effective protective device; it is not a particularly good energy absorber, but it blunts the striking edge of the impacting object and spreads the impact load to a larger area of the impacted surface. However, it appears possible to significantly increase the energy absorption capability by adding a highly deformable shock mitigating material between a thinner head shield (face plate) and the tank car head. Most railroad tank cars cover long distances over their operational life span. The additional dead weight of the thick steel head shields currently used would substantially increase the travelling cost. Therefore, it is of interest to find protective devices which are lighter than the steel head shields without sacrificing head protection and puncture resistance. The same basic concept of using a mitigator could be used in future railroad tank car designs, which could yield equivalent protection with lighter protective devices.

The mitigating materials would also solve a potential problem in current tank cars carrying steel head shields. This problem is the effect of low temperature on the impact resistance of steel plates. This is based on the fact that carbon steel in fracture tests exhibits a transition from ductile failure that requires high-impact fracture energy, to brittle failure that requires much lower energy. The effect of low temperature on the tank car head-impact performance is addressed and the degree of protection against head puncture rendered by mitigating materials at low temperature is assessed.

It is not practical from a cost-effective viewpoint to conduct full-scale testing to verify that a particular tank car design will perform satisfactorily in all possible impact situations because there are large combinations of tank car configurations and impact scenarios. Therefore, there is a need for reliable small-scale testing procedures to simulate the response of the tank car heads in impact situations.

Reliability of relating the small-scale model and prototype test results depends on the validity of scaling laws employed. In order to examine these laws, impact tests with models of two different scale factors under similar conditions are conducted. Analysis of the tests results of the two different scale models should help in establishing the scaling laws, which are used for

the prediction of the prototype performance.

The major catastrophy involved in the railroad tank car head puncture following a derailment or switchyard collision is the spillage of lading contained in the tank car. The ensuing spillage can lead to wide dispersion of highly toxic fumes for non-flammable cargo, or to quick ignition and conflagration for flammable cargo. Therefore, in this study the influence of lading on the threshold puncture velocity and energy is included.

The Federal Railroad Administration (FRA) scale-model puncture resistance program has considered only centerline impact tests. However, full-scale tank car head puncture resistance tests included two series of off-center impact tests, one test series conducted at 21 inches above the sill and the other test series conducted at 31 inches above the sill. This study also included an investigation of the vulnerability of the scale-model tank car heads under off-center impacts.

2. BACKGROUND AND PROCEDURES

2.1 OBJECTIVES

The objectives of this project are:

a. To assess the effectiveness of mitigating materials on increasing the puncture resistance of small-scale model aluminum tank car heads.

b. To evaluate the effect of low temperature on the threshold puncture energy of small-scale model aluminum tank car heads.

c. To test the validity of the scaling laws adopted on small-scale model aluminum tank car heads.

d. To study the influence of lading on the threshold puncture velocity of small-scale model aluminum tank car heads in horizontal impact situations.

e. To assess the vulnerability of small-scale model aluminum and high-alloy steel tank car heads under off-center impacts.

f. To develop a Finite Element Model for the prediction of the puncture resistance of small-scale model aluminum and high-alloy steel tank car heads.

2.2 DESCRIPTION OF SMALL-SCALE TEST PROGRAM

In order to achieve the objectives of this test program, a total of five series of impact tests were conducted with an ultimate goal of obtaining more insight into the tank car head impact phenomena. Thus, more efficient schemes can be developed to reduce the probability of tank car head puncture caused by impact during collision in derailment, switchyard operations, and accidents. Four series of center-impact tests were run on small-scale model aluminum tank

car heads and one series of off-center impact tests was run on model aluminum and high-alloy steel tank car heads. These impact tests involved two major testing schemes: vertical impact tests (drop weight) and horizontal impact tests (pendulum).

The first two series of center-impact tests were performed on 1/10-scale model aluminum tank car heads to evaluate and compare the effectiveness of different protective devices such as high-alloy steel head shields and steel face plates combined with different kinds of mitigating materials on increasing the puncture resistance of the model aluminum tank car heads. These tests were performed at ambient temperatures and also at low temperature of - 60 degree fahrenheit (^{o}F) with the intent of investigating the effect of low temperatures on the model behavior under varying impact conditions.

For the purpose of developing, establishing, and testing the scaling laws, the third series of center-impact tests was performed on 1/5-scale model aluminum tank car heads. Drop weights, head shields, and mitigating materials combined with steel face plates were scaled as close as possible to meet the ratio of the 1/5-scale. The results of this test series and those obtained from the first series of tests were then compared.

The fourth series of tests was conducted to evaluate the effect of lading on the threshold puncture velocity of model aluminum tank car heads in horizontal center-impact tests. A 1/5-scale model railroad tank car with removable head holder was used in this series of tests. These horizontal impact tests were performed on 1/5-scale model aluminum tank car bareheads in two impact conditions: (1) when the model tank car was filled with water to 90 percent of its volume, and (2) when the model tank car was loaded with weights to provide the same total weight of the tank car as in the first condition.

All previous drop-weight and pendulum impact tests were performed at the centerline of model aluminum tank car heads. The fifth test series in this study was conducted to investigate the vulnerability of the scale model aluminum and high-alloy steel tank car heads under off-center impacts. Drop-weight and pendulum impact tests were performed at two impact positions which were scaled to the full-scale test locations at 21 inches and 31 inches above the sill. These off-center impact tests were performed on bareheads, and heads that were covered by high-alloy steel head shields or combination of steel face plate and aluminum honeycomb material.

2.3 TEST FACILITY

The test facility employed includes a drop/pendulum tower made of wide-flanged steel I-beams, a railroad track, a small model railroad tank car, and an instrumentation room.

The tower is a four-legged free-standing structure, 46 feet high and has a large base area. The drop and pendulum impact tests can be performed at the tower base with a maximum drop height of 40 feet (34 miles per hour (mph) impact velocity), a 120 degree pendulum swing angle (30 mph impact velocity), and a lift of a 3,000 pound (lb) impact weight. Figure 1 shows photographs of the drop/pendulum tower from different angles. These photos also show the

Figure 1. Drop-pendulum tower photographs from different angles.

small model tank car and a railroad track. At the top of the tower there are safety rails surrounding a specially built steel platform which can be used to service the hoist periodically or in emergency situations and also to adjust the drop-weight guide cables. Steel rungs are attached to the towerside for safe access to the platform.

A 60 foot (ft) long portable railroad track laid on a gravel bed extends from the tower base at the pendulum side to guide the model tank car or any other object being impacted by the pendulum. The pendulum arm length can be adjusted by 1.5 inch (in) increments between 17.5 and 19.0 ft limits. Also, the pendulum impact weight is variable, and can be adjusted up to a 3,000 lb limit. The pendulum arm pivot rotates in two special duty flange bearings. These bearings together with their brackets are fixed at a height of 20 ft on the pendulum tower. A two-ton capacity hoist hanging at the top of the tower is used to lift either the pendulum or the drop impact weight. A remote controlled release hook is used to release the impact weight in either case. Figure 2 shows a photograph of the fast release hook.

An instrumentation trailer is situated near the tower to house the transient data acquisition equipment such as tape recorder, computer, oscilloscope and other instruments. An electrical power source (115 volts) is available in this trailer for operating the hoist and all electrical equipment. All the tests performed at the tower base area can be controlled from inside this trailer. A wide window faces the tower for the observation of the on-going experiments.

2.4 GENERAL PROCEDURES

The threshold puncture velocity will be determined approximately by progressively narrowing the gap of the velocities that cause puncture and non-puncture. The impact velocity in each test will be determined based on the previous test results. In general, puncture failure can be determined by visual inspection.

2.5 DROP WEIGHTS

Two drop weights were used for the drop-weight impact tests. The 1/10-scale test series used an impact weight of 263 lb. The 1/5-scale test uses 2,102 lb. These weights have been selected to represent the scale weight of the full-scale of the ram car.

2.6 DROP HEIGHT

An approximated initial drop height of 6.0 in of the 1/10-scale drop-weight was determined by equating the kinetic energy available at impact to the total energy which can be dissipated by plastic work of a 1/10-scale model aluminum tank car barehead up to the point of a material's shearing failure in a static test.

2.7 PENDULUM IMPACT WEIGHT

A pendulum impact weight of approximately 2,060 lb was used in the horizontal impact tests. The kinetic energies generated by this weight in the

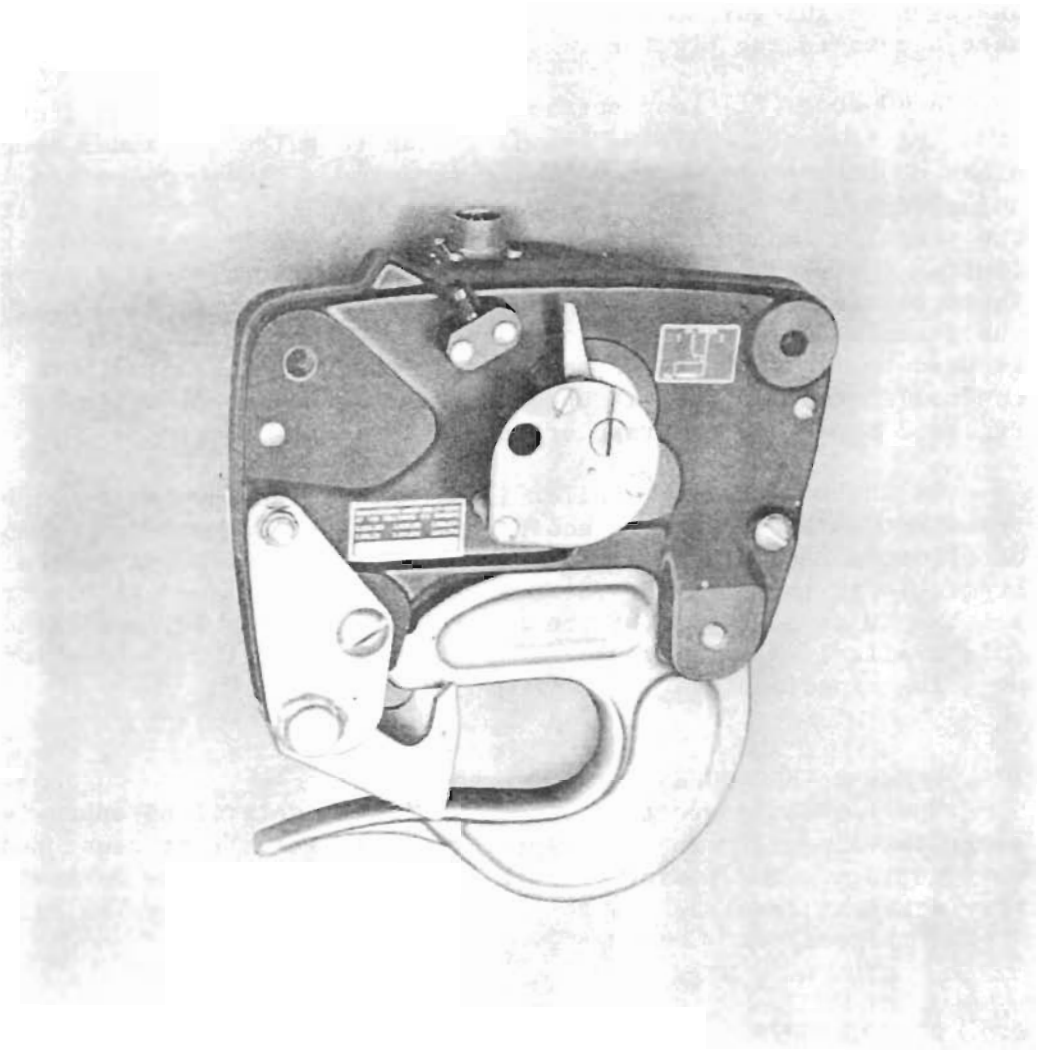

FIGURE 2. Mechanical Electrical Release Hook

pendulum test and by the drop weight in the 1/5-scale drop test are equivalent at impact when the swing-and drop-heights are the same.

2.8 TEST SERIES

Five series of impact tests were conducted in this test program and can be described as follows:

o Test Series No. 1 - Effect of mitigators (drop-weight impact tests)

The 1/10-scale model aluminum tank car heads were used in this series with the drop tower facility at temperatures above the transition temperature of the model material. Cases chosen include drop-weight impact tests on bareheads and heads that were covered by: (a) high-alloy steel head shields, (b) high-alloy steel face-plate and aluminum honeycomb materials, and (c) high-alloy steel face-plate and Tecspak materials. An average of six specimens were used in each case to determine the corresponding threshold puncture velocity. Figure 3 shows a photograph of a 1/10-scale model aluminum tank car barehead in a drop-weight impact test setup.

o Test Series No. 2 - Effect of low temperature (drop-weight impact tests)

The 1/10-scale model aluminum tank car heads were used in this test series with the drop tower facility at temperatures below the transition temperature of the model material. Similar drop-weight impact tests to that in the first test series were performed at low temperature. Liquid nitrogen was used as a coolant while a thermocouple and electronic thermometer were used to record the temperature.

o Test Series No. 3 - Validation of the scaling laws (drop-weight impact tests)

The 1/5-scale model aluminum tank car heads were used in this test series with the drop tower facility at temperatures above the transition temperature of the model material. Similar drop-weight impact tests to those in the first test series were performed including test conditions, materials, and procedures. Figure 4 shows a photograph of the 1/5-scale model aluminum tank car barehead in a drop-weight impact test setup.

o Test Series No. 4 - Effect of lading (pendulum impact tests)

The 1/5-scale model aluminum tank car heads were used in this test series with the pendulum facility at temperatures above the transition temperatures of the model material. The horizontal impact tests in this series were performed only on 1/5-scale model aluminum tank car bareheads under two conditions: (A) the model target car was filled with water to 90 percent of its total volume, and (B) the model target car was loaded with weights to provide the same total weight as in condition A.

o Test Series No. 5 - Effect of off-center impact (drop-weight and pendulum impact tests)

The 1/10- and 1/5-scale model aluminum and high-alloy steel tank car heads were used in this test series with the drop/pendulum tower facility at

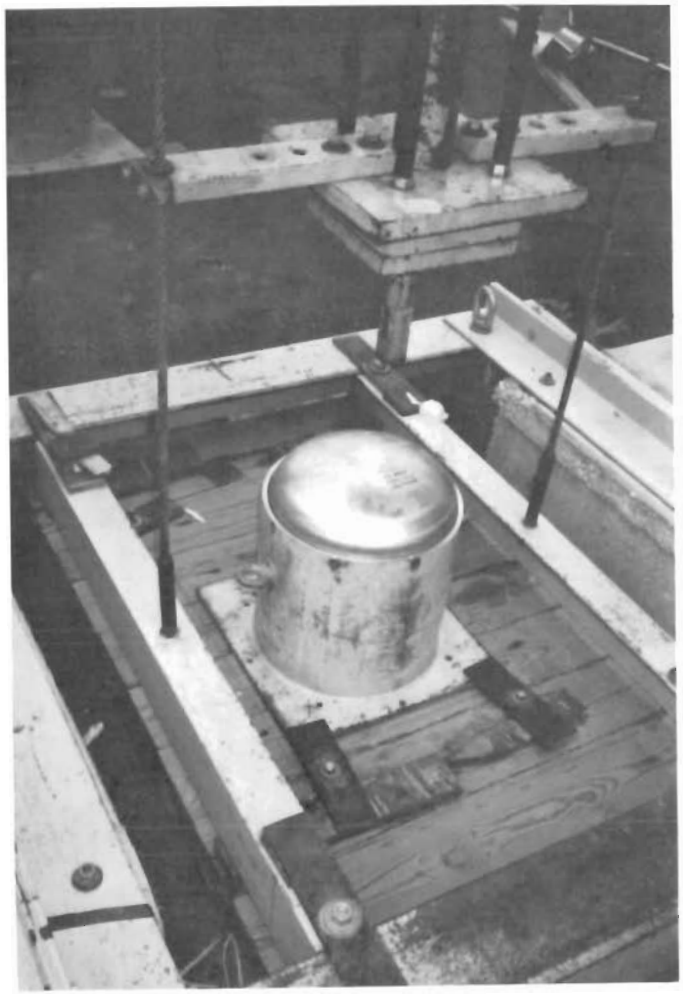

Figure 3. 1/10 scale model tank car barehead in drop-weight impact test setup.

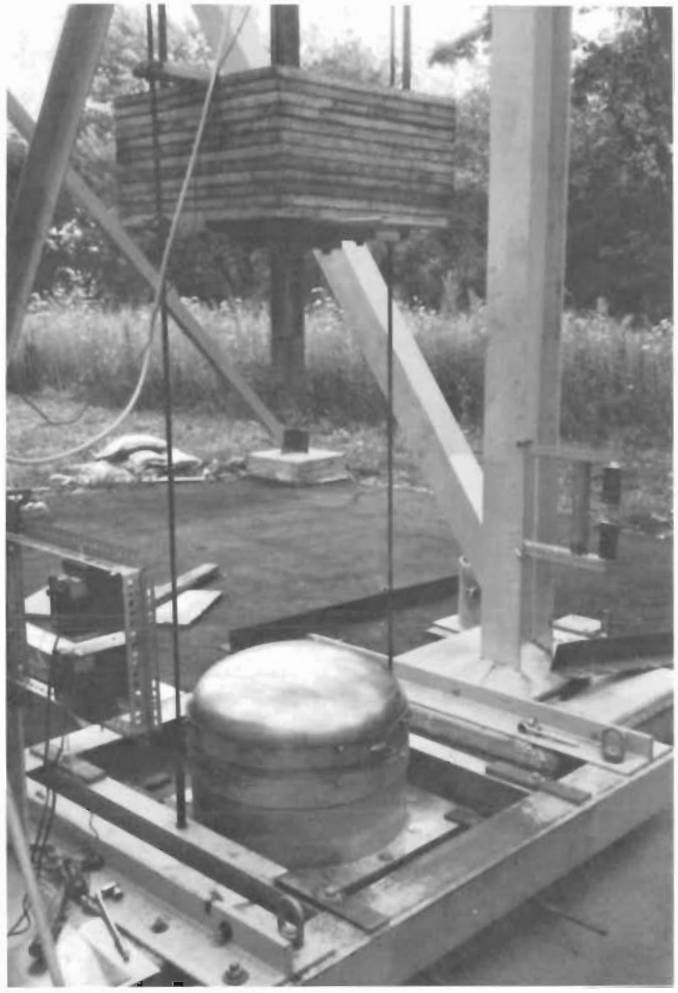

Figure 4. 1/5 scale model tank car barehead in drop-weight impact test setup.

temperatures above the transition temperature of model materials. These tests were performed at two different off-center impact positions which were scaled to the full-scale test locations at 21 and 31 inches above the sill. Similar drop-weight impact tests to those in the first and third test series, were performed with off-center impacts. The choice of one mitigating material (aluminum honeycomb) was allowed in these tests. To investigate the effect of horizontal off-center impacts, pendulum impact tests were performed on 1/5-scale model high-alloy steel tank car bareheads at the two off-center positions. The model target car was filled with water to 90 percent of its total volume.

2.9 MATERIALS AND GEOMETRY

2.9.1 Model Tank Car Heads

Based on the specifications in the A.A.R. Manual of Standards and Recommended Practices, Section C, Part III, several materials can be used to manufacture the tank car heads. Two of these materials were recommended and used in manufacturing the scale model tank car heads in this test program. Both materials are listed in the A.A.R. manual under "Approved Materials For Tanks Fabricated by Welding". The first material is listed in Table M1-B and identified as "Aluminum Alloy Plate - ASTM B209, Type 5052"; the second material is listed in Table M1-C and identified as "High-Alloy Steel Plate - ASTM A240, Type 304". The physical properties of these materials are within the A.A.R. manual recommendation and are listed in Table I.

The geometric specifications of the tank car heads are given in (ACF) Shipping Car Line Division, under "Tank Car Anatomy 15e Rev., Services Bulletin/May, 1972". These specifications were scaled to the 1/10- and 1/5-scale models and listed in Table I. Figure 5 shows a detailed drawing of the 1/10- and 1/5-scale model tank car heads.

2.9.2 Head Shield

In order to reduce the probability of DOT Class 112A and 114A railroad tank car head punctures, the Department of Transportation has required that one-half inch thick steel head shields be applied to these cars. They are to be spaced in front of the tank car heads and are to cover approximately the lower half of the head. Therefore, in this test program a single or double high-alloy steel thick plates (ASME A240, type 304), with scaled thicknesses were used to cover the model tank car heads in the 1/10- and 1/5-scale drop-weight impact tests.

2.9.3 Face Plate

The face plate is a relatively thin sheet of high-alloy steel metal, usually combined with mitigating materials and used as a protective device for the model tank car heads. The face plate can be used as: (1) a single sheet to cover the top of the mitigating material as in the case where Tecspak material was used as a mitigator; or (2) several sheets to separate several layers of the mitigating materials as in the case where the aluminum honeycomb material

TABLE I. SPECIFICATIONS AND PHYSICAL PROPERTIES OF THE 1/10- AND 1/5-SCALE MODEL TANK CAR HEADS

MATERIAL / SPECIFICATIONS AND PROPERTIES	ALUMINUM ALLOY 5052-0		HIGH-ALLOY STEEL A240 - TYPE 304	
SCALE	1/10	1/5	1/10	1/5
ELLIPTICAL	2:1	2:1	2:1	2:1
MAJOR DIAMETER (INCHES)	12	24	12	24
MINOR DIAMETER (INCHES)	6	12	6	12
PLATE THICKNESS (INCHES)	.068 - .070	.133 - .137	.052 - .058	.117 - .124
IMPACT AREA THICKNESS (INCHES)	.060 - .063	.110 - .117	.047 - .052	.097 - .109
TENSILE STRENGTH (PSI)	25,000	25,000	94,400	94,000
YIELD STRENGTH (PSI)	9,500	9,500	37,000	37,600
ELONGATION IN 2 INCHES (%)	19	20	62	59

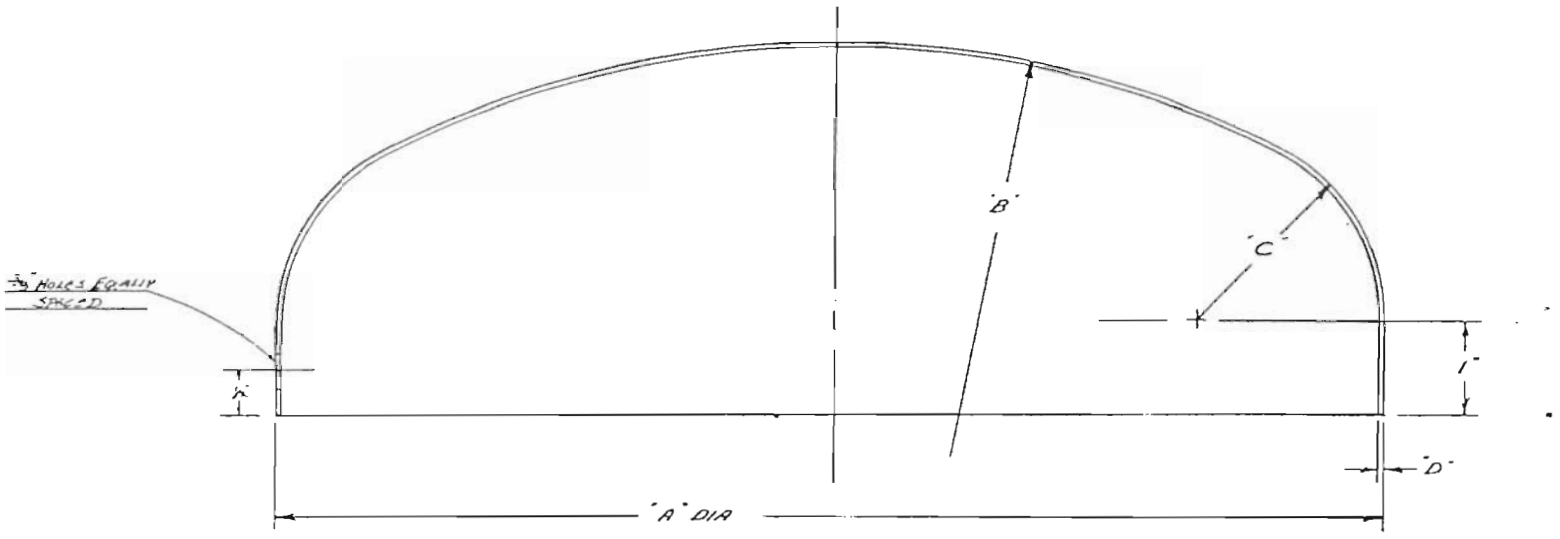

Dimension	A	B	C	D
1/10-Scale	12"	10.8"	2.06"	*
1/5-Scale	24"	21.6"	4.15"	*

*See plate thickness in Table 1.

Figure 5. The detail drawings of the 1/10- and 1/5-Scale Model Tank Car Heads.

was used as a mitigator.

2.9.4 Mitigating Materials

Several kinds of mitigating materials, such as aluminum honeycomb, aluminum foam, Kevlar material, Tecspak material, etc., were selected and examined in preliminary dynamic impact tests. Two of these materials were considered to be used as mitigators in the drop-weight impact tests. The first material was formed from several layers of TRUSSGRID aluminum honeycomb material combined with thin sheets of high-alloy steel face-plate. Figure 6 shows a photograph of a TRUSSGRID sample. The second material was formed from a single plate of Tecspak material covered by a thin sheet of high-alloy steel face-plate.

2.9.5 Couplers

The 1/10- and 1/5-scale model couplers were cut and machined from 2.5 inch and 4.5 inch 1045-CD carbon steel bars respectively. The ultimate and yield strengths of this carbon steel are 103,000 pounds per square inch (103K psi) and 90K psi respectively. Figure 7 shows a photograph of both scaled model couplers.

2.10 Test Procedure

2.10.1 Drop Weight Test

The 1/10- and 1/5-scale drop-weight impact tests were performed at the base area of the drop tower. The test procedure in both cases was similar and can be described by the following steps:

1. Use the hoist and a special weight stand to assemble the drop weight including the weight shaft, the weight plates, the guide arms, and the coupler. Figure 8 (a and b) shows the assembly drawing of the 1/10- and 1/5-scale drop weights respectively.

2. Align the guide cables with the guide arms so that the coupler and the drop weight can be guided to impact the specimen at a certain position.

3. Attach a release hook to the hoist, and hook the drop weight from its shaft. Secure the release hook, lift the drop weight to a certain height so that the test specimen preparation can be performed safely, and then remove the drop weight stand.

4. Place and fix a tank car head specimen on the specimen holder. Place the head-holder assembly on the drop tower base, and adjust its position so that the coupler will impact the specimen at the desired impact point. Tighten the head-holder assembly to the wooden base by the available clamps.

5. Prepare the tank car head specimen according to the test schedule with head shield, mitigating material, etc.

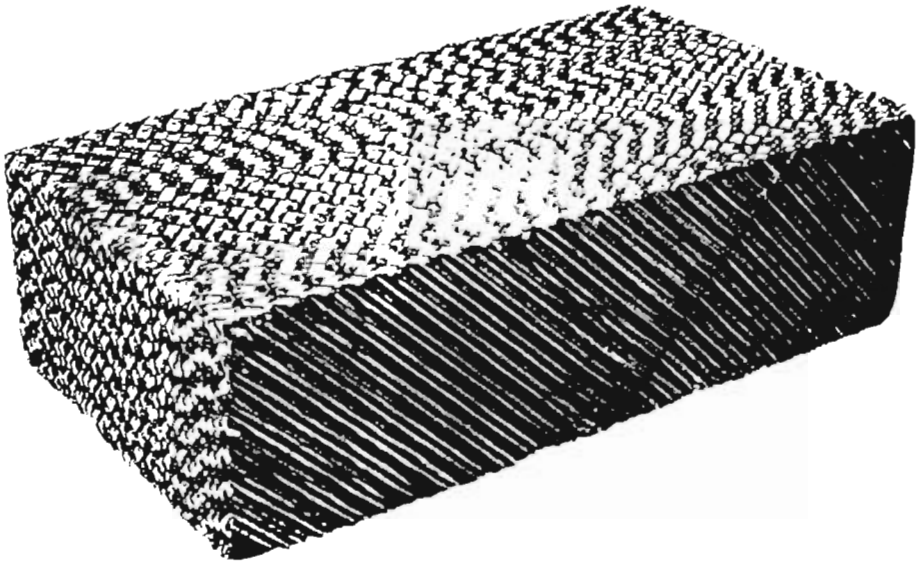

FIGURE 6. TRUSSGRID Aluminum Honeycomb Sample

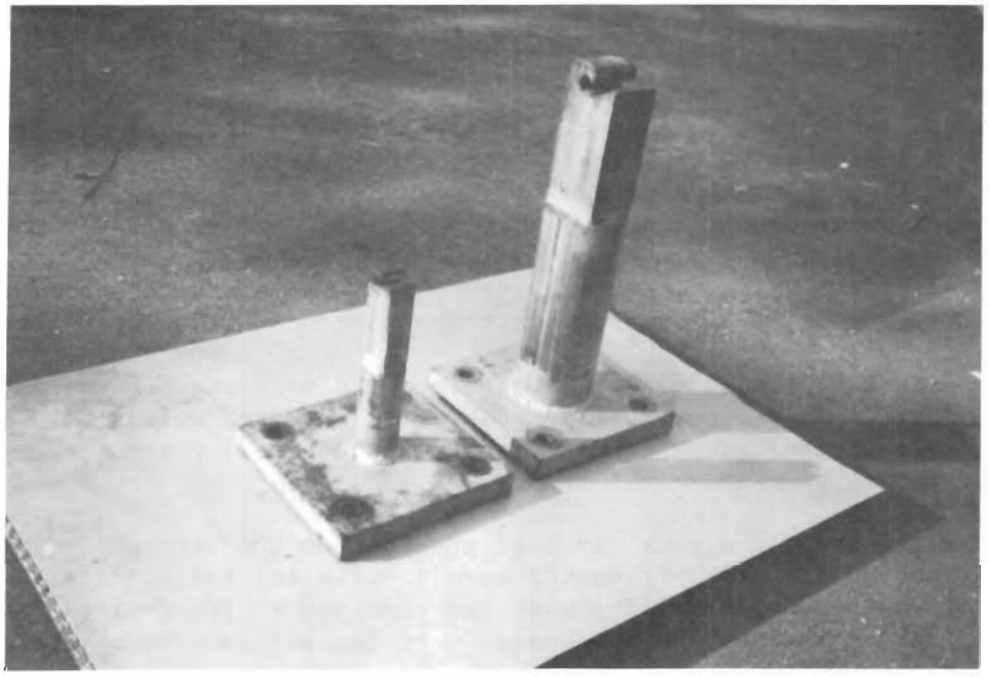

FIGURE 7. 1/10 - and 1/5 - Scale Model Couplers

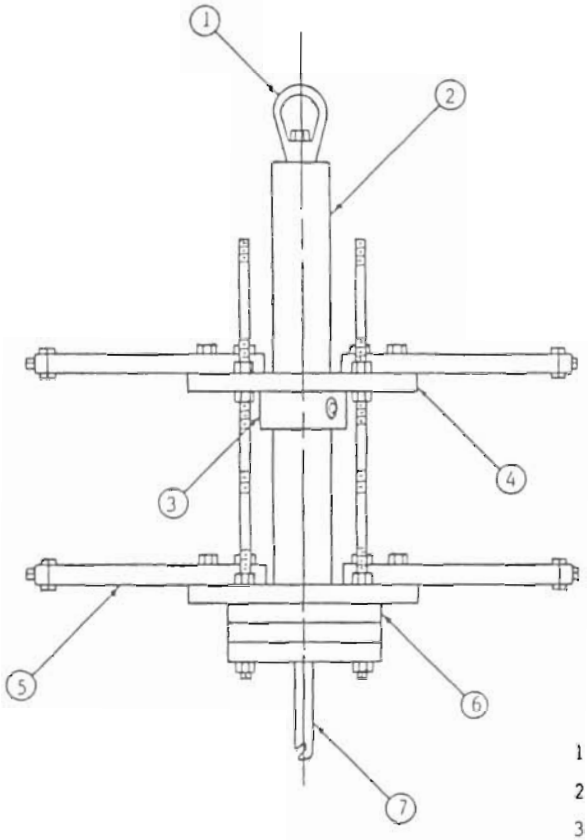

FIGURE 8a. 1/10-SCALE DROP WEIGHT ASSEMBLY

1 - Eye Nut
2 - Drop Weight Shaft
3 - Clamp
4 - Guide Plate
5 - Guide Arm
6 - Weight Plates
7 - Coupler

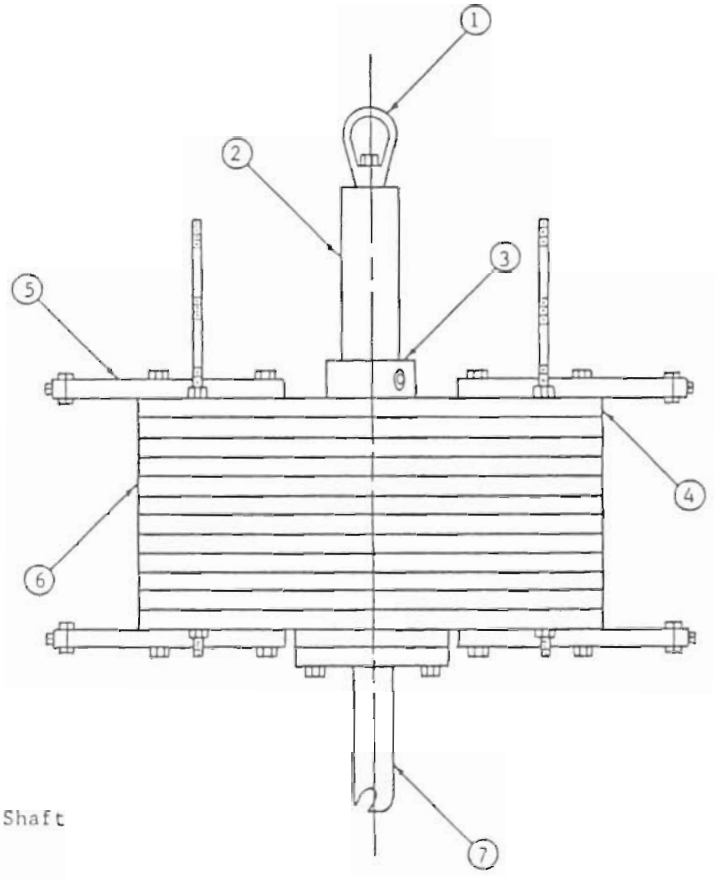

FIGURE 8b. 1/5-SCALE DROP WEIGHT ASSEMBLY

6. Use the hoist remote control to adjust the drop-weight height above the tank car head specimen. To check the desired impact height, measure the vertical distance between the coupler tip and the specimen surface at the impact point.

7. Activate the test instruments, computer, and tape recorder. Control and release the drop weight from inside the instrumentation room by using the release hook remote control.

8. Record the required measurements and readings, then deactivate all test instruments.

9. Lift the drop weight and secure it so that the tank car head specimen can be removed and inspected.

10. Repeat steps 4 to 9 for more drop impact tests. Figure 9 shows schematic drawings of the drop-weight impact test setup including all the instrumentation needed for the impact test.

2.10.2 Pendulum Test

The pendulum tests were performed only on the 1/5-scale model tank car heads at the base area of the pendulum tower. The test procedure can be described as follows:

1. Use the hoist and the lifting system available on the tower to assemble the pendulum head for the 1/5-scale horizontal impact tests. Figure 10 shows an assembly drawing of the 1/5-scale pendulum impact head.

2. Use a hydraulic lifter to jack-up the pendulum head to the desired height such that the coupler will impact the specimen at the desired position. Tighten and fix the pendulum head at this horizontal level with the available nuts and special pins.

3. Place and fix a tank car head specimen on the specimen holder. Place the head-holder assembly in position on the model tank car, adjust and fasten it.

4. Load the model tank car with weights or fill it with water according to the test schedule.

5. While the pendulum is in a vertical position, push the model tank car toward the pendulum head until the coupler tip is touching the model tank head surface at the desired position. Apply the brakes to the model tank car wheels.

6. Hook the pendulum head with a special sling and the release hook. Pull-up the pendulum to a desired height by using the hoist.

7. Activate the test instruments, computer, and tape recorder. Control and release the pendulum from inside the instrumentation room by using remote

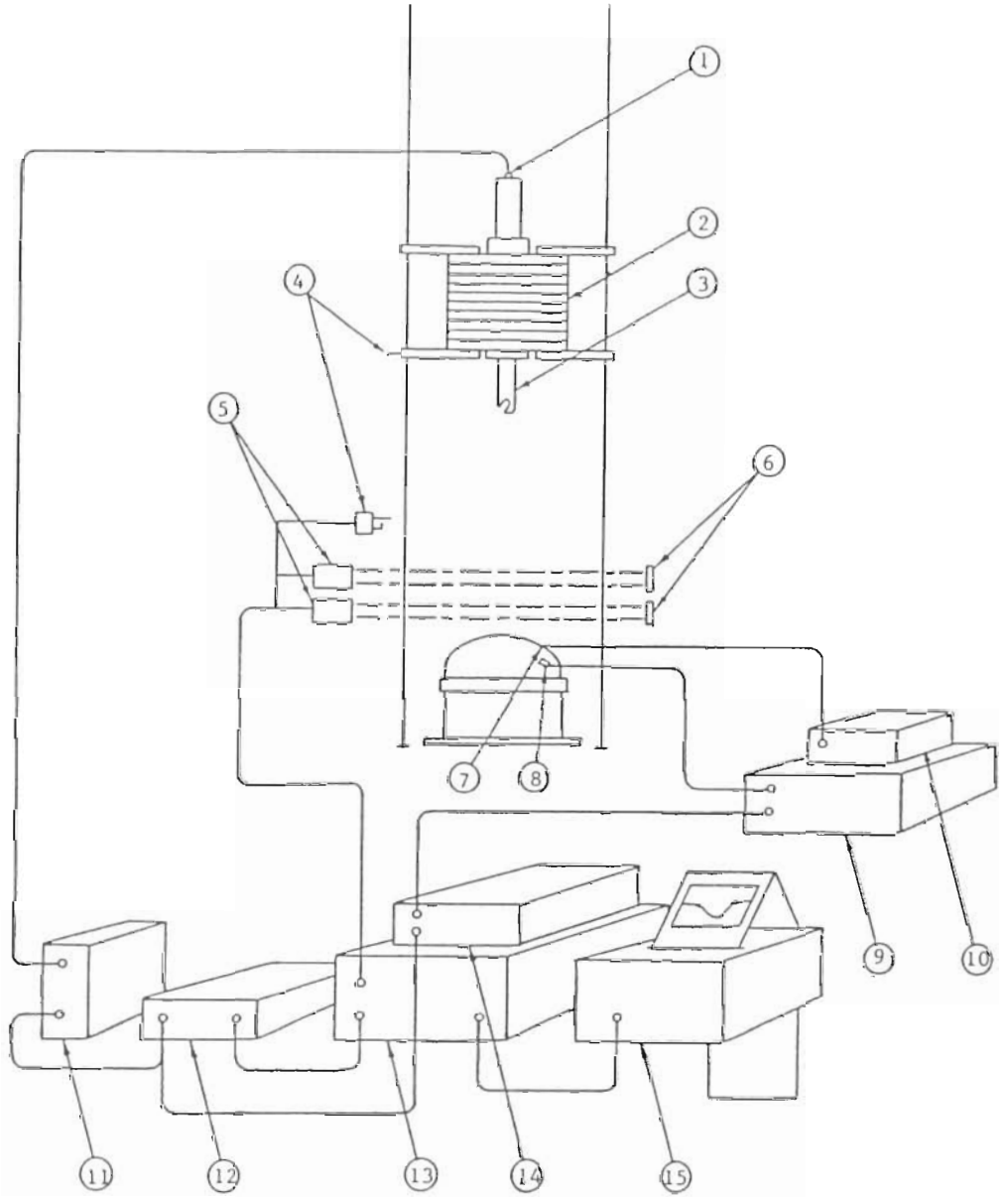

1 - Accelerometer
2 - Impact Weight
3 - Coupler
4 - Triggering System
5 - Infrared Photoelectric Relay
6 - Reflectors
7 - Thermocouple
8 - Strain Gauge
9 - Strain Gauge Indicator
10 - Thermocouple Thermometer
11 - Charge Amplifier
12 - Filter
13 - Mini-Computer
14 - Tape Recorder
15 - Printer

FIGURE 9. DROP-WEIGHT IMPACT TEST SETUP

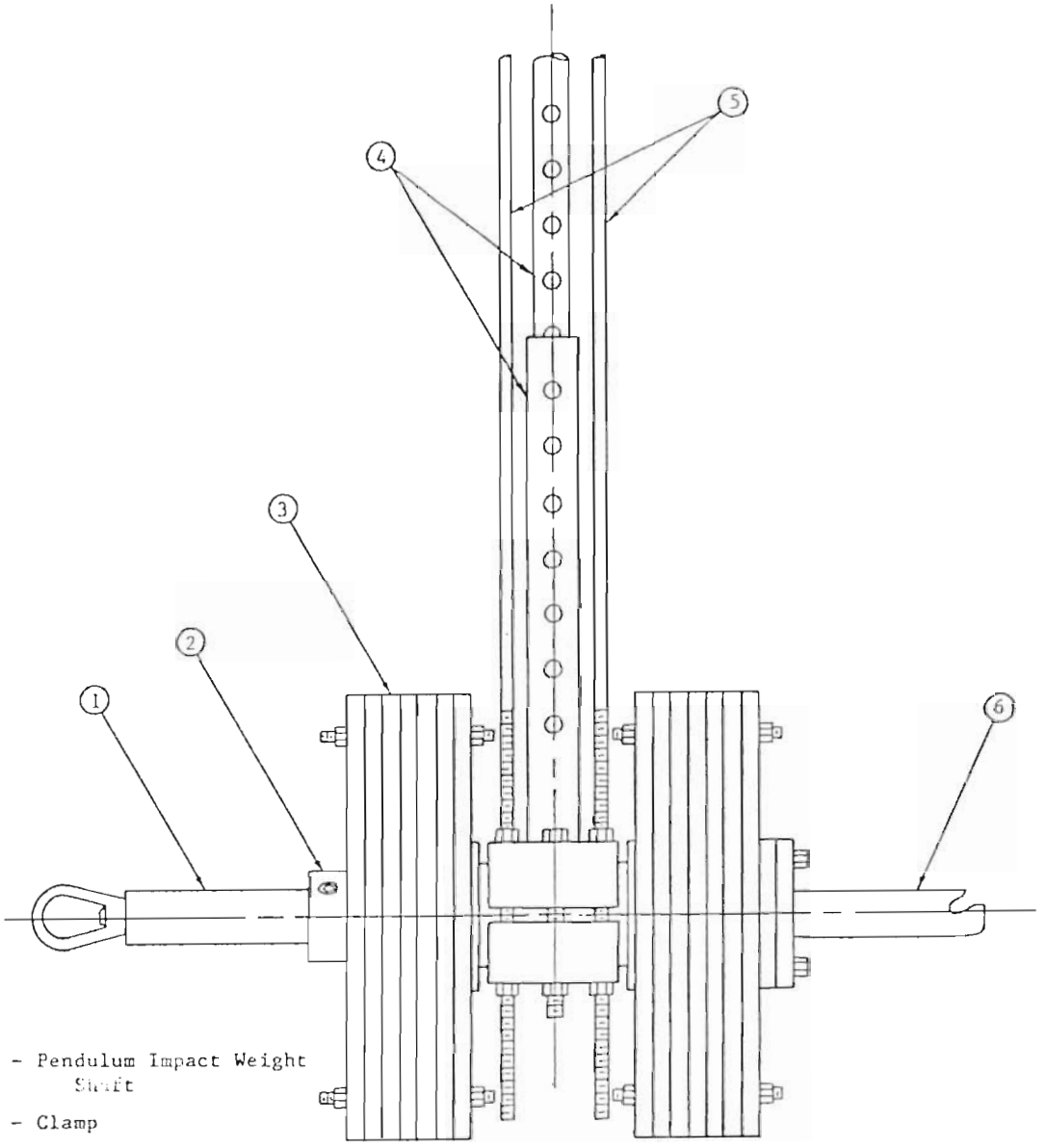

1 - Pendulum Impact Weight Shaft

2 - Clamp

3 - Pendulum Impact Weight Plates

4 - Adjustable Pendulum Arm

5 - Pendulum Arm Rods

6 - Coupler

FIGURE 10. PENDULUM IMPACT WEIGHT ASSEMBLY IN HORIZONTAL TEST

control.

8. Record the required measurements and readings; then deactivate the test instruments.

9. After the pendulum completely stops, remove the tank car head specimen from the model tank car for inspection.

10. Repeat steps 3 to 9 for more horizontal impact tests. Figure 11 shows an illustrative drawing for a pendulum impact test setup.

2.11 INSTRUMENTATION

Figure 9 shows schematic drawings of the drop impact test setup including the instruments and devices which were needed to measure and monitor the various quantities and signals involved, during the test. These instruments can be described as follows:

a. Accelerometer - A calibrated accelerometer mounted on the impact weight shaft was used to monitor the deceleration during the impact. The output will give a direct measure of the deceleration from which the maximum deceleration can be obtained and the maximum impact force can be computed.

b. Charge amplifier - A charge amplifier was used to amplify the acceleration signals so that it can be read and recorded. This charge amplifier was also used in the process of calibrating the accelerometer.

c. Tape recorder - A magnetic four-channels tape recorder was used to record all the signals from the different devices in the impact tests.

d. Filter - A band-pass filter was used with these instruments to eliminate the undesirable signals such as noise and test signals at undesirable frequencies.

e. Triggering system - A simple triggering system was used with these instruments to activate a minicomputer so that test signals can be recorded and stored.

f. Infrared photoelectric relay system - This system consists of two infrared photoelectric relays and reflectors; it was installed at a level above the model tank car head specimens. At this level an average velocity of the impact weight can be measured, which in turn can be used to calculate the impact weight velocity at the impact point.

g. Thermocouple and thermometer system - A thermocouple and electronic digital thermometer were used in the low-temperature drop impact tests to measure temperatures around -60^{o} F.

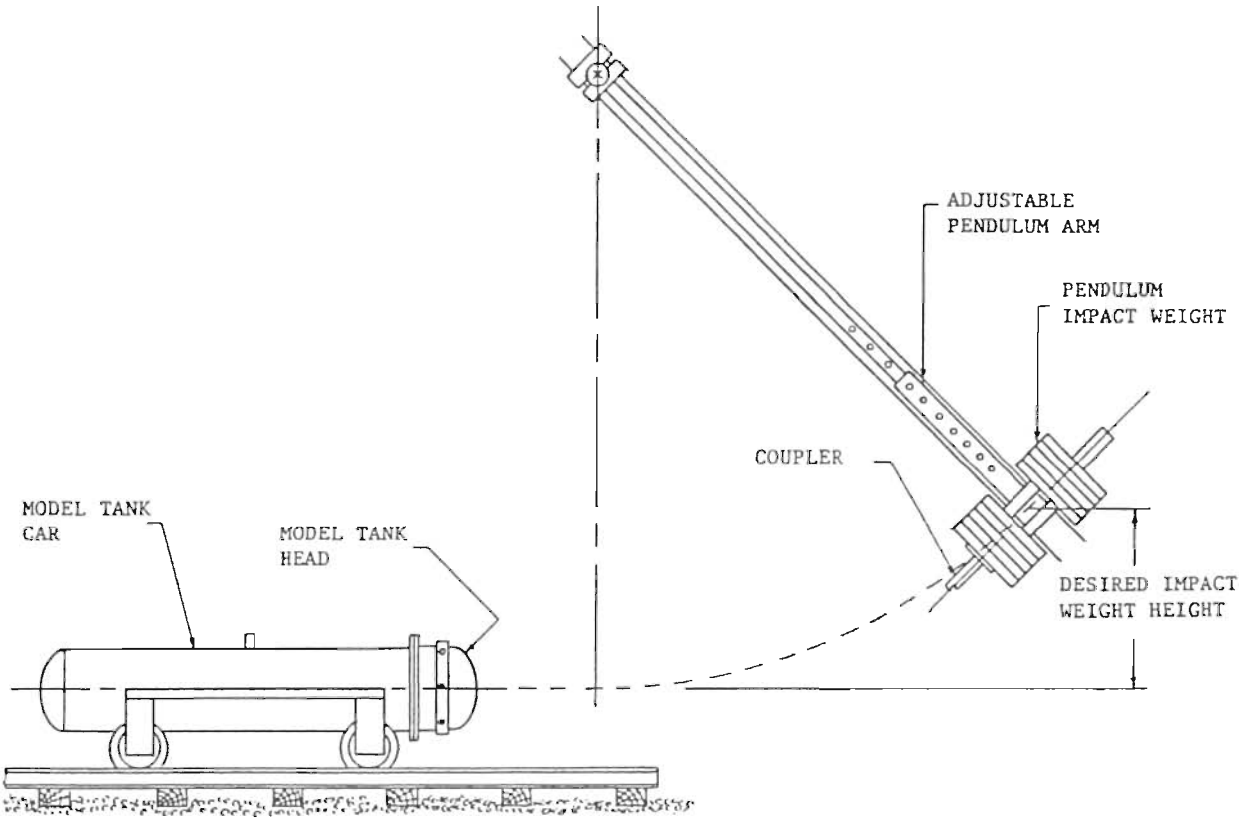

FIGURE 11. PENDULUM IMPACT TEST SETUP

h. Strain gauges and strain gauge indicator system - This system was used to measure and compare the strain rate of the model tank car head materials in the 1/10- and 1/5-scale drop impact tests.

i. Minicomputer - A computer with ADC (Analog to Digital Converter) was used with this system to store different test signals instantly during the impact tests. These signals are discretized, digitized, and then manipulated through a computer program to provide readable data for the impact tests. Some of these data are displayed in graphic form on the monitor and/or by the printer.

3. TEST RESULTS AND DISCUSSION

3.1 Determination of the Initial Drop-Weight Height

Prior to performing the 1/10-scale drop-weight impact tests, it was convenient to establish an approximate initial drop-weight height. Therefore, a preliminary static test was performed on a 1/10-scale model aluminum tank car head. A static load was applied by a hydraulic testing machine (Tinius Olson) through the 1/10-scale model coupler at the specimen's surface center. The test was conducted to determine the total energy which can be dissipated by plastic work by the model specimen up to the point of incipient shear failure (Threshold Puncture). The static test data is given in Table II, and the load-deflection curve obtained from these data is shown in Figure 12.

The total energy (E) dissipated by plastic work by the model specimen in the static test is represented by the area under the load-deflection curve. This area was measured and the total energy was computed as 124.5 foot-pounds (ft-lbs).

A scaled drop-weight (W) of 263 lb attached to the scale model coupler was used in the 1/10-scale drop-weight impact tests. The initial drop-weight height (h) was calculcated from the energy formula:

$E = Wh$, thus
$h = E/W = 124.5/263 = 0.473$ ft or
$h = 5.68$ in

Previous results indicated that the energy required to produce the same amount of deflection (depth of dent) at the center of the test specimen in a dynamic impact test was more than that in a static test. This observation was obtained when the static and dynamic tests were performed on scale model high-alloy steel tank car heads in Reference 5 and also to initiate a threshold puncture by using coke can lids as a model in scale model testing in reference 6.

3.2 Evaluation of the Mitigating Material Effectiveness

As described above in Section 2.8, the impact tests in this program were started by using the 1/10-scale model aluminum tank car heads in drop-weight impact tests. These tests were performed on bareheads and heads that were covered by head shields or face-plate mitigating materials combination.

TABLE II. STATIC TEST DATA FOR 1/10-SCALE MODEL ALUMINUM TANK CAR HEAD

FORCE (LBS)	100	190	280	250	280	320	430	540	650
DEFLECTION (IN)	.03125	.0625	.09375	.15625	.21875	.28125	.40625	.53125	.65625
FORCE (LBS)	785	935	1060	1160	1235	1395	1575	1795	1980
DEFLECTION (IN)	.78125	.90625	.96875	1.03125	1.15625	1.28125	1.40625	1.53125	1.65625

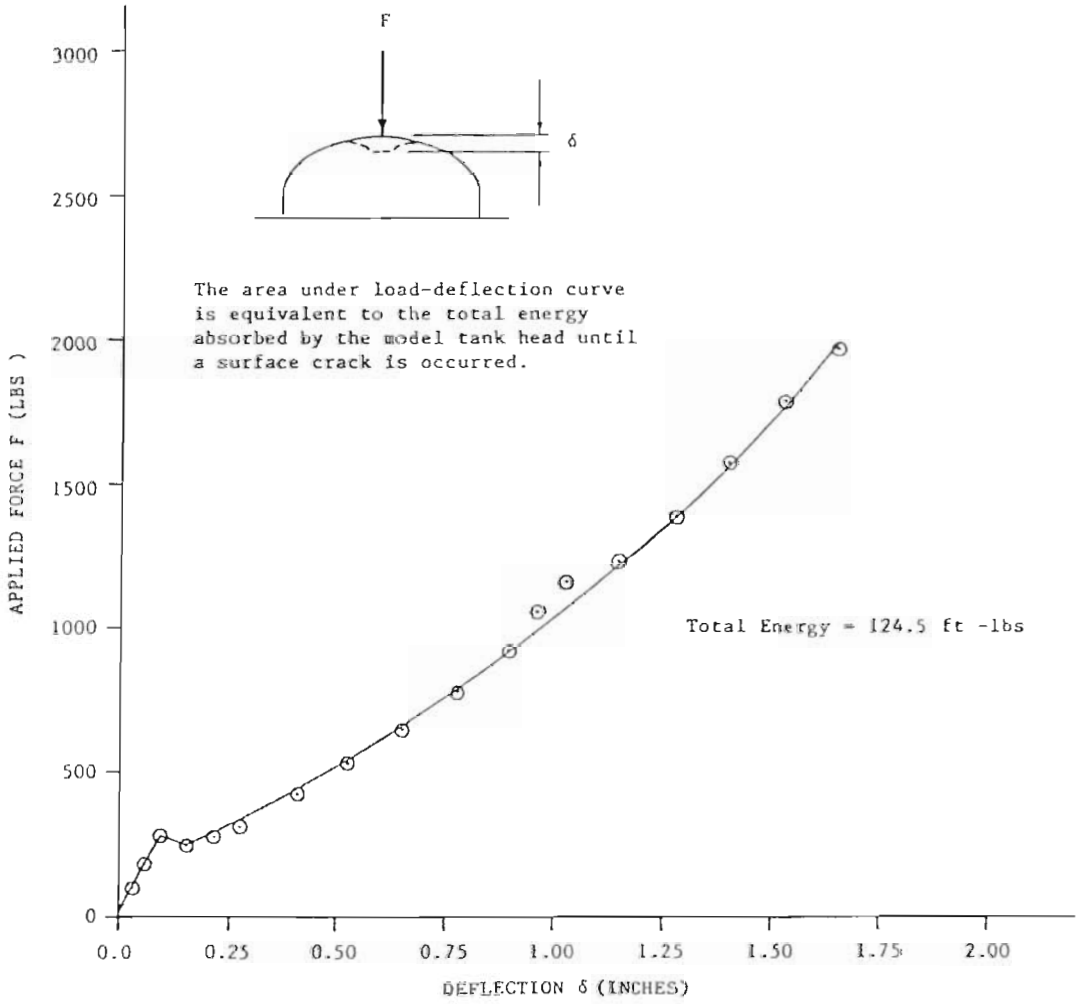

FIGURE 12. FORCE VS DEFLECTION AT THE APEX OF 1/10-SCALE MODEL ALUMINUM TANK CAR HEAD IN THE STATIC TEST.

Several kinds of mitigating materials were selected and examined in preliminary dynamic impact tests to determine the most suitable material combination with the most energy-absorbing capacity which can be used in impact situations. In order to achieve a satisfying comparison between these mitigating materials, similar face-plate mitigating material combinations were selected, and similar test procedures were followed in all cases.

Test results revealed a possible choice of two face-plate mitigating material combinations which can be used to provide a good protection to the 1/10- and 1/5-scale model tank car heads in the drop-weight impact tests. These materials can be described as follows: high-alloy steel face-plates combined with (a) TRUSSGRID aluminum honeycomb of American Cynamide Company and (b) Tecspak of Miner Enterprises, Inc. The TRUSSGRID honeycomb material has the advantage of a plane of high strength and rigidity in all three plane dimensions, which makes the material suitable for use where the direction of the impact load cannot be predicted. The "Tecspak" material is based on DUPONT Hytrel Polyester Elastomer, which has the ability to spread the impact forces on a larger area of the specimen surface, and has the advantage of high strength in compression and shearing.

Since there is a high concern about reducing railroad tank cars dead load, which is partially created by the existing steel-plate head shields, an attempt was made in this study to compare the puncture resistance-effectiveness versus material weight between the scale model steel head shield and the selected mitigating materials. Also from Reference 5, results indicated that a backup material to the scale model tank car heads was needed to reduce the excessive deformation to the specimen surface which occurred under impact forces without any sign of cracks or puncture. A slight difference in the threshold puncture velocity of 2.4 percent was registered when water and uncompacted dry sand were used as backup materials to the 1/10-scale model high-alloy steel tank car heads in drop-weight impact tests. A lower threshold puncture velocity in the water case indicated the worst situation in these impact tests. Because of the difficulty to control the water in a vertical position, the uncompacted dry sand was selected and used in the 1/10- and 1/5-scale drop-weight impact tests.

A total of forty-two (42) 1/10-scale model aluminum tank car heads were used in the drop-weight impact tests as required in the first and the second series of tests. These tests were performed to investigate the effectiveness of two different mitigating materials in increasing the puncture resistance of the model tank car heads in impact situations. The test results of the first and second series of tests are tabulated in Tables III and IV respectively. These results consist of data from the drop-weight impact tests which were performed on 1/10-scale model aluminum tank car heads at ambient temperature between 75° F and 90° F (Table III) and at low temperature between -55° F and -60° F (Table IV). The impact velocities contained in these tables are calculated according to the theoretical velocity formula $V = \sqrt{2\,gs}$, where "V" denotes the velocity of the drop-weight at impact, "g" denotes the gravity acceleration, and "s" denotes the vertical distance between the specimen surface at the point of impact and the tip of the scale model coupler.

For easier comparison and interpretation of the test data in Table III, the threshold puncture velocity, energy, and the corresponding depth of dent in

TABLE III. 1/10-SCALE MODEL DROP IMPACT TEST DATA (WITH BARE HEADS AND HEADS PROTECTED WITH FACE PLATE - HONEYCOMB, FACE PLATE - TECSPAK COMBINATION MATERIALS, OR STAINLESS STEEL HEAD SHIELDS) FOR MODEL ALUMINUM TANK CAR HEADS

MODEL - TEST NO.	TEST* CONDITION	DROP WEIGHT (LBS)	DROP HEIGHT (IN)	IMPACT SPEED		KINETIC ENERGY (FT- LBS)	MAXIMUM DECEL. (G'S)	MAX. IMPACT FORCE (LBS)	IMPACT RESULT	DEPTH OF DENT (IN)
				FT/SEC	MPH					
1-6	B	263	5	5.18	3.53	110	7.85	2065	DENT	1.375
2-50	B	263	7	6.13	4.18	153	8.10	2130	DENT	1.625
3-4	B	263	8	6.55	4.47	175	12.27	3227	TP*	1.688
4-5	B	263	9	6.95	4.74	197	13.49	3548	PUNCTURE	1.563
5-7	B	263	10	7.33	5.00	219	14.72	3871	PUNCTURE	1.438
6-2	B	263	12	8.02	5.47	263	15.46	4066	PUNCTURE	1.313
1-32	F-HC	263	40	14.65	9.99	876	39.25	10,323	DENT	2.250
2-39	F-HC	263	43	15.19	10.36	942	41.21	10,838	TP*	2.313
3-33	F-HC	263	46	15.71	10.71	1008	36.80	9678	PUNCTURE	2.375

NOTE: UNCOMPACTED DRY SAND WAS USED IN ALL 1/10-SCALE MODEL DROP IMPACT TESTS AS A BACK-UP MATERIAL FOR THE TANK HEADS

* B : BARE HEAD HC: HONEYCOMB MATERIAL
F : FACE PLATE TP: THRESHOLD PUNCTURE

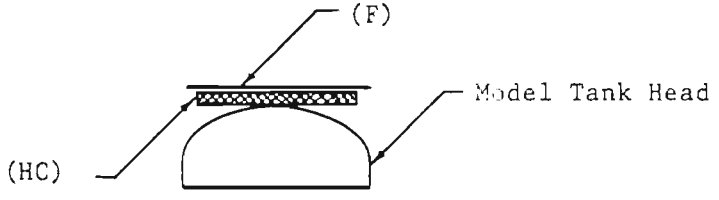

TABLE III. (CONTINUED)

MODEL-TEST NO.	TEST* CONDITION	DROP WEIGHT (LBS)	DROP HEIGHT (IN)	IMPACT SPEED		KINETIC ENERGY (FT - LBS)	MAXIMUM DECEL. (G'S)	MAX. IMPACT FORCE (LBS)	IMPACT RESULT	DEPTH OF DENT (IN)
				FT/SEC	MPH					
1-14	HS	263	32	13.10	8.93	701	40.72	10709	DENT	2.000
2-19	HS	263	40	14.65	9.99	876	46.61	12258	DENT	2.250
3-13	HS	263	46	15.71	10.71	1008	50.05	13163	TP*	2.438
4-15	HS	263	52	16.71	11.39	1140	51.52	13550	PUNCTURE	2.438
5-16	HS	263	62	18.24	12.44	1359	53.48	14065	PUNCTURE	2.500
1-9	F-T	263	16	9.27	6.32	351	21.83	5741	DENT	1.750
2-10	F-T	263	32	13.10	8.93	701	33.34	8768	DENT	2.188
3-11	F-T	263	38	14.28	9.74	833	35.33	9292	DENT	2.375
4-17	F-T	263	40	14.65	9.99	876	40.72	10709	TP*	2.438
5-12	F-T	263	46	15.71	10.71	1008	40.23	10580	PUNCTURE	2.313

* HS: HEAD SHIELD
TP: THRESHOLD PUNCTURE
F : FACE PLATE
T : TECSPAK MITIGATING MATERIAL

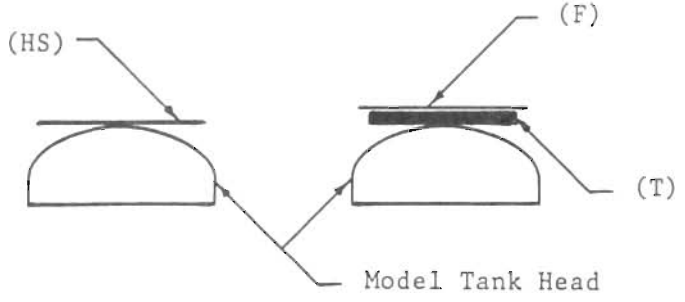

TABLE IV. 1/10-SCALE MODEL DROP IMPACT TEST DATA AT LOW TEMPERATURE (WITH BARE HEADS AND HEADS PROTECTED WITH HEAD SHIELDS OR FACE PLATE - HONEYCOMB COMBINATION MATERIAL) FOR MODEL ALUMINUM TANK CAR HEADS

MODEL-TEST NO.	TEST* CONDITION	DROP WEIGHT (LBS)	DROP HEIGHT (IN)	IMPACT SPEED		KINETIC ENERGY (FT-LBS)	MAXIMUM DECEL. (G'S)	MAX. IMPACT FORCE (LBS)	IMPACT RESULT	DEPTH OF DENT (IN)
				FT/SEC	MPH					
1-21	B-L	263	8	6.55	4.47	175	11.78	3098	DENT	1.705
2-22	B-L	263	11	7.68	5.24	241	17.17	4516	TP*	1.875
3-23	B-L	263	14	8.67	5.91	307	18.15	4773	PUNCTURE	1.875
1-24	HS-L	263	40	14.65	9.99	876	49.56	13,034	DENT	2.337
2-25	HS-L	263	52	16.71	11.39	1140	60.65	15,951	DENT	2.312
3-26	HS-L	263	62	18.24	12.44	1359	69.92	18,389	DENT	2.612
4-27	HS-L	263	72	19.66	13.40	1578	74.82	19,678	TP*	2.487
5-28	HS-L	263	82	20.98	14.30	1798	77.28	20,325	PUNCTURE	2.337
1-35	F-HC-L	263	40	14.65	9.99	876	37.78	9936	DENT	2.188
2-36	F-HC-L	263	46	15.71	10.71	1008	43.67	11,485	DENT	2.338
3-37	F-HC-L	263	52	16.71	11.39	1140	52.74	13,871	DENT	2.388
4-38	F-HC-L	263	62	18.24	12.44	1359	58.88	15,485	TP*	2.588
1-29	F-T-L	263	40	14.65	9.99	876	41.70	10,965	PUNCTURE	2.250

NOTE: UNCOMPACTED, DRY SAND WAS USED IN ALL 1/10-SCALE MODEL DROP IMPACT TESTS AS A BACK-UP MATERIAL FOR THE TANK HEADS

* B : BARE HEAD
L : LOW TEMPERATURE
HS: HEAD SHIELD
T : TECSPAK
F : FACE PLATE
HC: HONEYCOMB
TP: THRESHOLD PUNCTURE

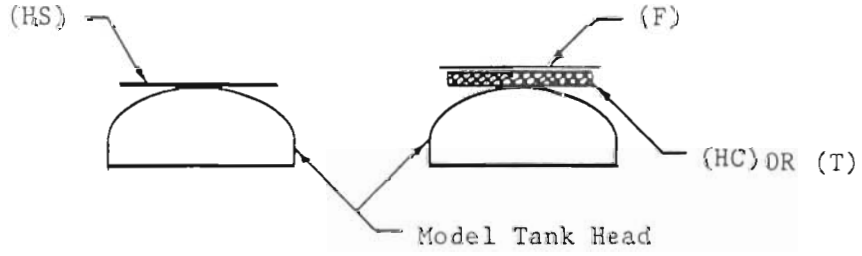

each case are tabulated in Table V. Graphs relating the dent depth versus kinetic energy at impact for the different cases in Table III are displayed in Figure 13 and also displayed in Appendix A.

It can be noticed from Figures 13 and A1 that the dent depth at the center of the 1/10-scale model aluminum tank car heads decreased after the threshold puncture situation in two cases of the drop-weight impact tests, and increased in the other cases. An examination of the punctured specimens in these tests revealed that the impact puncture in the first two cases was initiated by concentrated impact forces at the edge of the model coupler where a shearing failure occurred. In the other two cases the impact forces were spread on a bigger area of the specimens surface and the puncture failure was initiated where an excessive deformation occurred.

As can be seen from Table V, the puncture resistance of the 1/10-scale model aluminum tank car heads has increased by more than 500 percent by using head protection devices. This improvement figure can be obtained from Table V by comparing the threshold puncture energy in each case with the energy for the barehead.

Thus far the results of the drop-weight impact tests for the 1/10-scale model aluminum tank car heads indicate that the high-alloy steel head shields provide the most protection to the scale model tank car heads in impact situations. It can be seen from Table V that the impact energy absorbed by the head shield at the threshold puncture is greater than that for face-plate honeycomb or face-plate Tecspak combinations.

To assist in visualizing the deformation patterns and magnitude of damage to the impacted 1/10-scale model aluminum tank car heads, the specimens were photographed and their pictures are displayed in Appendix B. For additional information, a number of selected deceleration versus time curves for each case of the 1/10- and 1/5-scale model aluminum tank car heads in the drop-weight impact tests and also in the pendulum impact tests are displayed in Appendix C. These curves represent an accelerometer response of the impact collision between the scale model coupler and the scale model tank car heads. Impact results, maximum impact deceleration, and impact duration can be obtained from these curves. Three curves from each group in the 1/10-scale drop-weight impact tests are displayed to assist in visualizing the difference between situations where the impact results were dent, threshold puncture, and puncture. The first curve in each group represents the case when impact dent occurred at the center of the specimen. This curve is usually smooth at the bottom part where the maximum deceleration is reached because there is no sudden change in the impact weight deceleration. A little disturbance at the bottom part of the curve indicates a threshold puncture situation, while a large disturbance will indicate a puncture situation.

An examination of the quantities shown in Table V revealed that the high-alloy steel head shield absorbed the impact energy in a shorter period of time than the aluminum honeycomb or tecspak materials. Table V shows the average duration of the impact for each case of the 1/10-scale drop-weight impact tests.

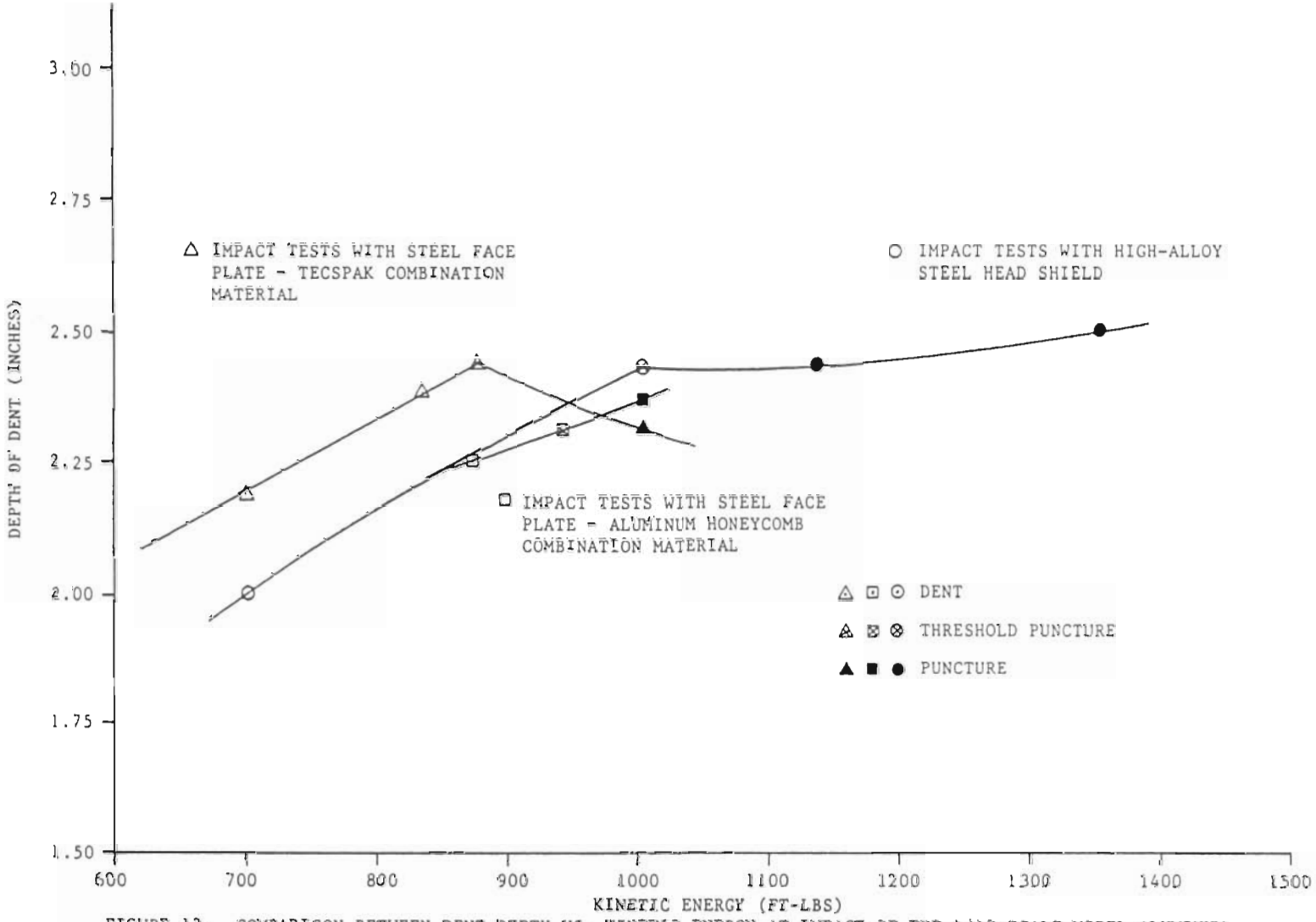

FIGURE 13. COMPARISON BETWEEN DENT DEPTH VS. KINETIC ENERGY AT IMPACT OF THE 1/10-SCALE MODEL ALUMINUM TANK CAR HEADS IN DROP-WEIGHT IMPACT TESTS

TABLE V. THRESHOLD PUNCTURE ENERGIES AND CORRESPONDING DEPTH OF DENT FROM TABLES III AND IV, ALSO THE AVERAGE IMPACT DURATION FROM THE DECELERATION VS. TIME CURVES

TEST / SHIELD MATERIAL	DROP-WEIGHT VELOCITY AT IMPACT (FT / SEC)		THRESHOLD PUNCTURE ENERGY (FT - LBS)		DEPTH OF DENT (INCHES)		AVERAGE IMPACT DURATION (M-SEC)	
	ROOM TEMP.	LOW TEMP.	ROOM TEMP.	LOW TEMP.	ROOM TEMP.	LOW TEMP.	ROOM TEMP.	LOW TEMP.
BAREHEAD	6.55	7.68	175	241	1.686	1.875	45	44
HIGH-ALLOY STEEL HEAD SHIELD	15.71	19.66	1008	1578	2.438	2.487	32	30
FACE-PLATE AND ALUMINUM HONEYCOMB	15.19	18.24	942	1359	2.313	2.588	40	37
FACE-PLATE AND TECSPAK MATERIAL	14.65	-	876	-	2.438	-	42	-

It is of interest to compare the dynamic response between test models 2-19, 1-32, and 4-17 in Table III. These models were protected by high-alloy steel head shield, steel face plate-aluminum honeycomb material, and steel face plate-Tecspak material respectively. All models were subjected to the same drop-weight impact conditions with 40 in drop-weight height and 263 lbs drop-weight, thereby all were subjected to the same impact energy. The impact duration of these models were 30, 40, and 42 milliseconds (ms) and corresponding maximum impact forces were 12,258 lbs, 10,323 lbs, and 10,709 lbs, respectively. The results from reference 5 indicated that at the same impact energy, the model with the smaller impact duration should be subjected to a higher value of the maximum impact forces. However, an examination of the above data indicates that this notion is not applied in all cases with different mitigating materials.

3.3 LOW-TEMPERATURE EFFECT

The 1/10-scale model aluminum tank car heads with different protective devices were used in this series of tests to examine the effect of low temperature on the threshold puncture energy in each case. Liquid nitrogen was used to cool down the test specimens including the model aluminum tank car heads, the high-alloy steel head shields, and the combined materials of steel face-plates and different kinds of mitigating materials. These impact tests were performed at low temperatures around - 60^{o}F. The test results are tabulated in Table IV, and the comparison between these results and those at room temperature are tabulated in Table V. According to these data, the threshold puncture energy at low temperature was higher than the energy at room temperature in all test conditions except the case when the Tecspak material was used as a mitigator. This material became brittle at such low temperature, and smashed under the impact load without providing an effective protection to the model aluminum tank car heads. The increase in the threshold puncture energy in each case was calculated as follows: 38 percent with bareheads, 57 percent with high-alloy steel head shields, and 44 percent with steel face plate-aluminum honeycomb mitigating materials. However, the threshold puncture energy decreased by more than 13 percent in the case when steel face-plate Tecspak material was used as protective device at low temperature. For easier comparison, graphs relating dent depth versus kinetic energy at impact at low and room temperatures are displayed in Figure 14. Also, these graphs are displayed separately in Appendix A in Figures A1 to A7. Based on this information, it may be concluded that low temperature has the effect of increasing the threshold puncture energy of the model aluminum tank car heads in all impact cases except in the case where Tecspak materials was used as a mitigator.

3.4 VALIDITY OF SCALING LAWS

3.4.1 Scaling Laws

In the development of small-scale simulation tests, it is very important to adopt appropriate scaling laws so that model results can be extrapolated to the full-scale cases. The scaling laws adopted in this study were developed by Gorman (Reference 6), using dimensional analysis. Similar dimensional analysis

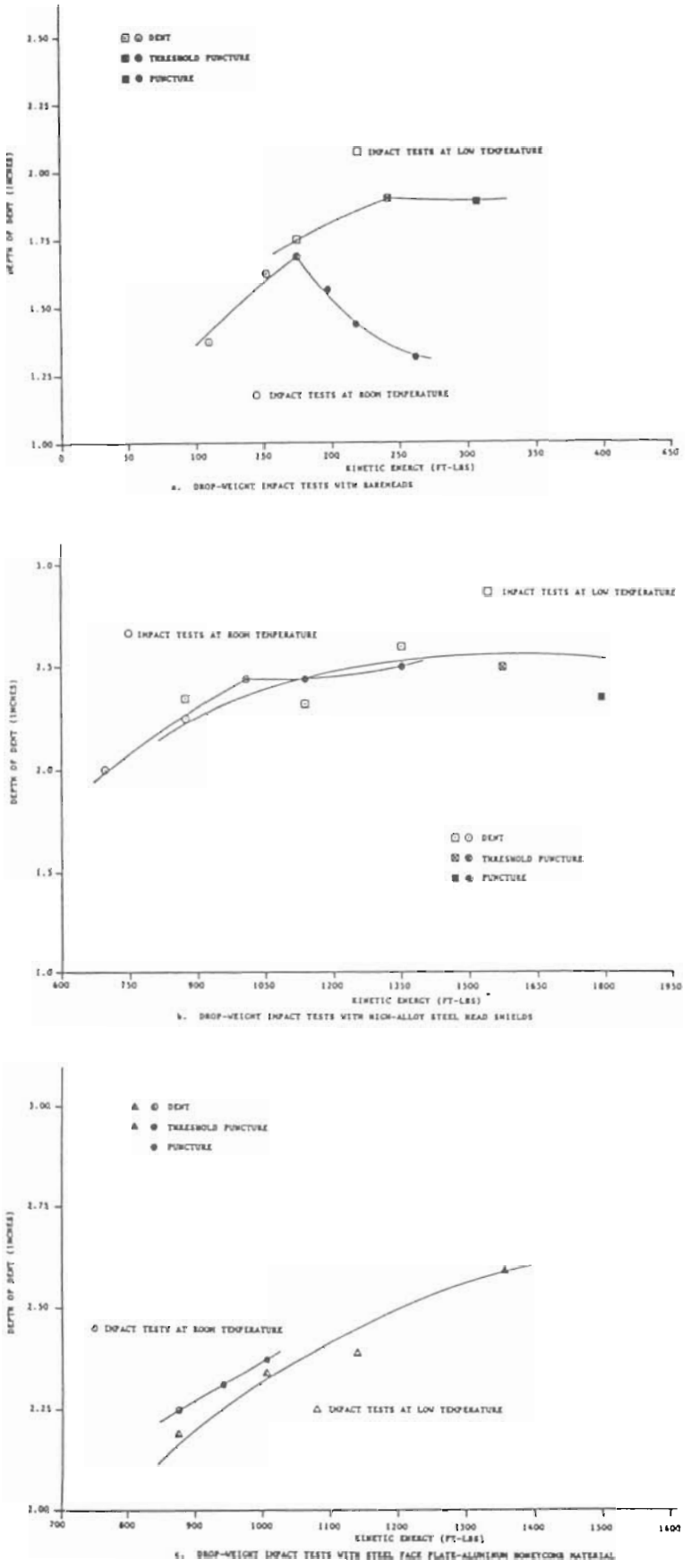

Figure 14. Comparison of Dent Depth Vs. Kinetic Energy at Impact of the 1/10-Scale Model Aluminum Tank Car Heads at Low and Room Temperatures in Drop-Weight Impact Tests

were also done in References 3 and 7 to 11. The details of this dimensional analysis are displayed in Appendix D.

3.4.2 Applying and Testing the Scaling Laws

All previous drop-weight impact tests in this program were performed on the 1/10-scale model aluminum tank car heads. However, for the purpose of applying and testing the scaling laws adopted, a series of drop-weight impact tests were also performed on 1/5-scale model aluminum tank car heads. The head shields, the face plates, and the mitigating materials used in this series of tests were selected according to the scaling laws specifications so that accurate comparison between the two models can be made.

A total of nineteen (19) 1/5-scale model aluminum tank car heads were used to cover all the required impact tests in this series. The test results of the 1/5-scale drop-weight impact tests are tabulated in Table VI. Graphs relating the dent depth versus kinetic energy at impact for each case in Table VI are displayed in Appendix A in Figures A8 to A12. Also, for easier comparison, these graphs are displayed together in Figures 15 and 16. It can be noticed from Figures 15 and A8 that the dent depth at the center of the 1/5-scale model aluminum tank car heads decreased after the threshold puncture situation in three cases of the drop-weight impact tests and undetermined in the case where the aluminum honeycomb was used as a mitigator. In these cases the impact puncture was initiated by concentrated impact forces at the edge of the model coupler where a shearing failure occurred. Similar results were obtained in Section 3.2 in the 1/10-scale drop-weight impact tests with model aluminum tank car bareheads and when Tecspak material was used as a mitigator.

It can be seen from Table VI, that the threshold puncture data in some cases could not be determined directly by the drop-weight impact tests. However, these data can be estimated approximately by interpolating or extrapolating the required data points on the dent depth versus kinetic energy graphs as shown in Figure 15. The threshold puncture data point should be located on the graph between two consecutive data points where the impact test results indicate dent and puncture respectively. Also, it can be located on the graph after the deepest dent data point. The location of the threshold puncture data point is controlled by the condition of the impacted specimens. An examination of these specimens can be a guide to determine whether the threshold puncture data point is located near the dent data point or the puncture data point.

This procedure was followed in some cases of the 1/5-scale model aluminum drop-weight impact tests to determine the location of the threshold puncture data points on the dent depth versus kinetic energy graphs as shown in Figures 15 and A8. The threshold puncture energy for each data point was obtained from the graphs and the corresponding threshold puncture velocity was calculated for each case as follows: 1,315 ft-lbs at 4.33 mph with bareheads, 5,675 ft-lbs at 8.99 mph with high-alloy steel head shields, and 7,532 ft-lbs at 10.36 mph with steel face plate-aluminum honeycomb material.

As can be seen from Table VI and these data, the puncture resistance of the 1/5-scale model aluminum tank car heads has increased by an average of 4.5

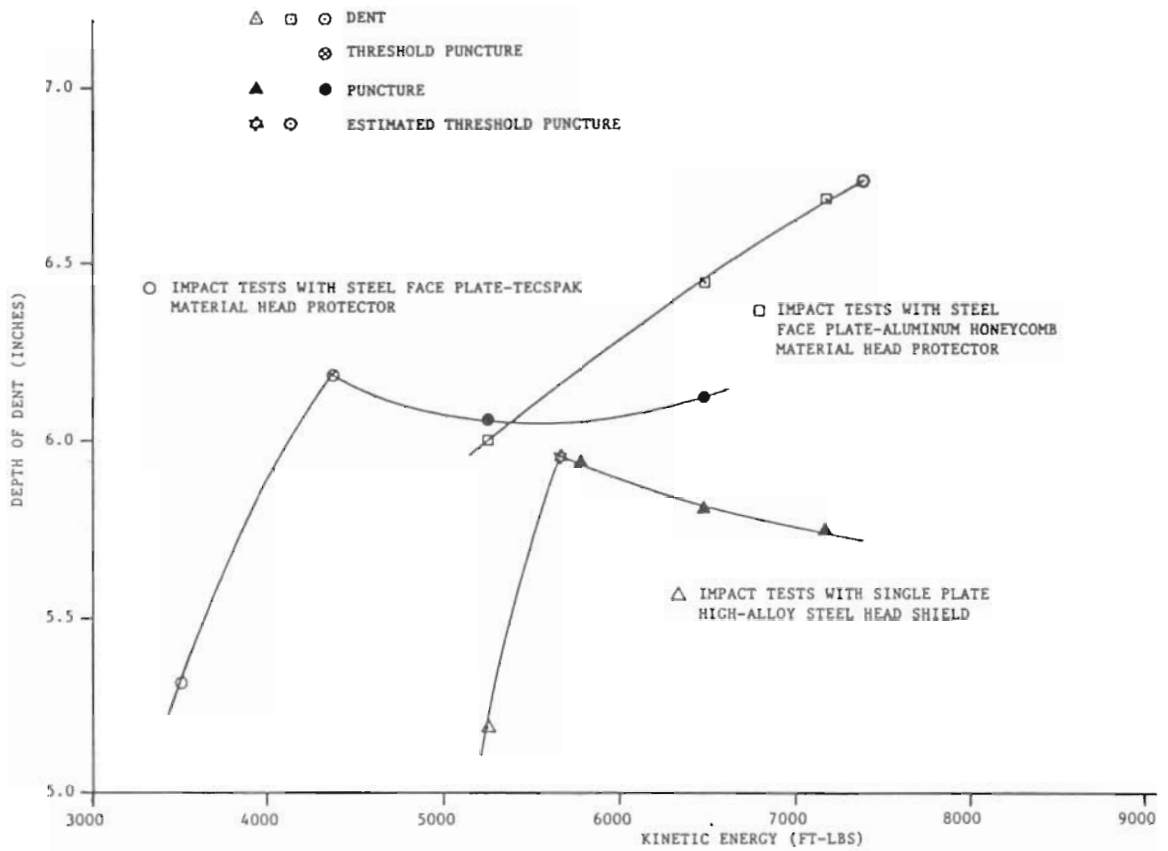

FIGURE 15. COMPARISON OF DENT DEPTH VS. KINETIC ENERGY AT IMPACT OF THE 1/5-SCALE MODEL ALUMINUM TANK CAR HEADS IN DROP-WEIGHT IMPACT TESTS

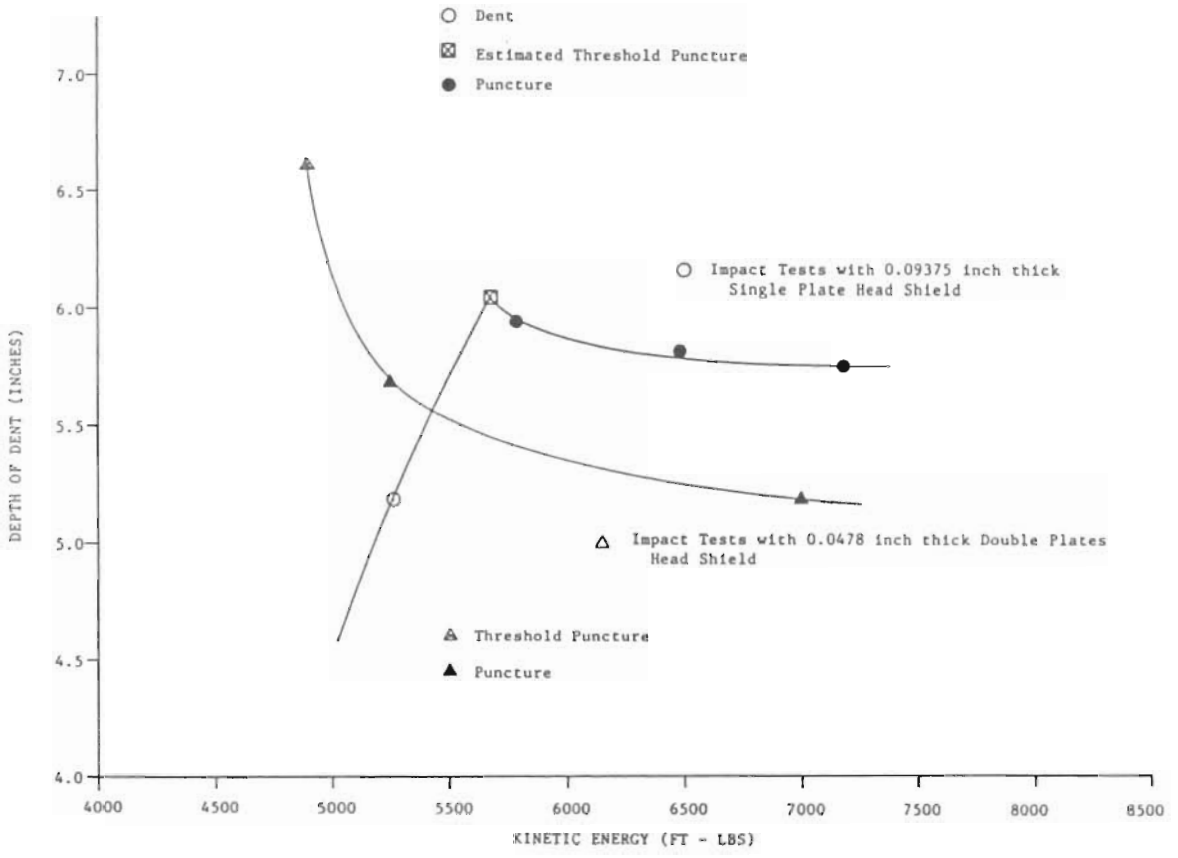

Figure 16. Comparison of Dent Depth vs. Kinetic Energy at impact of the 1/5-scale model aluminum tank car heads with high-alloy steel head shields in drop-weight impact tests.

TABLE VI. 1/5-SCALE MODEL DROP IMPACT TEST DATA (WITH BARE HEADS AND HEADS PROTECTED WITH HEAD SHIELDS, FACE PLATE - HONEYCOMB, OR FACE PLATE - TECSPAK COMBINATION MATERIALS) FOR MODEL ALUMINUM TANK CAR HEADS

MODEL-TEST NO.	TEST* CONDITION	DROP WEIGHT (LBS)	DROP HEIGHT (IN)	IMPACT SPEED		KINETIC ENERGY (FT LBS)	MAXIMUM DECEL. (G'S)	MAX. IMPACT FORCE (LBS)	IMPACT RESULT	DEPTH OF DENT (IN)
				FT/SEC	MPH					
1-54	B	2102	6	5.67	3.87	1049	**	**	DENT	3.88
2-53	B	2102	8	6.55	4.47	1400	9.32	19,591	PUNCTURE	4.31
3-52	B	2102	10	7.33	5.00	1754	**	**	PUNCTURE	4.19
1-82	HS-1	2102	30	12.69	8.65	5256	18.89	39,706	DENT	5.19
2-80	HS-1	2102	33	13.31	9.07	5782	16.44	34,557	PUNCTURE	5.94
3-79	HS-1	2102	37	14.09	9.61	6480	18.64	39,181	PUNCTURE	5.81
4-78	HS-1	2102	41	14.83	10.11	7178	19.63	41,262	PUNCTURE	5.75
1-63	HS-2	2102	28	12.26	8.36	4906	16.19	34.031	TP*	6.62
2-56	HS-2	2102	30	12.69	8.65	5256	18.40	38,677	PUNCTURE	5.69
3-55	HS-2	2102	40	14.65	9.99	7005	19.14	40,232	PUNCTURE	5.19

NOTE: UNCOMPACTED DRY SAND WAS USED IN ALL 1/5-SCALE MODEL DROP IMPACT TESTS AS A BACK-UP MATERIAL FOR THE TANK HEADS

* B : BARE HEAD HS-1: SINGLE PLATE OF .09375 INCH THICK HIGH-ALLOY STEEL HEAD SHIELD
TP: THRESHOLD PUNCTURE HS-2: DOUBLE PLATES OF .0478 INCH THICK HIGH-ALLOY STEEL HEAD SHIELD

** MISSING DATA OCCURRED IN SITUATIONS WHEN SEVERE PUNCTURE OR MEASURING DIFFICULTIES WERE ENCOUNTERED

TABLE VI. (CONTINUED)

MODEL-TEST NO.	TEST* CONDITION	DROP WEIGHT (LBS)	DROP HEIGHT (IN)	IMPACT SPEED		KINETIC ENERGY (FT - LBS)	MAXIMUM DECEL. (G'S)	MAX. IMPACT FORCE (LBS)	IMPACT RESULT	DEPTH OF DENT (IN)
				FT/SEC	MPH					
1-57	F-HC	2102	30	12.69	8.65	5256	7.85	16,501	DENT	6.00
2-58	F-HC	2102	37	14.09	9.61	6480	14.72	30,941	DENT	6.44
3-59	F-HC	2102	41	14.83	10.11	7178	14.96	31,446	DENT	6.69
4-81	F-HC	2102	45	15.54	10.60	7882	17.17	36,091	DENT	5.50**
1-65	F-T	2102	20	10.36	7.06	3503	11.04	23,206	DENT	5.31
2-62	F-T	2102	25	11.58	7.90	4377	12.76	26,822	TP*	6.19
3-61	F-T	2102	30	12.69	8.65	5256	11.53	24,236	PUNCTURE	6.06
4-60	F-T	2102	37	14.09	9.61	6480	11.04	23,206	PUNCTURE	6.13

* F : FACE PLATE T : TECSPAK MATERIAL
HC: HONEYCOMB TP: THRESHOLD PUNCTURE

** THE HONEYCOMB MATERIAL USED IN THIS TEST WAS THICKER AND LESS DENSE.

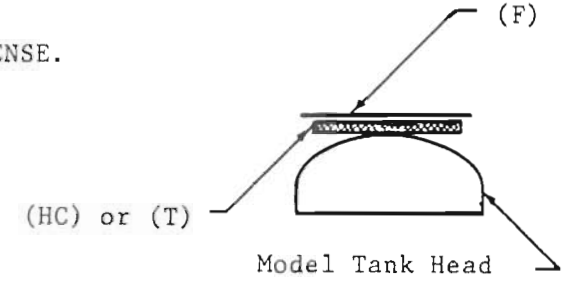

times by using head protection devices. This improvement figure can be obtained by comparing the threshold puncture energy in each case and the threshold puncture energy for the barehead. Also, the steel face plate-honeycomb material has absorbed the most impact energy (7,532 ft-lbs) before puncture; this indicates that layers of aluminum honeycomb material combined with thin sheets of high-alloy steel can provide more protection to the model tank car heads than that provided by the corresponding single plate high-alloy steel head shield or steel face plate-Tecspak materials.

3.4.3 Comparison Between the 1/10- and 1/5-Scale Model Test Results

According to the scaling laws adopted in this study (from Appendix D), the threshold puncture velocities of the model tank car head and the prototype should be the same. These scaling laws can also be applied to the 1/10- and 1/5-scale model aluminum tank car heads. It was proved theoretically from the analyses of the scaling laws in Appendix D that if the effect of the strain rate is taken into account for the above case, a scaling factor of two will yield a difference of 1.0 percent in the threshold puncture velocities between the 1/10- and 1/5-scale models.

In comparing the impact test results from Tables III and VI, and the data in Section 3.4.2, a difference of 3.0 percent in the threshold puncture velocities between the two scale model aluminum bareheads was found. This difference is slightly higher than the theoretical 1.0 percent difference obtained from the analyses of the scaling laws in Appendix D. However this result can be considered as a good agreement with the scaling laws in this case. As expected, this difference will be higher in the other cases because of the additional materials used as protective devices.

The comparison between the impact test results in the 1/10- and 1/5-scale model aluminum tank car heads where high-alloy steel head shields, and steel face plate-Tecspak materials were used as protective devices, revealed that the difference in the threshold puncture velocities between the two models were higher as expected, and were calculated as 16.0 percent and 21.0 percent respectively. On the other hand, by investigating the case where steel face plate-aluminum honeycomb material was used as a protective device, it can be noticed that there was no difference in the threshold puncture velocity between the two scale models.

This result may be attributed to a special characteristic of the aluminum honeycomb material which is the ability to absorb the impact energy constantly during the crushing process under an impact load up to 70 percent of its thickness. The data at the threshold puncture of the 1/10- and 1/5-scale models are shown in Table VI-I.

3.5 EFFECT OF LADING

The effect of lading on the threshold puncture energy of the model aluminum tank car heads was examined through a series of horizontal impact tests conducted on the pendulum tower. A total of eleven (11) 1/5-scale model aluminum tank car heads were used as required in the forth test series. A movable model tank car mounted on a railroad track with a brake system attached to the front wheels was used to perform the horizontal impact tests. A

TABLE VI-I COMPARISON OF THE DATA AT THE THRESHOLD PUNCTURE OF THE 1/10- AND 1/5-SCALE DROP-WEIGHT IMPACT TESTS

MODEL-TEST NO.	MODEL SCALE	TEST CONDITION	DROP-WEIGHT (LBS)	DROP-HEIGHT (IN)	IMPACT SPEED		KINETIC ENERGY (FT - LBS)	IMPACT* RESULT	DEPTH OF DENT (IN)
					FT/SEC	MPH			
3-4	1/10	B	263	8.0	6.55	4.47	175	TP	1.688
3-13	1/10	HS	263	46.0	15.71	10.71	1008	TP	2.438
2-39	1/10	F-HC	263	43.0	15.19	10.36	942	TP	2.313
4-17	1/10	F-T	263	40.0	14.65	9.99	876	TP	2.438
	1/5	B	2102	7.5 **	6.35 **	4.33 **	1315 **	TP	4.400 **
	1/5	HS-1	2102	32.4 **	13.19 **	8.99 **	5675 **	TP	6.045 **
	1/5	F-HC	2102	43.0 **	15.19 **	10.36 **	7532 **	TP	6.700 **
2-62	1/5	F-T	2102	25.0	11.58	7.90	4377	TP	6.190

* B : BAREHEAD
HS: HEAD SHIELD
F : FACE PLATE
HC: HONEYCOMB
T : TECSPAK
HS-1: SINGLE PLATE HEAD SHIELD
TP : THRESHOLD PUNCTURE

** These vales were calculated and not from actual impact tests as explained in Section 3.4.2.

removable 1/5-scale head holder (the same head holder used in the 1/5-scale drop-weight impact tests) was used to mount the test specimens on the model tank car. The horizontal impact tests were performed on the 1/5-scale model aluminum tank car bareheads under two conditions: (A) the model target tank car was filled with water to 90 percent of its total volume, and (B) the model target tank car was loaded with weights to provide the same total weight as in Condition A. The test results are listed in Table VII. For easier comparison, graphs relating dent depth versus kinetic energy for the horizontal center-impact tests are displayed in Figure 17. It can be seen from these graphs that the threshold puncture energy in the impact Condition A (7,970 ft-lbs) is lower than the energy in the impact Condition B (8,408 ft-lbs) at impact speeds of 10.65 mph and 10.94 mph respectively. Also, the corresponding depth of dent in Case B is deeper than the depth of dent in Case A.

It may be concluded that the scale model aluminum tank car heads with empty tank car is susceptible to a deeper dent and less susceptible to an impact puncture than the one backed up with fluids; lading has the effect of increasing the scale model tank car head vulnerability to impact puncture.

3.6 EFFECT OF THE OFF-CENTER IMPACTS

Thus far, the drop-weight and pendulum impact tests conducted in this program were performed at the centerline of the 1/10- and 1/5-scale model aluminum tank car heads. However, the Federal Railroad Administration (FRA) full-scale puncture resistance tests included two series of off-center impact tests, which were performed at 21 inches and 31 inches above the sill. Since the scale model data for these two conditions are lacking, a test series, including off-centerline drop-weight and pendulum impact tests was added to this test program. Aluminum and high-alloy steel model tank car heads, with and without head protection devices, were used in this test series. The off-center impact positions were scaled to the full-scale test locations defined above. Also, two test settings with each impact position were used in the 1/10-scale model aluminum off-center drop weight impact tests. In one test setting the head holder was tilted by a certain angle, such that the impact direction will be perpendicular to the specimen surface. Figures 18 and 19 show photographs of 1/10-scale model aluminum tank car heads in the off-center impact test settings at scaled positions of 31 inches and 21 inches above the sill respectively. The other off-center test setting was arranged by adjusting and fixing the head holder in the vertical position so that the impact direction will be parallel to the centerline of the test specimen. Figure 20 shows the 1/10-scale model aluminum tank car head in a vertical off-center drop-weight impact test setting. The 1/5-scale model high-alloy steel tank car heads were used also in off-center drop-weight impact tests with only vertical test setting. Uncompacted dry sand was used in all center and off-center drop-weight impact tests as a backup material to the model tank car heads.

A total of forty-five (45) 1/10- and 1/5-scale model aluminum and high-alloy steel tank car heads were used in the off-center impact tests as required in this test series. The test results are tabulated in Tables VIII, IX, X, and XI. Performing these impact tests at similar impact conditions and ambient temperature is a base for the comparison between the test data.

TABLE VII. 1/5-SCALE MODEL HORIZONTAL IMPACT TEST DATA (WITH BARE HEADS AND: EMPTY TANK OR THE TANK FILLED WITH WATER TO 90 PERCENT OF ITS VOLUME) FOR MODEL ALUMINUM TANK CAR HEADS

MODEL-TEST NO.	TEST* CONDITION	PENDULUM IMPACT WEIGHT (LBS)	SWING HEIGHT (IN)	IMPACT SPEED		KINETIC ENERGY (FT - LBS)	MAXIMUM DECEL. (G'S)	MAX. IMPACT FORCE (LBS)	IMPACT RESULT	DEPTH OF DENT (IN)
				FT/SEC	MPH					
1-45	B-E	2060	30	12.69	8.65	5256	2.26	4656	DENT	6.188
2-46	B-E	2060	45	15.54	10.60	7882	2.50	5150	DENT	8.188
3-48	B-E	2060	48	16.05	10.94	8408	3.93	8096	TP*	8.250
4-47	B-E	2060	55	17.18	11.71	9634	4.66	9600	PUNCTURE	6.938
1-40	B-W	2060	10	7.33	5.00	1754	2.94	6056	DENT	3.188
2-41	B-W	2060	20	10.36	7.06	3503	3.19	6571	DENT	5.000
3-42	B-W	2060	30	12.69	8.65	5256	3.43	7066	DENT	6.188
4-43	B-W	2060	45	15.54	10.60	7882	3.68	7581	DENT	7.563
5-51	B-W	2060	46.5	15.80	10.77	8148	3.93	8096	PUNCTURE	6.563
6-49	B-W	2060	48	16.05	10.94	8408	4.05	8343	PUNCTURE	6.250
7-44	B-W	2060	60	17.94	12.23	10,505	4.42	9105	PUNCTURE	6.438

NOTE: ALL OF THE HORIZONTAL TESTS WERE PERFORMED WITHOUT BACK-UP CARS AND THE BRAKES WERE ON.

* B : BARE HEAD
E : EMPTY TANK CAR
W : TANK CAR FILLED WITH WATER
TP: THRESHOLD PUNCTURE

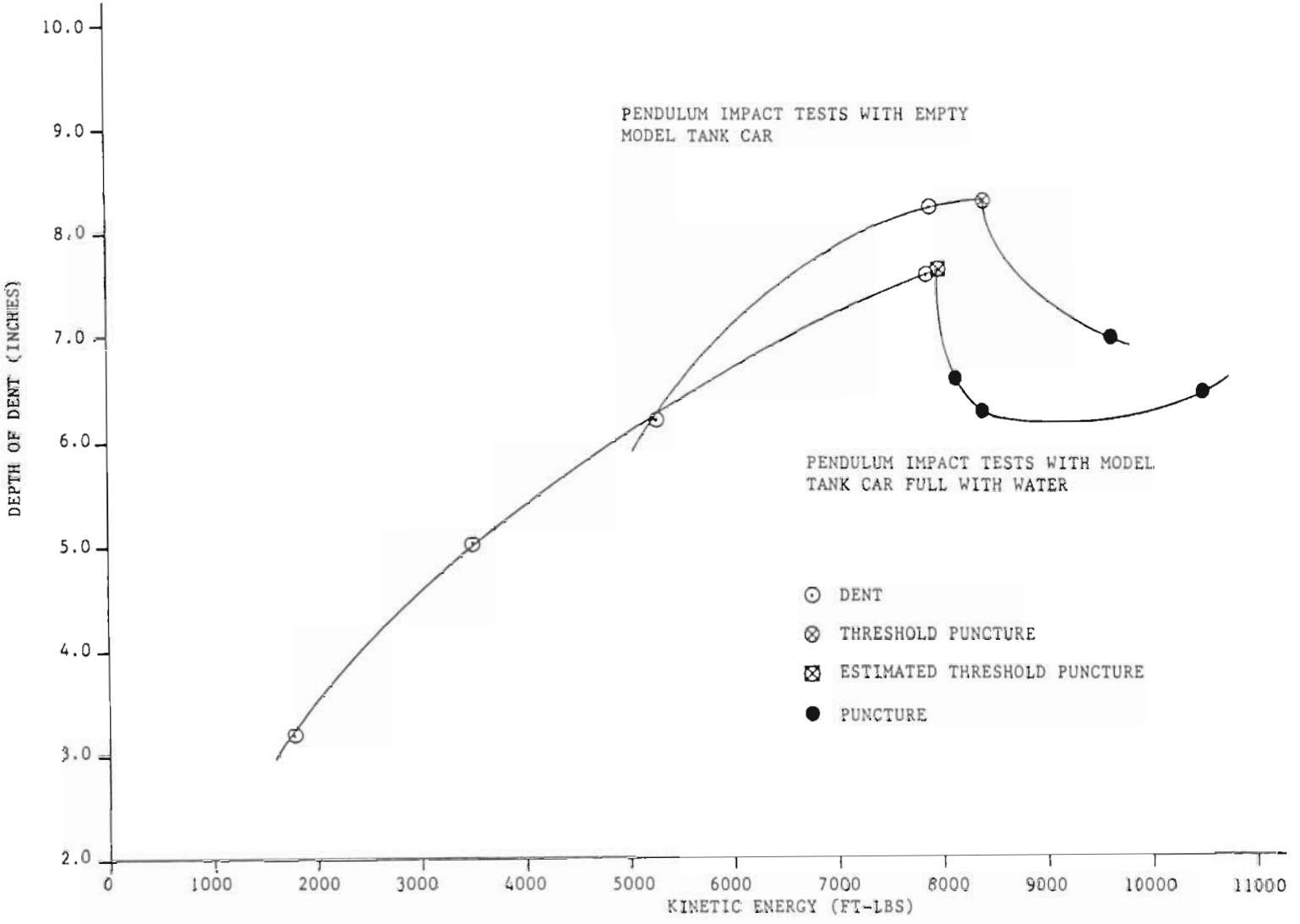

FIGURE 17. COMPARISON OF DENT DEPTH VS. KINETIC ENERGY AT IMPACT OF THE 1/5-SCALE MODEL ALUMINUM TANK CAR HEADS IN HORIZONTAL IMPACT TESTS WITH AND WITHOUT WATER IN THE MODEL TANK CAR

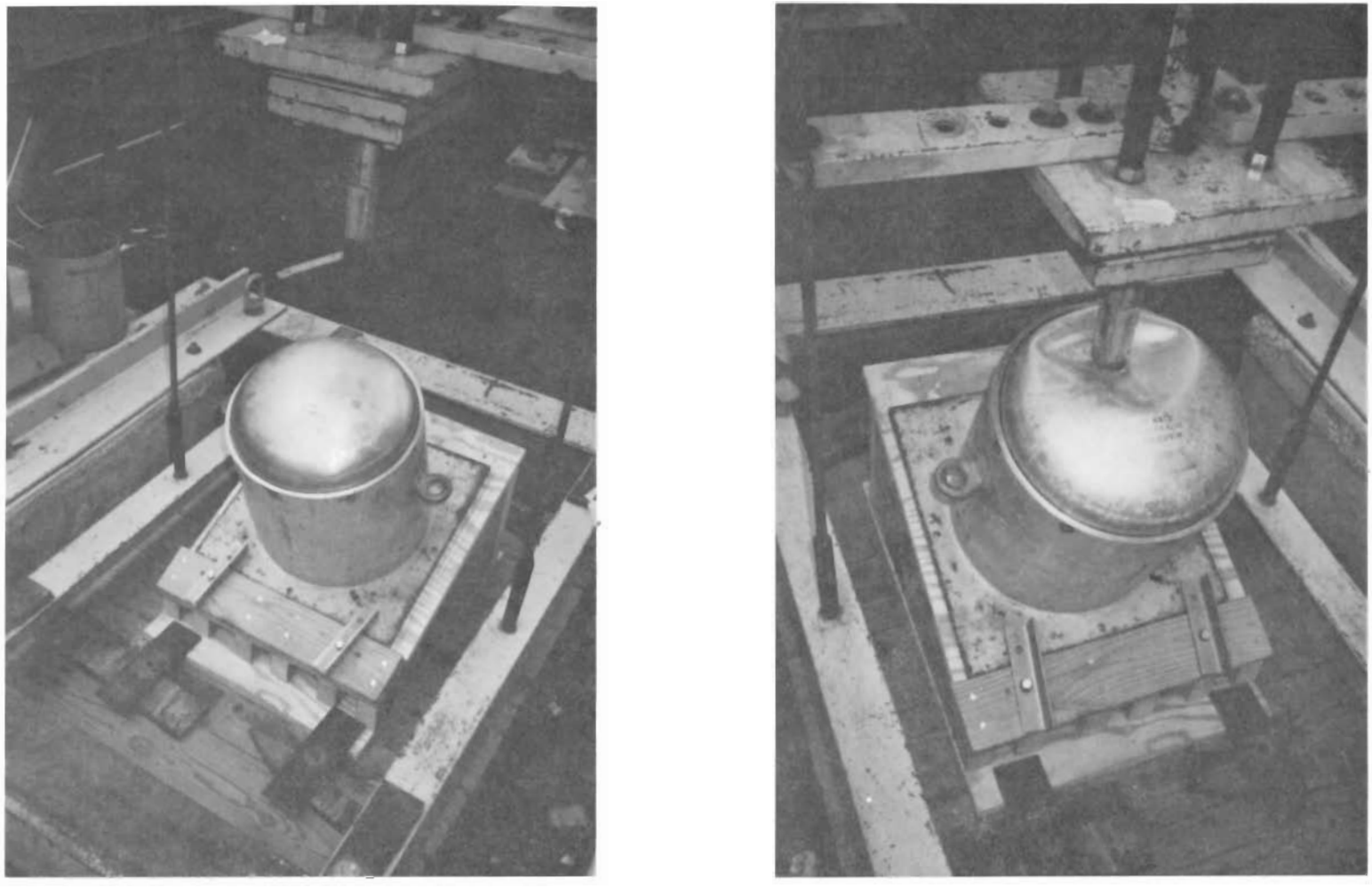

Figure 18. 1/10 scale model aluminum tank car barehead in off-center impact test setup at scaled position of 31 inches above the sill before and after the impact.

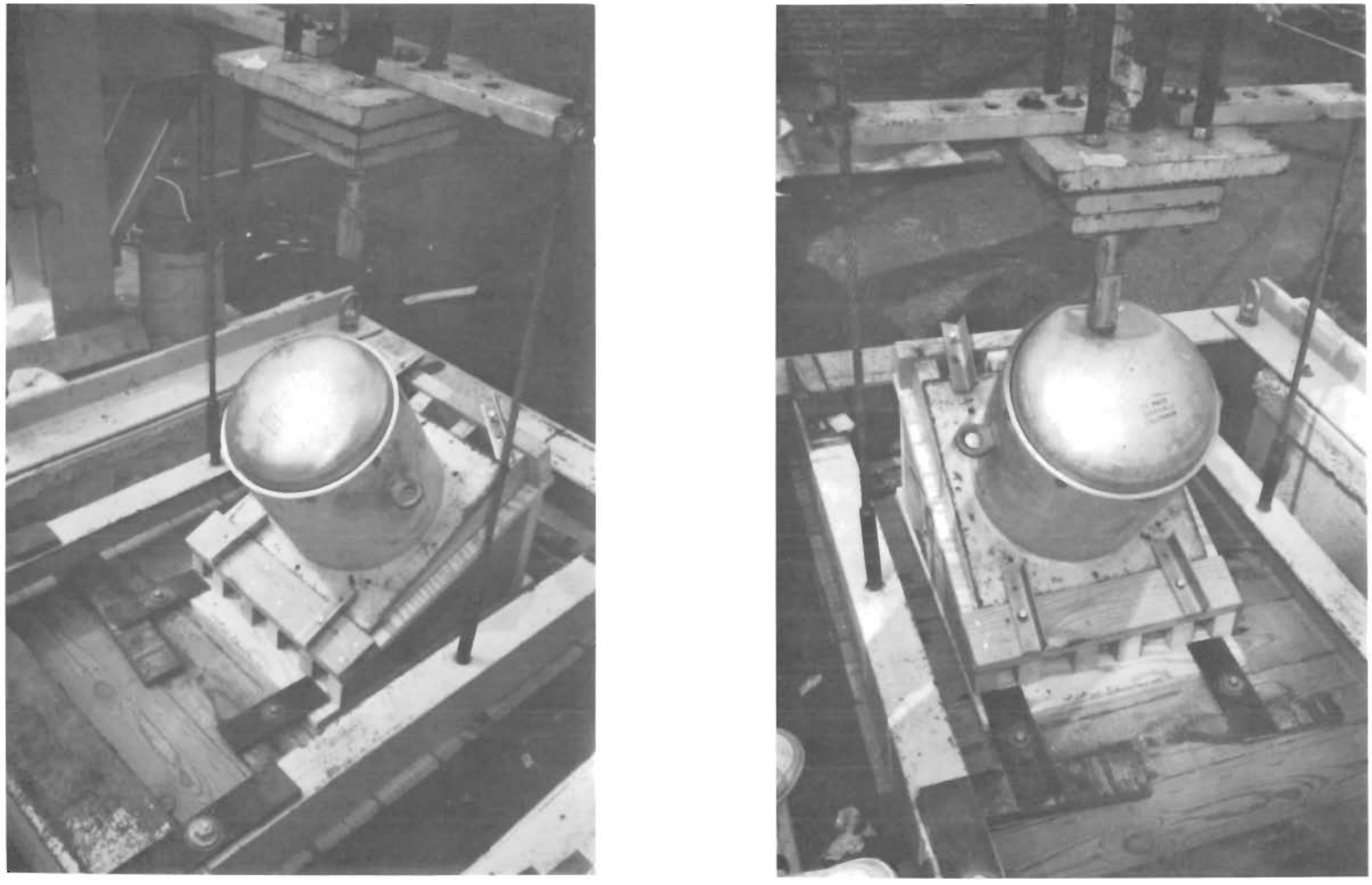

Figure 19. 1/10 scale model aluminum tank car bare head in off-center impact test setup at scaled position of 21 inches above the sill before and after the impact.

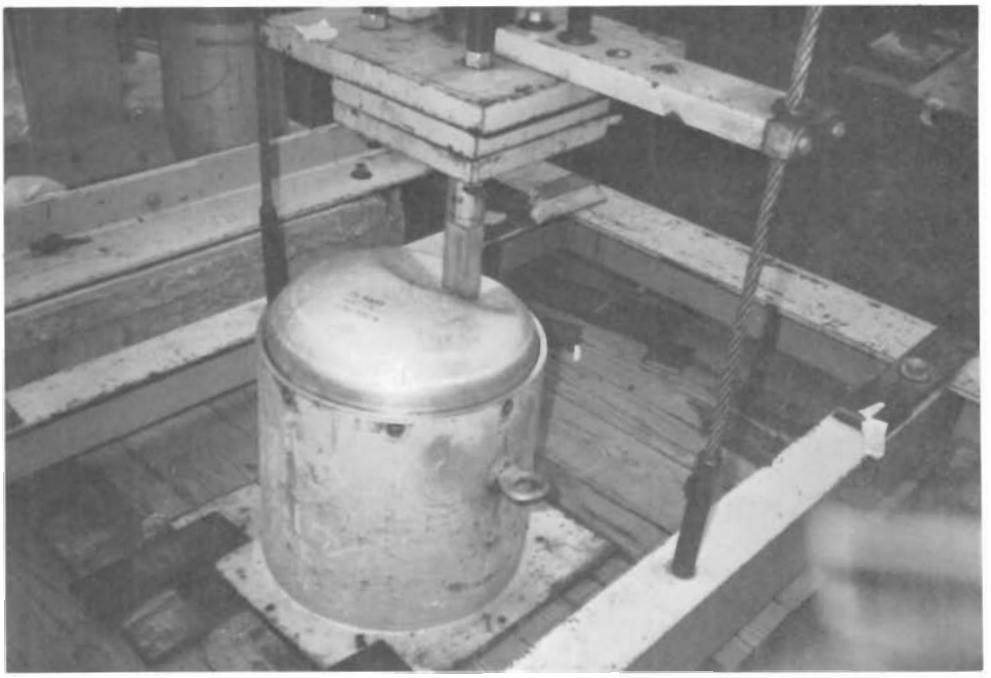

Figure 20. 1/10 scale model aluminum tank car barehead in off-center impact test setup with impact direction parallel to the specimen center line.

Tables III and VIII contains the center and off-center drop-weight impact test data of the 1/10-scale model aluminum tank car bareheads. For the same impact speed of 4.18 mph these data indicate an impact puncture in the vertical off-center impact tests (A-B-VI) and (A-B-V2), an impact dent in the perpendicular off-center impact tests (A-B-P1) and (A-B-P2), and also an impact dent in the center impact test (2-50). It can be seen from these data that the worst impact condition is developed in the vertical off-center impact tests. The impact puncture in these two off-center impact positions was initiated at the edge of the model coupler and caused by shearing stress. However, an examination of the test specimens revealed that the worst impact case was developed in the impact test (A-B-V2) where the impact energy was dissipated in a shearing process more than a deformation process. Also, it can be noticed from these impact data in the center impact tests (6-2) and (3-71) that there is a difference in the depth of dent as well as the maximum impact force between these two models, even though the impact speeds and test results are the same. These two impact tests were conducted at similar impact conditions but different ambient temperatures.

The data in Table IX were also obtained from the center and off-center drop-weight impact tests when the 1/10-scale model aluminum tank car heads were covered by either high-alloy steel head shields, or steel face plate-aluminum honeycomb materials and backed up by uncompacted dry sand. From the data and careful examination of the impacted test specimens, it can be seen that the puncture resistance at impact points farther from the specimen center was generally higher than that at the center. These results are opposite to those obtained from the off-center barehead vertical impact tests. These differences are caused in part by the presence of the head shields or the mitigating materials. These protective devices blunt the leading edge of the impact coupler and spread the impact forces to a larger surface area. Further impact-force reduction will be created during the side sliding motion of the model coupler, which is caused by the tangential impact force component at the specimen surface.

Table X shows the data of the center and off-center drop-weight impact tests for the 1/5-scale model high-alloy steel tank car heads where uncompacted dry sand was used as a backup material. Since the test results of the 1/10-scale off-center drop-weight impact tests revealed that the minimum puncture resistance was recorded when the impact direction was parallel to the centerline of the model tank car bareheads, this test setting was selected to be used in the 1/5-scale off-center drop-weight impact tests. It can be seen from the data in Table X that the puncture resistance of the 1/5-scale model high-alloy steel tank car bareheads was maximum at the specimen center. Also, by careful examination of the impacted test specimens when high-alloy steel head shields or steel face plate-aluminum honeycomb materials were used as protective devices, it was noticed that a close agreement between the test results and the previous test results with the 1/10-scale models exists.

Besides the 1/10- and 1/5-scale center and off-center drop-weight impact tests, a series of horizontal impact tests was performed on 1/5-scale model high-alloy steel tank car bareheads where water was used as a backup material. The pendulum impact-weight height was adjusted for the horizontal impact tests at the centerline and two scaled off-centerline impact positions. The data

TABLE VIII. 1/10-SCALE DROP-WEIGHT IMPACT TEST DATA FOR MODEL ALUMINUM TANK CAR BAREHEADS WITH CENTER AND OFF-CENTER IMPACTS

MODEL-TEST NO.	TEST* CONDITION	DROP WEIGHT (LBS)	DROP HEIGHT (IN)	IMPACT SPEED		KINETIC ENERGY (FT-LBS)	MAX. DECEL. (G's)	MAX. IMPACT FORCE (LBS)	IMPACT RESULT	DEPTH OF DENT (IN)
				FT/SEC	MPH					
1-4	A-B-C	263	8	6.55	4.47	175	12.27	3,227	TP*	1.69
2-5	A-B-C	263	9	6.95	4.74	197	13.49	3,548	PUNCTURE	1.56
3-71	A-B-C	263	12	8.02	5.47	263	12.14	3,193	PUNCTURE	2.10
4-68	A-B-P1	263	7	6.13	4.18	153	6.50	1,710	DENT	1.69
5-69	A-B-P1	263	9	6.95	4.74	197	7.24	1,904	DENT	2.06
6-70	A-B-P1	263	12	8.02	5.47	263	8.22	2,162	PUNCTURE	2.35
7-73	A-B-P2	263	7	6.13	4.18	153	5.89	1,549	DENT	1.69
8-74	A-B-P2	263	10	7.33	5.00	219	7.36	1,936	DENT	2.06
9-75	A-B-P2	263	12	8.02	5.47	263	8.22	2,162	TP*	2.25
10-72	A-B-V1	263	7	6.13	4.18	153	6.87	1,807	PUNCTURE	1.81
11-89	A-B-V2	263	7	6.13	4.18	153	6.21	1,633	PUNCTURE	1.69

NOTE: UNCOMPACTED DRY SAND WAS USED IN ALL 1/10-SCALE DROP-WEIGHT IMPACT TESTS AS A BACK-UP MATERIAL FOR THE TANK CAR HEADS

*A : ALUMINUM MATERIAL
B : BAREHEAD
C : CENTER IMPACT
TP: THRESHOLD PUNCTURE

P1, P2: THE IMPACT DIRECTION IS PERPENDICULAR TO THE SPECIMEN SURFACE AT SCALED IMPACT POSITIONS OF 31" and 21" ABOVE THE SILL RESPECTIVELY

V1, V2: THE IMPACT DIRECTION IS PARALLEL TO THE SPECIMEN CENTERLINE AT SCALED IMPACT POSITIONS OF 31" AND 21" ABOVE THE SILL RESPECTIVELY

TABLE IX. 1/10-SCALE DROP-WEIGHT IMPACT TEST DATA FOR PROTECTED MODEL ALUMINUM TANK CAR HEADS WITH HEAD SHIELDS AND FACE PLATE-HONEYCOMB MATERIAL IN CENTER AND OFF-CENTER IMPACTS

MODEL-TEST NO.	TEST* CONDITION	DROP WEIGHT (LBS)	DROP HEIGHT (IN)	IMPACT SPEED		KINETIC ENERGY (FT - LBS)	MAX. DECEL. (G's)	MAX. IMPACT FORCE (LBS)	IMPACT RESULT	DEPTH OF DENT (IN)
				FT/SEC	MPH					
1-32	A-F-HC-C	263	40	14.65	9.99	877	39.25	10,323	DENT	2.25
2-97	A-F-HC-C	263	41.5	14.92	10.17	910	41.65	10,954	TP*	2.50
3-39	A-F-HC-C	263	43	15.19	10.36	942	41.21	10,838	PUNCTURE	2.313
4-33	A-F-HC-C	263	46	15.71	10.71	1,008	36.80	9,678	PUNCTURE	2.375
5-96	A-F-HC-V1	263	40	14.65	9.99	877	33.12	8,711	DENT	2.38
6-98	A-F-HC-V2	263	41.5	14.92	10.17	910	29.93	7,872	DENT	3.00
1-14	A-HS-C	263	32	13.10	8.93	701	40.72	10,709	DENT	2.00
2-19	A-HS-C	263	40	14.65	9.99	876	46.61	12,258	DENT	2.25
3-13	A-HS-C	263	46	15.71	10.71	1,008	50.05	13,163	TP*	2.438
4-99	A-HS-C	263	49	16.22	11.06	1,074	44.65	11,743	PUNCTURE	3.00
5-15	A-HS-C	263	52	16.71	11.39	1,140	51.52	13,550	PUNCTURE	2.438
6-16	A-HS-C	263	62	18.24	12.44	1,359	53.48	14,065	PUNCTURE	2.500
7-77	A-HS-P1	263	46	15.71	10.71	1,008	45.39	11,935	TP*	3.19
8-100	A-HS-V1	263	49	16.22	11.06	1,074	44.65	11,743	DENT	2.69
9-101	A-HS-V2	263	49	16.22	11.06	1,074	38.27	10,065	DENT	3.19

NOTE: UNCOMPACTED DRY SAND WAS USED IN ALL 1/10-SCALE DROP-WEIGHT IMPACT TESTS AS A BACK-UP MATERIAL FOR THE TANK CAR HEADS

*A : ALUMINUM MATERIAL
C : CENTER IMPACT
HC: HONEYCOMB
HS: HEAD SHIELD
TP: THRESHOLD PUNCTURE
F: FACE PLATE

P1: THE IMPACT DIRECTION IS PERPENDICULAR TO THE SPECIMEN SURFACE AT SCALED IMPACT POSITION OF 31" ABOVE THE SILL
V1, V2: THE IMPACT DIRECTION IS PARALLEL TO THE SPECIMEN CENTERLINE AT SCALED IMPACT POSITIONS OF 31" AND 21" ABOVE THE SILL

TABLE X, 1/5-SCALE DROP-WEIGHT IMPACT TEST DATA FOR HIGH-ALLOY STEEL MODEL TANK CAR HEADS

MODEL-TEST NO.	TEST* CONDITION	DROP WEIGHT (LBS)	DROP HEIGHT (IN)	IMPACT SPEED		KINETIC ENERGY (FT - LBS)	MAX. DECEL. (G's)	MAX. IMPACT FORCE (LBS)	IMPACT RESULT	DEPTH OF DENT (IN)
				FT/SEC	MPH					
1-102	S-B	2,102	38	14.28	9.74	6,656	22.08	46,412	DENT	4.69
2-103	S-B1	2,102	38	14.28	9.74	6,656	16.68	35,061	PUNCTURE	5.13
3-109	S-B2	2,102	35	13.71	9.35	6,135	15.95	33,527	PUNCTURE	4.44
1-104	S-HS	2,102	72	19.66	13.40	12,616	40.48	85,089	DENT	5.06
2-105	S-HS	2,102	80	20.72	14.13	14,013	42.93	90,239	DENT	5.00
3-106	S-HS1	2,102	80	20.72	14.13	14,013	34.35	72,204	DENT	5.53
4-107	S-HS1	2,102	90	21.98	14.99	15,769	32.38	68,063	DENT	5.31
5-110	S-HS1	2,102	92	22.22	15.15	16,116	39.25	82,504	DENT	5.44
1-108	S-HC-F	2,102	73	19.79	13.49	12,783	31.40	66,003	PUNCTURE	4.75
2-111	S-HC1-F	2,102	92	22.22	15.15	16,116	38.27	80,444	DENT	4.88

NOTE: UNCOMPACTED DRY SAND WAS USED IN ALL 1/5-SCALE DROP-WEIGHT IMPACT TESTS AS A BACK-UP MATERIAL FOR THE TANK CAR HEADS

*S : HIGH-ALLOY STEEL
B : BAREHEAD (CENTER IMPACT)
HS: HEAD SHIELD (CENTER IMPACT)
HC: HONEYCOMB (CENTER IMPACT)
F: FACE PLATE

B1, B2: BAREHEAD WITH IMPACT DIRECTION PARALLEL TO THE SPECIMEN CENTERLINE AT SCALED IMPACT POSITIONS OF 31" AND 21" ABOVE THE SILL RESPECTIVELY

HS1, HC1: THE IMPACT DIRECTION IS PARALLEL TO THE SPECIMEN CENTERLINE AT SCALED IMPACT POSITION OF 31" ABOVE THE SILL. THE PROTECTIVE DEVICES ARE HEAD SHIELD AND FACE-PLATE HONEYCOMB MATERIAL RESPECTIVELY.

TABLE XI. 1/5-SCALE HORIZONTAL IMPACT TEST DATA WITH HIGH-ALLOY STEEL BAREHEADS

MODEL-TEST NO.	TEST* CONDITION	DROP WEIGHT (LBS)	DROP HEIGHT (IN)	IMPACT SPEED		KINETIC ENERGY (FT- LBS)	MAXIMUM DECEL. (G's)	MAX. IMPACT FORCE (LBS)	IMPACT RESULT	DEPTH OF DENT (IN)
				FT/SEC	MPH					
1-88	S-B	2,102	90	21.98	14.99	16,470	13.25	29,084	DENT	6.5
2-83	S-B1	2,102	63	18.39	12.54	11,529	10.30	22,608	DENT	5.06
3-84	S-B1	2,102	70	19.38	13.21	12,804	13.00	28,535	DENT	5.38
4-86	S-B1	2,102	80	20.72	14.13	14,640	12.02	26,384	DENT	5.00
5-85	S-B1	2,102	93	22.34	15.23	17,019	11.53	25,308	PUNCTURE	6.12
6-87	S-B2	2,102	90	21.98	14.99	16,470	16.19	35,537	TP*	5.31

NOTE: THE SCALE MODEL TANK CAR WAS FILLED WITH WATER to 90 PERCENT OF ITS VOLUME

*S : HIGH-ALLOY STEEL
B : BAREHEAD, CENTER IMPACT
TP: THRESHOLD PUNCTURE

B1, B2: BAREHEAD WITH SCALED IMPACT POSITIONS AT 31" AND 21" ABOVE THE SILL RESPECTIVELY

obtained from this series of tests are tabulated in Table XI. It can be noticed from the data in Tables X and XI where the 1/5-scale model high-alloy steel tank car heads were used in drop-weight and pendulum impact tests respectively, that there are relatively big differences in the impact speeds and maximum impact forces at similar impact situations such as puncture and threshold puncture. The same situation can be observed in the drop-weight and the pendulum impact tests where model aluminum tank car heads were used as test specimens.

In the drop-weight impact tests the impact energy was dissipated by the test specimen and the backup material. A solid platform supported by solid ground was used to support the head holder and the test specimen. In this case the movement of the platform in the vertical direction under the impact forces was negligible. On the other hand in the horizontal impact tests, the impact energy was dissipated by the test specimen, the backup material, and the displacement of the model railroad tank car. In this case, the movement of the tank car in the horizontal direction under the impact forces was large and was against the front wheel brakes of the tank car.

From Table XI and carefull examination of the impacted test specimens, it can be seen that the puncture resistance of the 1/5-scale model high-alloy steel tank car bareheads in horizontal impact tests was maximum at the specimen center and reduced at the impact points farther from the center.

It may be concluded that the off-center impacts on the scale model aluminum and high-alloy steel tank car bareheads are more likely to cause puncture than the center impacts. However, the presence of the head protection devices in the off-center impact tests will blunt the leading edge of the model coupler as well as help deflect and reduce the concentration of the impact forces at the specimen surface. This will increase the required impact energy for the threshold puncture over the energy required in the center impact.

3.7 FINITE ELEMENT SIMULATION

The ability to predict the large plastic deformation encountered during an impact process has improved in recent years. The calculation of the response of any damage to a shell such as a tank car head from a localized impact is within the capability of a number of finite element computer programs. The ADINA program is well suited for such analyses. Therefore, it has been used to simulate the experimental situation to complement the test results. The work was divided into two phases, validation and prediction. The use of ADINA to predict the response of the model aluminum and high-alloy steel tank car heads under a static load at the centerline was validated first. The dynamic response was then obtained and analyzed for the prediction of the puncture resistance of the tank car heads.

3.7.1 Finite Element Model

The finite element work was performed to simulate the structure response of the 1/10-scale model aluminum and high-alloy steel tank car heads under center impact. The scale-model tank car heads in the static and dynamic tests were considered as axisymmetric structures. The impacting coupler creates a

dent which, although not perfectly axisymmetric, could be approximated axisymmetrically. Since both the loading and the geometry are axisymmetric, the two dimensional (2D) axisymmetric element was chosen. Various meshes ranging from 2 by 12 to 5 by 24 have been tested for convergence and compared with static experimental results for solution accuracy. A final choice of 2 by 12 variable mesh with very small elements under and near the impact region was made (Figure 21). This model gave reasonably good results while maintaining solution efficiency, especially in dynamic analyses.

In addition to the 2D elements, two truss elements and one gap element were used to simulate the impacting coupler and to connect the coupler and the tank head during impact. The two truss elements were linear while the gap element was actually a nonlinear truss element. This gap element was specified such that it transmitted an impact load when in a compressed configuration. Furthermore, in order to evenly distribute the load over a small region around the apex with a 0.4 inch diameter, displacement constraints were applied to the first two elements from the apex. The constraints were such that the downward deflections of the nodes located on the upper surface had the same values. The displacement boundary conditions were also applied at the lower edge of the model to simulate the clamped bottom ring.

In the dynamic response calculation, the impacting coupler was given an initial velocity while positioned at 0.1 inch above the apex of the tank car head. The proper time step size used in the analysis was chosen to be 0.25 to 0.5 millisecond.

The Von Mise yield criteria was used for the failure prediction. The effective stresses at integration points in element 21, located at about 1 inch from the apex, were averaged and compared with the ultimate stress of the material investigated. The model was considered to be punctured at the instant when the average effective stress reached a value higher than the ultimate stress. It should be pointed out that one might think that any location between element 22 and 24 was equally good for failure prediction. However, given this particular model, the stress distribution in element 22 to 24 was disturbed due to the application of displacement constraints. Therefore, element 21 was the most suitable element to use for the failure prediction purpose.

3.7.2 High-alloy Steel Tank Car Head

In the stainless steel tank head finite model, the numerical values used for the material properties, yield stress, ultimate stress, and strain hardening modulus are listed as follows:

Youngs Modulus	$E = 2.8 \times 10^7$ psi
Poissons Ratio	$\nu = 0.3$
Density	$\rho = 0.000777$ lb-sec^2/in^4
Yield Stress	$\sigma_y = 7.4 \times 10^4$ psi

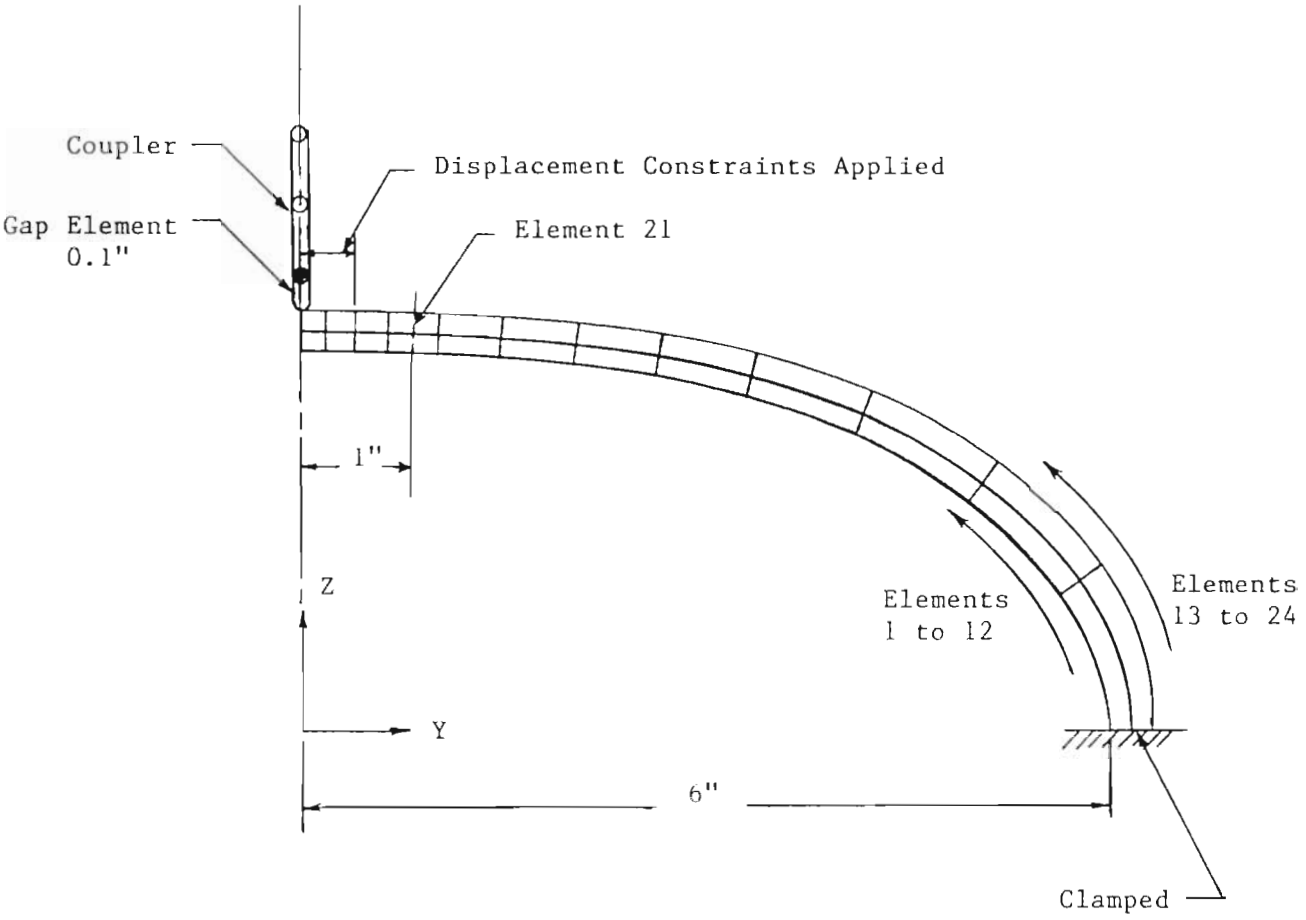

Figure 21. Finite Element Mesh for the 1/10-Scale Model Tank Car Head.

Ultimate Stress $\sigma_u = 9.44 \times 10^4$ psi

Strain Hardening Modulus $E_T = 3.6 \times 10^5$ psi

Maximum dent time histories corresponding to various initial impacting velocities are plotted in Figure 22 and the corresponding data are tabulated in Table XII. Effective stress (σ_e) in element 21 was checked at each time-step to determine if the test specimen was punctured. For the two cases where the initial velocity (V_o) is equal to 12.0 or 14.0 ft/sec, the effective stress was determined at the end of the impact at 88K and 90K psi, respectively. The comparison between these results and the ultimate stress (u) of the tank car head material indicated that with these initial velocities the impact results would be only a dent. However, for the case with V_o = 16.0 ft/sec the effective stress reached 95.7K psi at the time (t) $\doteq$ 19 msec. This stress value exceeded the ultimate stress of the material which indicated a puncture case. The experiment result showed that the threshold puncture velocity was around 15.97 ft/sec, which was in good agreement with the finite element prediction. It is concluded, therefore, that this finite element model can be used for the prediction of the puncture resistance of tank car heads. However, no full scale tests were used to verify these results and the model may require modification.

3.7.3 Aluminum Tank Car Head

The same finite element procedure as described in the previous section was repeated for the aluminum tank car head finite element model. The following parameters were used in this procedure:

$E = 1.02 \times 10^7$ psi

$\nu = 0.3$

$\rho = 0.00026$ lb-sec^2/in^4

$\sigma_y = 1.9 \times 10^4$ psi

$\sigma_u = 2.3 \times 10^4$ psi

$E_T = 9.0 \times 10^4$

Maximum dent time histories corresponding to various initial impacting velocities are plotted in Figure 23 and the corresponding data are tabulated in Table XIII. The result in the first case with an initial velocity of 6 ft/sec indicated a dent at the apex of the model with maximum effective stress of 22K psi. However, the results of the remaining two cases with initial velocities of 7 and 8 ft/sec indicated penetration with effective stresses exceeded the ultimate stress of the model material. The impact test results of the 1/10-scale model aluminum tank car bareheads indicated a threshold puncture at impact velocity of 6.55 ft/sec. Therefore, the finite element prediction is in good agreement with impact test results.

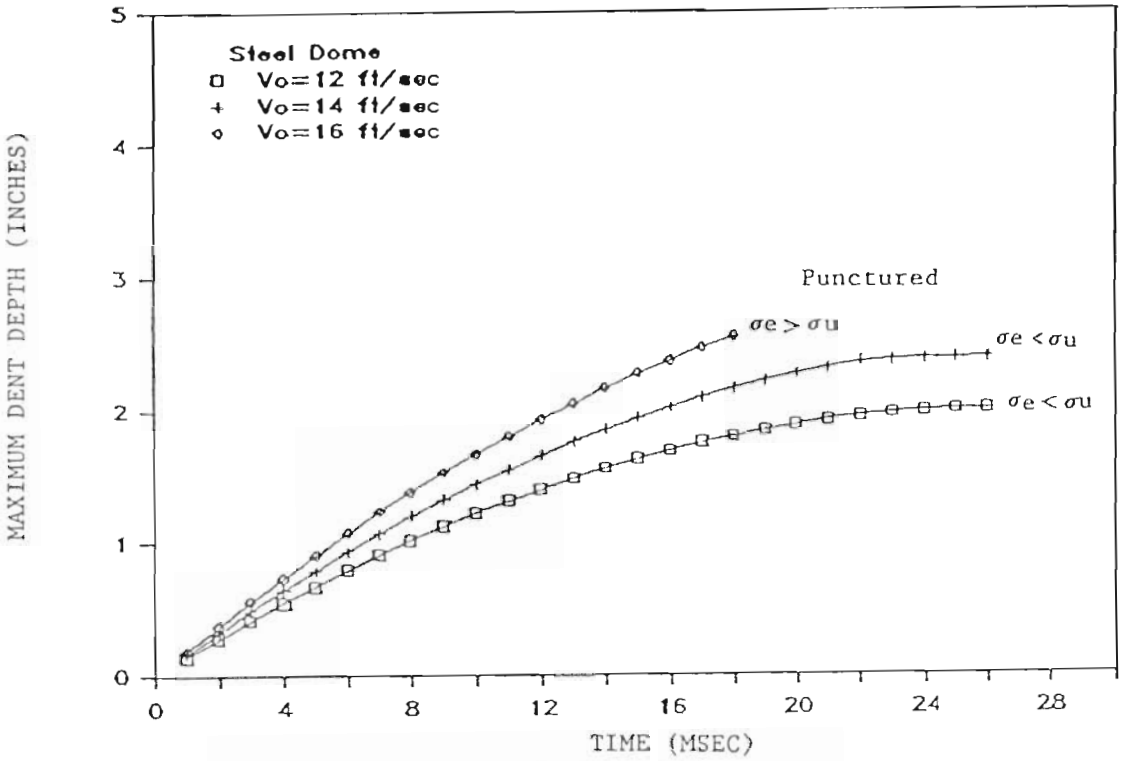

Figure 22. Maximum Depth Of Dent At Apex Under Different Impact Velocities For Steel Tank Car Heads.

Table XII. Maximum Depth Of Dent Data For Steel Tank Car Head With Different Initial Velocities in Finite Element Model

TIME (MSEC)	MAXIMUM DEPTH OF DENT (IN)		
	at 12 ft/sec	at 14 ft/sec	at 16 ft/sec
1	0.1428	0.1667	0.1906
2	0.2816	0.329	0.3767
3	0.4158	0.4867	0.5578
4	0.545	0.6392	0.7333
5	0.6697	0.7859	0.9034
6	0.7893	0.9272	1.0677
7	0.9039	1.0627	1.2263
8	1.0132	1.1928	1.3787
9	1.117	1.3169	1.525
10	1.216	1.435	1.665
11	1.309	1.547	1.799
12	1.397	1.653	1.926
13	1.478	1.753	2.047
14	1.554	1.846	2.16
15	1.624	1.933	2.267
16	1.687	2.014	2.367
17	1.746	2.0878	2.46
18	1.798	2.1556	2.546
19	1.844	2.2128	2.624
20	1.884	2.264	
21	1.917	2.309	
22	1.945	2.351	
23	1.967	2.365	
24	1.983	2.377	
25	1.993	2.382	
26	1.996	2.384	

TABLE XIII - Maximum Depth of Dent Data For Aluminum Tank Car Head With Different Initial Velocities in Finite Element Model

TIME (MSEC)	MAXIMUM DEPTH OF DENT (IN)		
	at 6 ft/Sec	at 7 ft/Sec	at 8 ft/Sec
1	0.0718	0.08378	0.0958
2	0.1428	0.1665	0.19
3	0.2129	0.2479	0.2836
4	0.2819	0.328	0.3754
5	0.3499	0.4065	0.4657
6	0.4167	0.4837	0.5545
7	0.4824	0.5594	0.6418
8	0.5469	0.6337	0.727
9	0.61	0.7064	0.812
10	0.6723	0.7777	0.894
11	0.7332	0.8474	0.975
12	0.7928	0.9156	1.055
13	0.8511	0.9823	1.132
14	0.9082	1.047	1.208
15	0.9639	1.111	1.283
16	1.018	1.173	1.356
17	1.07	1.233	1.427
18	1.123	1.292	1.496
19	1.174	1.349	1.564
20	1.222	1.405	1.63
21	1.27	1.459	1.695
22	1.316	1.511	1.757
23	1.36	1.562	1.818
24	1.404	1.611	1.877
25	1.446	1.659	1.934
26	1.486	1.704	1.99
27	1.525	1.748	2.044
28	1.562	1.791	2.096
29	1.598	1.832	2.146
30	1.632	1.871	
31	1.665	1.908	
32	1.696	1.944	
33	1.726	1.978	
34	1.754	2.01	
35	1.781	2.04	
36	1.806	2.07	
37	1.83	2.1	
38	1.852	2.123	
39	1.87	2.147	
40	1.89	2.17	
41	1.91	2.19	
42	1.924		
43	1.938		
44	1.95		
45	1.96		
46	1.97		
47	1.98		
48	1.986		
49	1.99		

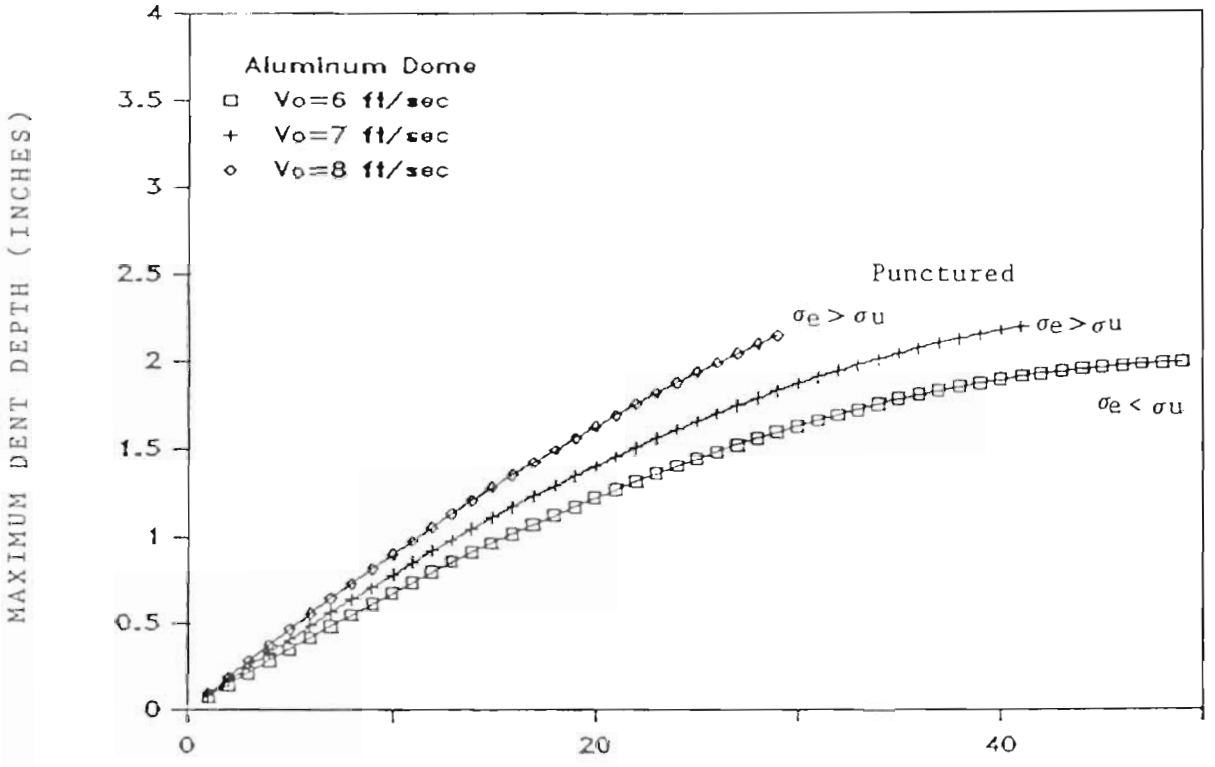

Figure 23. Maximum Depth Of Dent At Apex Under Different Impact Velocities For Aluminum Tank Car Heads.

4. CONCLUSIONS

1. All protective devices used in this test program increase the puncture resistance of the scale model aluminum and high-alloy steel tank car bareheads, the most increase was 500 percent.

2. The high-alloy steel head shield is a good protective device, it absorbs the impact energy, blunts the coupler edges, and spreads the impact forces to some extent over a larger surface area. However, during the impact duration, it bends and deforms to the coupler shape which increases the chances to develop a puncture to the specimen surface.

3. The combination of TRUSSGRID aluminum honeycomb layers and thin sheets of high-alloy steel face-plates improved the property of this mitigating material in absorbing the impact energy and spreading the impact forces to a larger surface area. Also, this material combination blunts the model coupler edges and forms a smooth surface against the specimen surface at the end of the impact duration. This material combination provides more protection to the scale model tank car heads than the protection provided by the steel head shield.

4. The combination of the Tescpak material and a thin sheet of high-alloy steel face-plate improved the performance of this mitigating material over the performance when it was used by itself with the 1/10- and 1/5-scale model high-alloy steel tank car heads in center drop-weight impact tests (Reference 5). However, this mitigating material ranked third in this test program for improving the puncture resistance of the model tank car heads after the aluminum honeycomb material and the high-alloy steel head shields.

5. The effect of low temperature on the model aluminum tank car heads, the high-alloy steel head shields, and the mitigating materials combined with steel face-plates was varied. It raised the threshold puncture energy of the model tank car heads and increased the protection performance of the high-alloy steel head shields and the face-plate aluminum honeycomb materials. On the other hand, it affected the Tecspak material so that it became brittle and smashed under the impact load without providing an effective protection to the model tank car heads.

6. The test results in this study show a difference of 3.0 percent in the threshold puncture velocities between the 1/10- and 1/5-scale model aluminum tank car bareheads. This difference is slightly higher than the theoretical 1.0 percent difference obtained from the non-dimensional analysis of the scaling laws adopted (Appendix D). However, this result can be considered a good agreement with the scaling laws in this case. The difference in the threshold puncture velocities between the two scale models in the other impact cases were calculated at 16.0 percent with high-alloy steel head shield and 21.0 percent with steel face plate-Tecspak material. These higher

difference percentages occurred because of the additional materials which were used as protective devices. On the other hand, the investigation of the case where steel face plate-aluminum honeycomb material was used as a protective device, showed no difference in the threshold puncture velocity between the two scale models. This may have happened because of the ability of the aluminum honeycomb to constantly absorb the impact energy during the crushing process under impact load up to 70 percent of its thickness.

7. The scale model aluminum tank car heads with empty model tank car are susceptible to deeper dents and less susceptible to impact punctures than the heads backed up with fluids; lading has the effect of increasing the scale-model tank car head vulnerability to impact puncture.

8. The off-center impacts on the scale models aluminum and high-alloy steel tank car bareheads are more likely to cause puncture than the center impacts. However, the presence of the head protection devices in the off-center impact tests will blunt the leading edge of the model coupler as well as help deflect and reduce the concentration of the impact forces at the specimen surface. This will increase the required impact energy for the threshold puncture over the energy required in the center impact.

9. The finite element model and procedure established in this work proves to be very indicative in the prediction of the puncture resistance of scale tank heads. The choice of the element for stress output for failure detection is critical for a meaningful and accurate interpretation of the finite element results. This model can be readily modified to include the effect of the backup material (fluid). For the analysis of the effectiveness of the mitigating material, however, more effort needs to be made, since it becomes a nonlinear contact problem.

5. REFERENCES

1. Peters, D. A., B. A. Szabo and W. B. Diboll, "Tank Car Head Puncture Mechanisms," Washington University, St. Louis, Missouri, FRA-OR&D-76-269, April, 1980.

2. Orringer, O. and P. Tong, "Results and Analysis of the Switchyard Impact Tests," DOT Transportation Systems Center, FRA-OR&D-80-6, January, 1980.

3. Phillips, E. and L. Olson, "Final Phase 05 Report on Tank Car Head Study," RPI-AAR Tank Car Safety Research Project, RA-05-1-17, July 14, 1972.

4. Shang, J. C. and J. E. Everett, "Impact Vulnerability of Tank Car Head," The Shock and Vibration Bulletin, No. 42, Part 1, Naval Research Laboratory, January, 1972, pp. 197-210.

5. Lishaa, M., J. Chen, J. C. S. Yang, and R. Kao, "Small Scale Impact Simulation Tests," Advanced Technology and Research, Inc., Report for Contract DOT/DTFR53-83-C-00290, December, 1984.

6. Gorman, J. J., "Applicability of Scale Model Testing to Rail Tank Car Head Impact Phenomena," Aeroelastic and Structures Research Laboratory, MIT, Interim Report for Contract DOT/TSC-1143, December, 1976.

7. Baker, W. E., et al., "Similarity Methods in Engineering Dynamics," Hyaden Book Co., Inc., Rochelle Park, New Jersey, 1971.

8. Langhaar, H. L., "Dimensional Analysis and Theory of Methods," John Wiley and Son, Inc., 1951.

9. Murphy, G., "Similitude in Engineering," Press Co., New York, 1950.

10. Goodier, J. N. and Thomson, W. T., "Applicability of Similarity Principles to Structural Models," NACA TN-933, July, 1944.

11. Haerta, M., "Analysis; Scale Modeling, and Full Scale Tests of a Truck Spent-Nuclear-Fuel Shipping System in High Velocity Impacts Against a Rigid Barrier," Report No. SAND77-0270, Sandia Laboratories, Albuquerque, New Mexico, April, 1978.

12. Monjoine, M. J., "Influence of Rate of Strain and Temperature on Yield Stresses of Mild Steel," Transaction of the ASME, Journal of Applied Mechanics, Vol. 66, December, 1944, pp. A-211 - A-218.

13. Baron, H. C., "Stress-Strain Curves of Some Metal and Alloys at Low Temperatures and High Rates of Strain," Journal of the Iron and Steel Institute, Vol. 182, April, 1956.

A P P E N D I X A

Graphs Relating the Dent-Depth Versus Kinetic Energy at Impact For Different Cases of the 1/10- and 1/5- Scale Drop-Weight Impact Tests

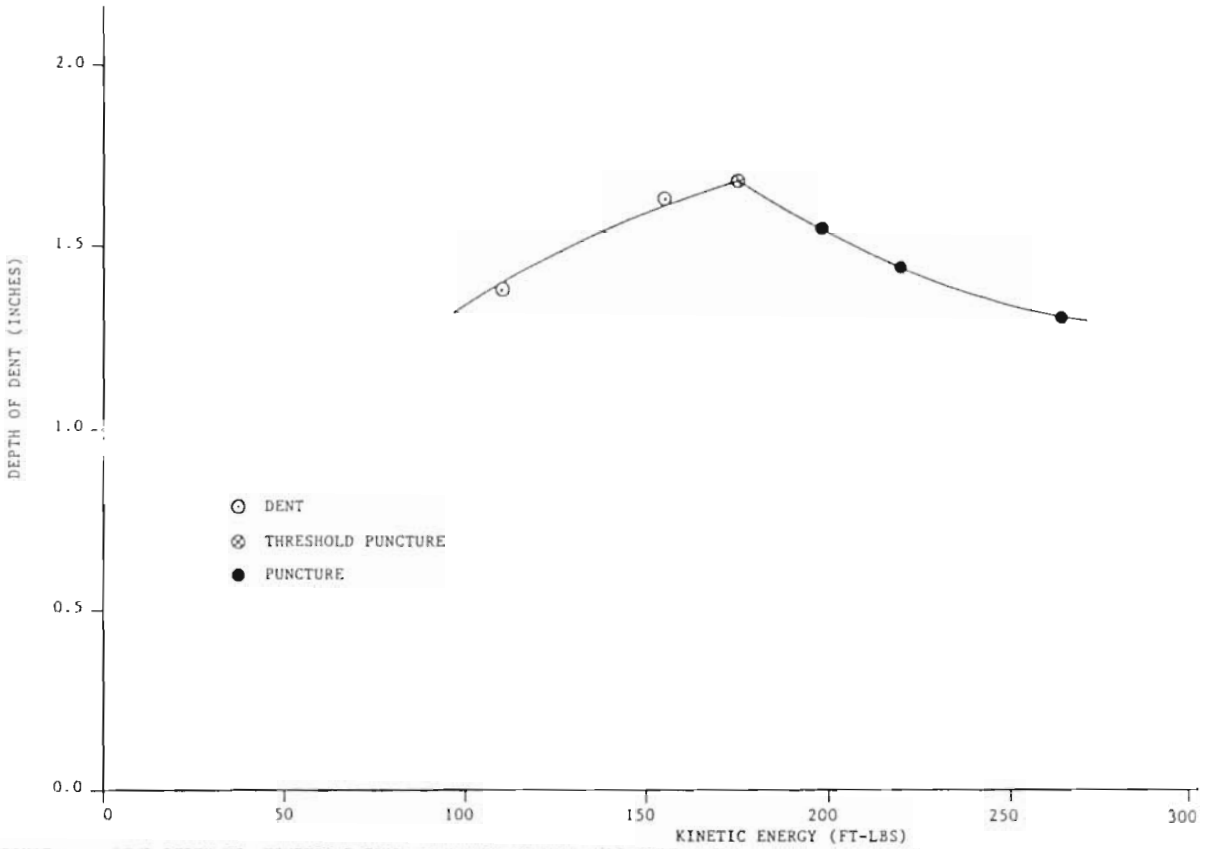

FIGURE A1. DENT DEPTH VS. KINETIC ENERGY AT IMPACT OF THE 1/10-SCALE MODEL ALUMINUM TANK CAR BAREHEADS IN DROP-WEIGHT IMPACT TESTS

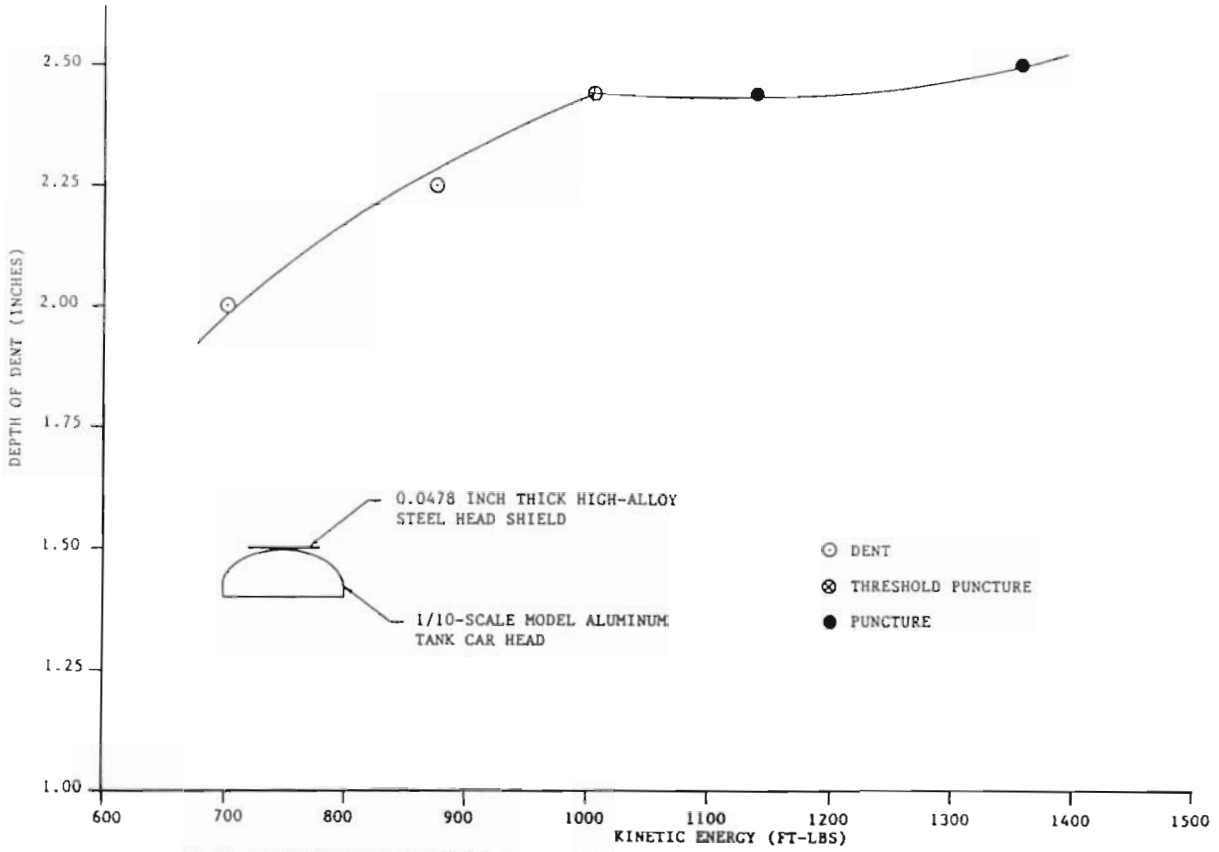

FIGURE A2. DENT DEPTH VS. KINETIC ENERGY AT IMPACT OF THE 1/10-SCALE MODEL ALUMINUM TANK CAR HEEADS WITH HIGH-ALLOY STEEL HEAD SHIELDS IN DROP-WEIGHT IMPACT TESTS

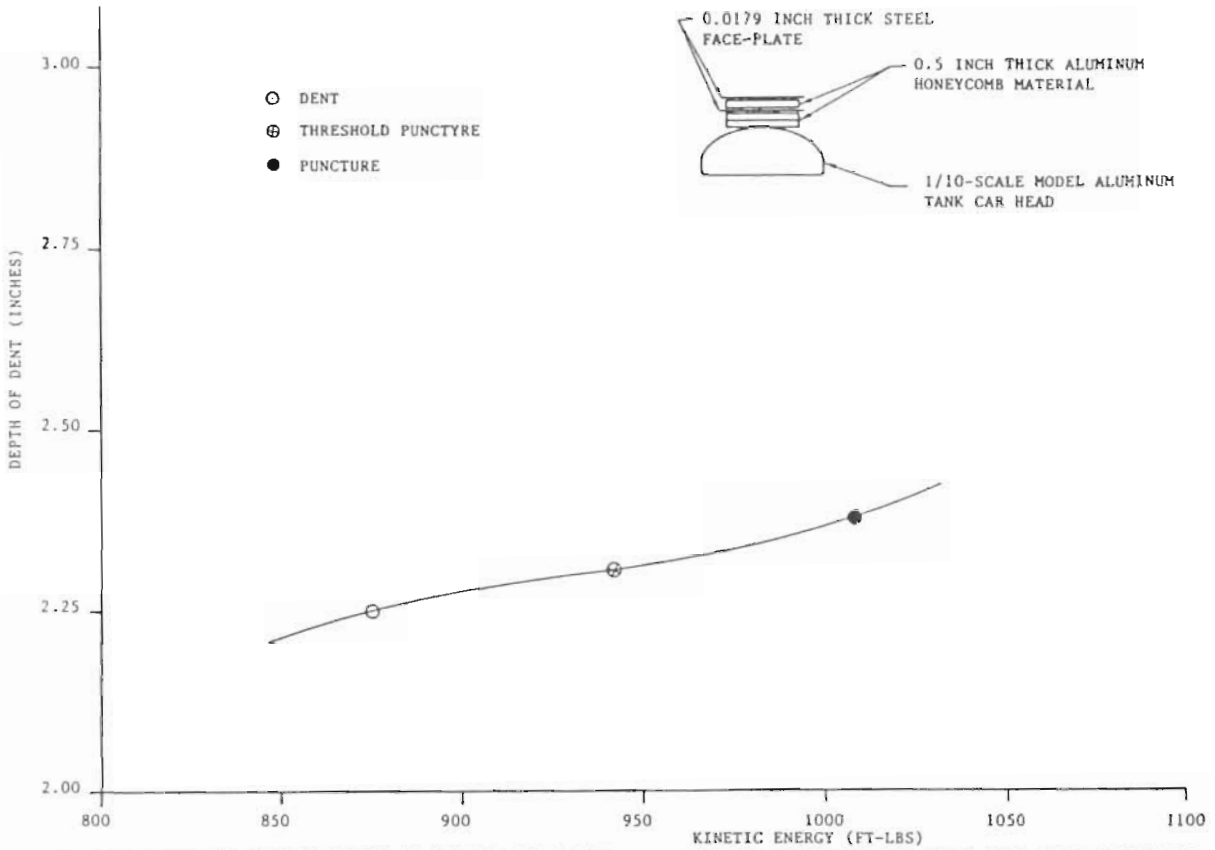

FIGURE A3. DENT DEPTH VS. KINETIC ENERGY AT IMPACT OF THE 1/10-SCALE MODEL ALUMINUM TANK CAR HEADS WITH STEEL FACE PLATE-ALUMINUM HONEYCOMB MATERIAL IN DROP-WEIGHT IMPACT TESTS

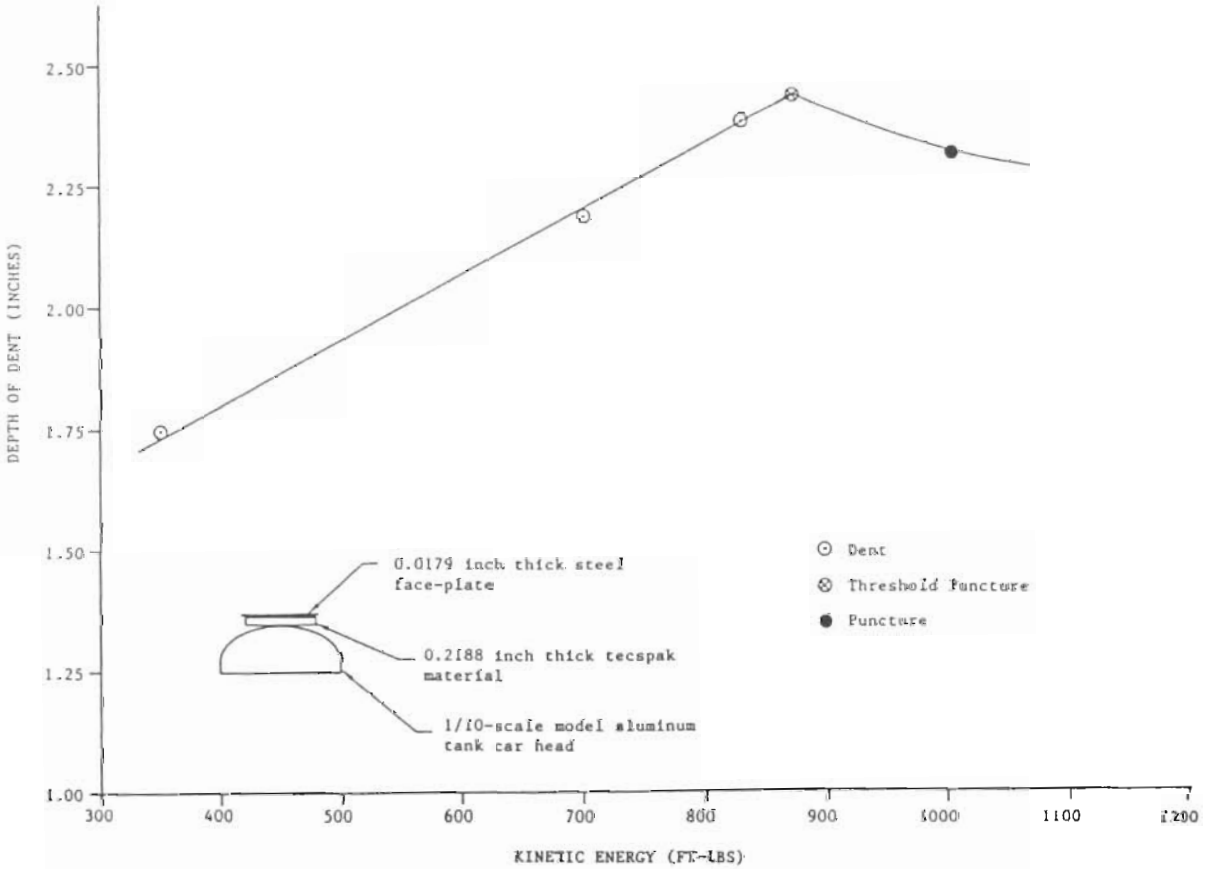

Figure A4. Dent depth vs. kinetic energy at impact of the 1/10-scale model aluminum tank car heads with steel face plate - Tecspak material in drop-weight impact tests.

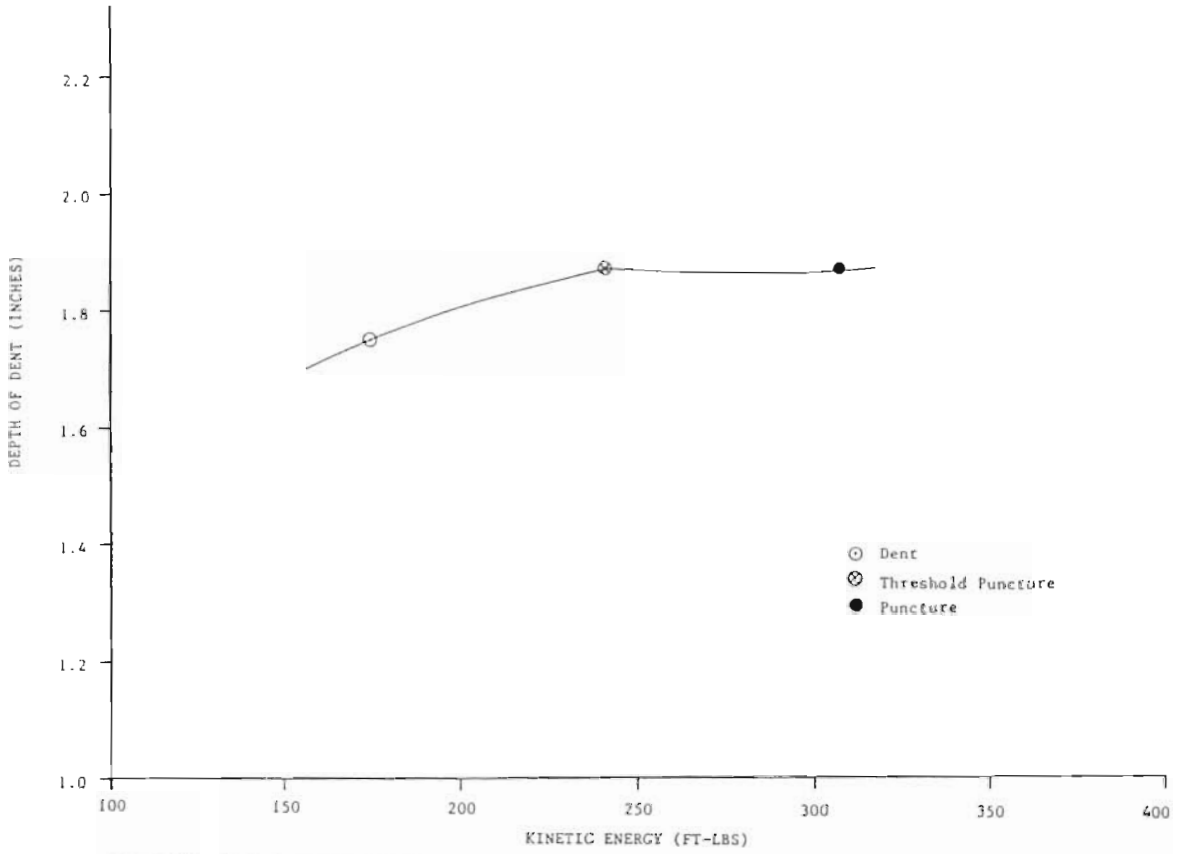

Figure A5. Dent depth vs. kinetic energy at impact of the 1/10-scale model aluminum tank car bareheads in drop-weight impact tests at low temperature.

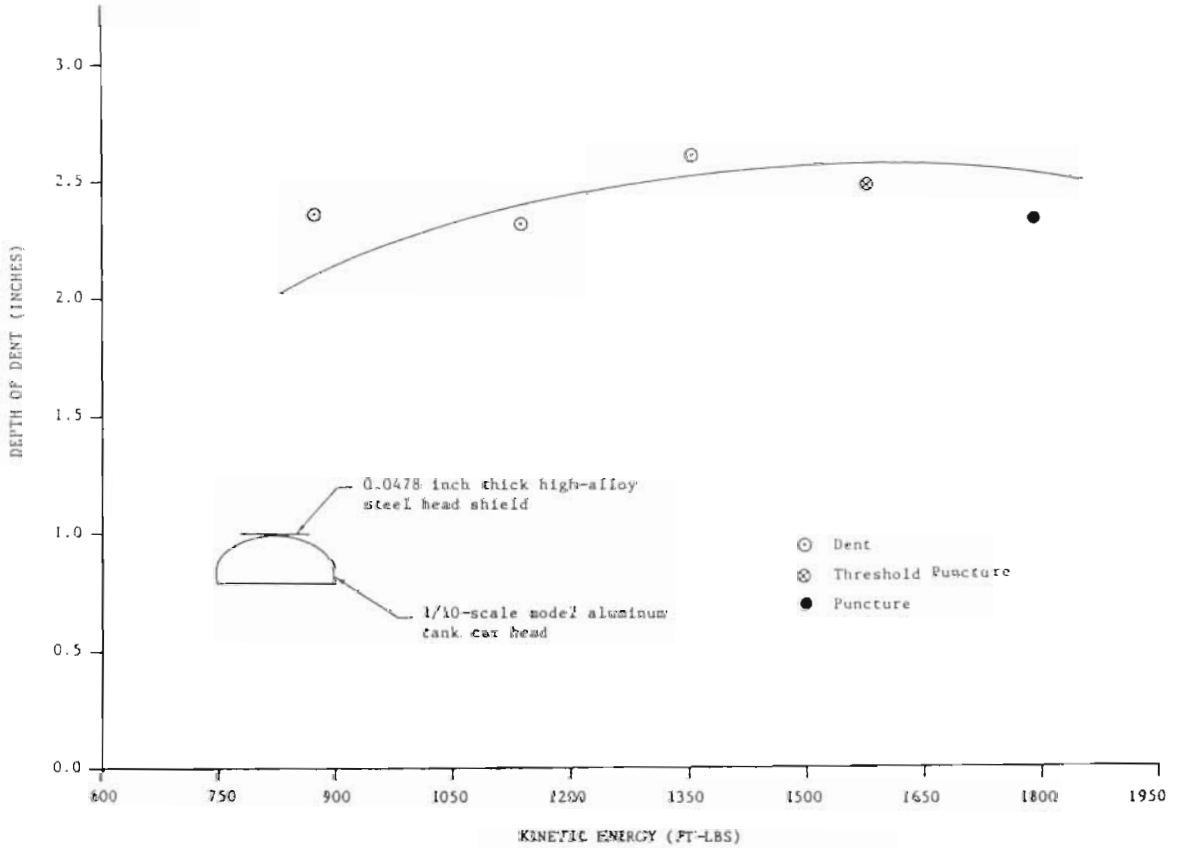

Figure A6. Dent depth vs. kinetic energy at impact of the 1/10-scale model aluminum tank car heads with high-alloy steel head shields at low temperature in drop-weight impact tests.

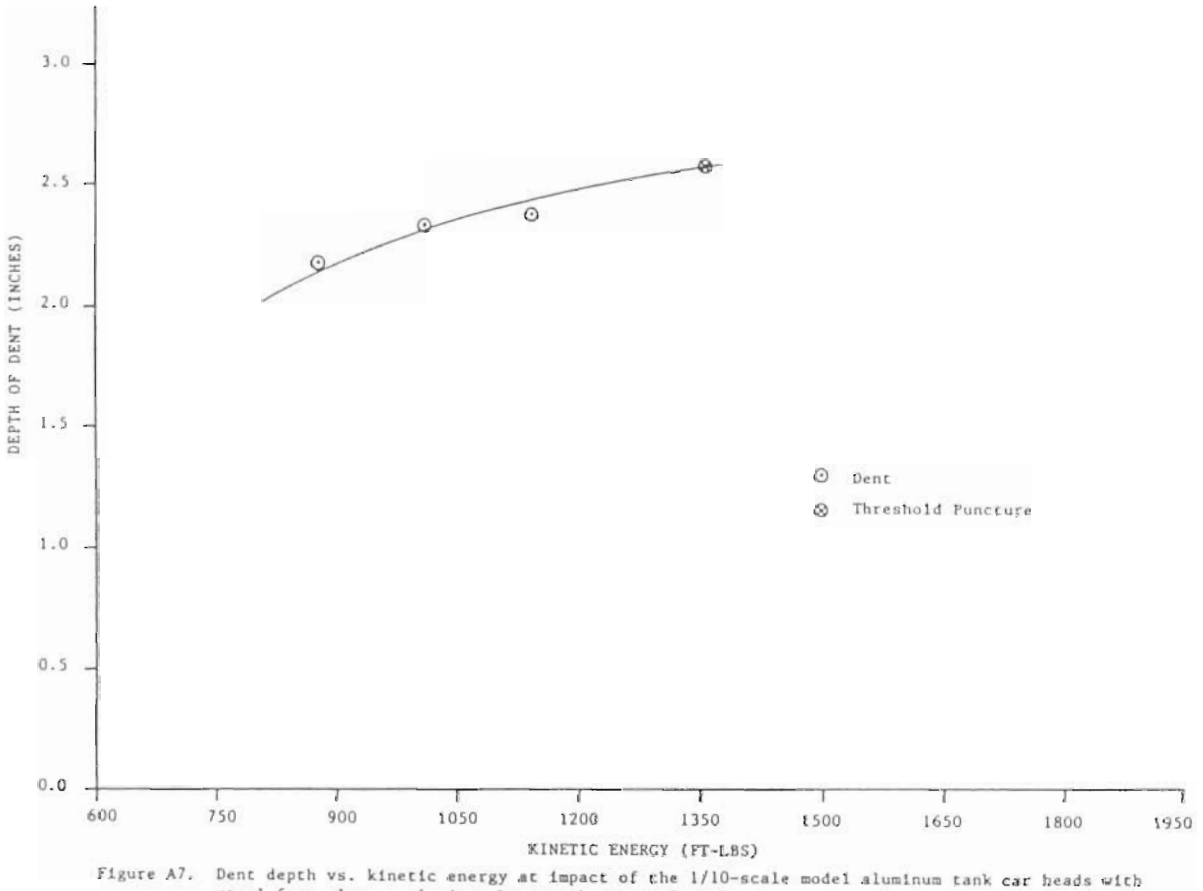

Figure A7. Dent depth vs. kinetic energy at impact of the 1/10-scale model aluminum tank car heads with steel face plate - aluminum honeycomb material at low temperature in drop-weight impact tests.

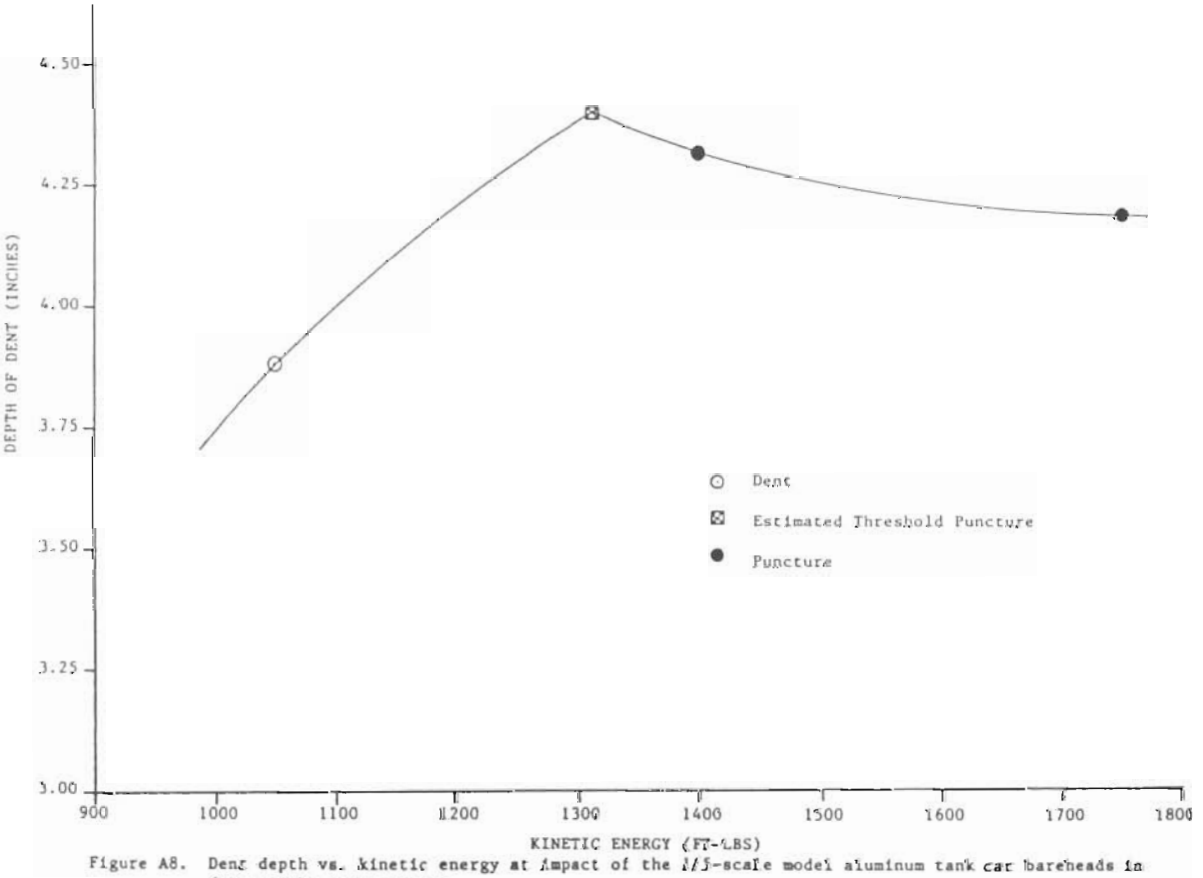

Figure A8. Dent depth vs. kinetic energy at impact of the 1/5-scale model aluminum tank car bareheads in drop-weight impact tests.

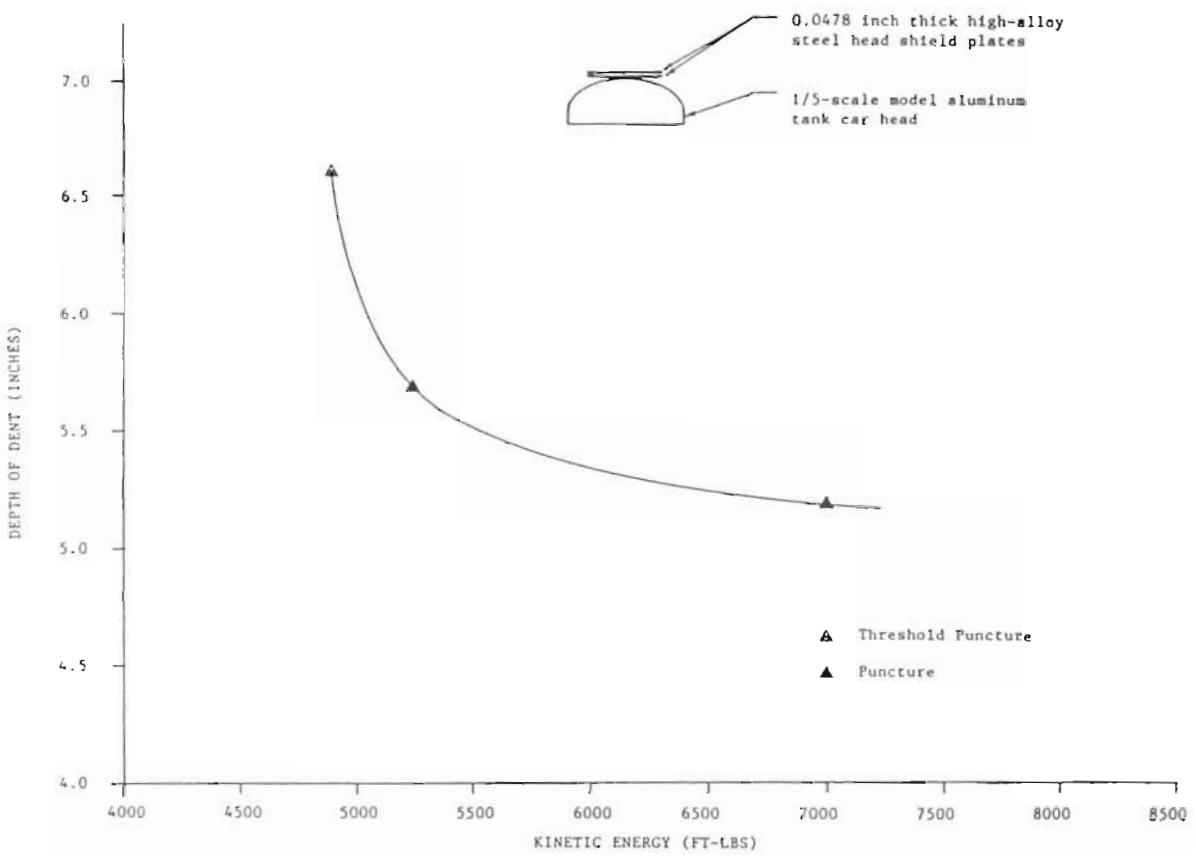

Figure A9. Dent depth vs. kinetic energy at impact of the 1/5-scale model aluminum tank car heads with double plate high-alloy steel head shield in drop-weight impact tests.

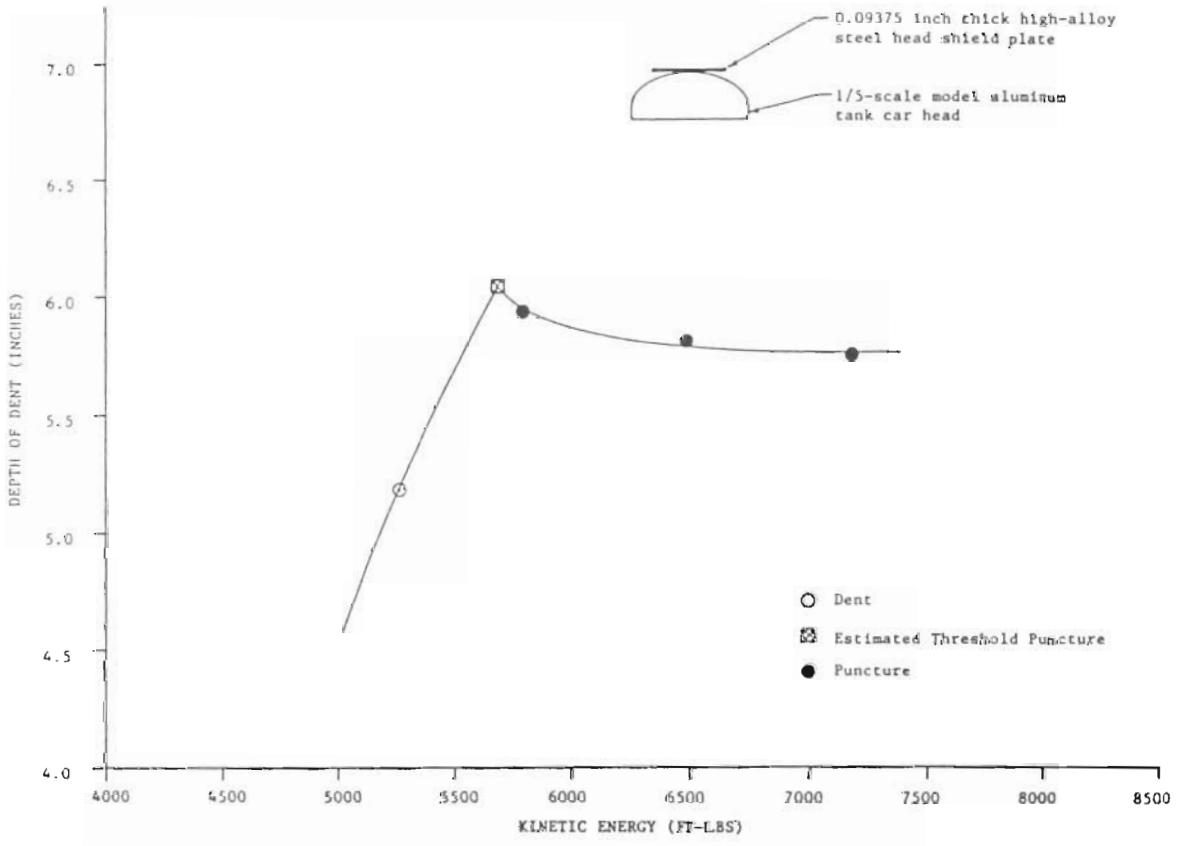

Figure A10. Dent depth vs. kinetic energy at impact of the 1/5-scale model aluminum tank car heads with single plate high-alloy steel head shield in drop-weight impact tests.

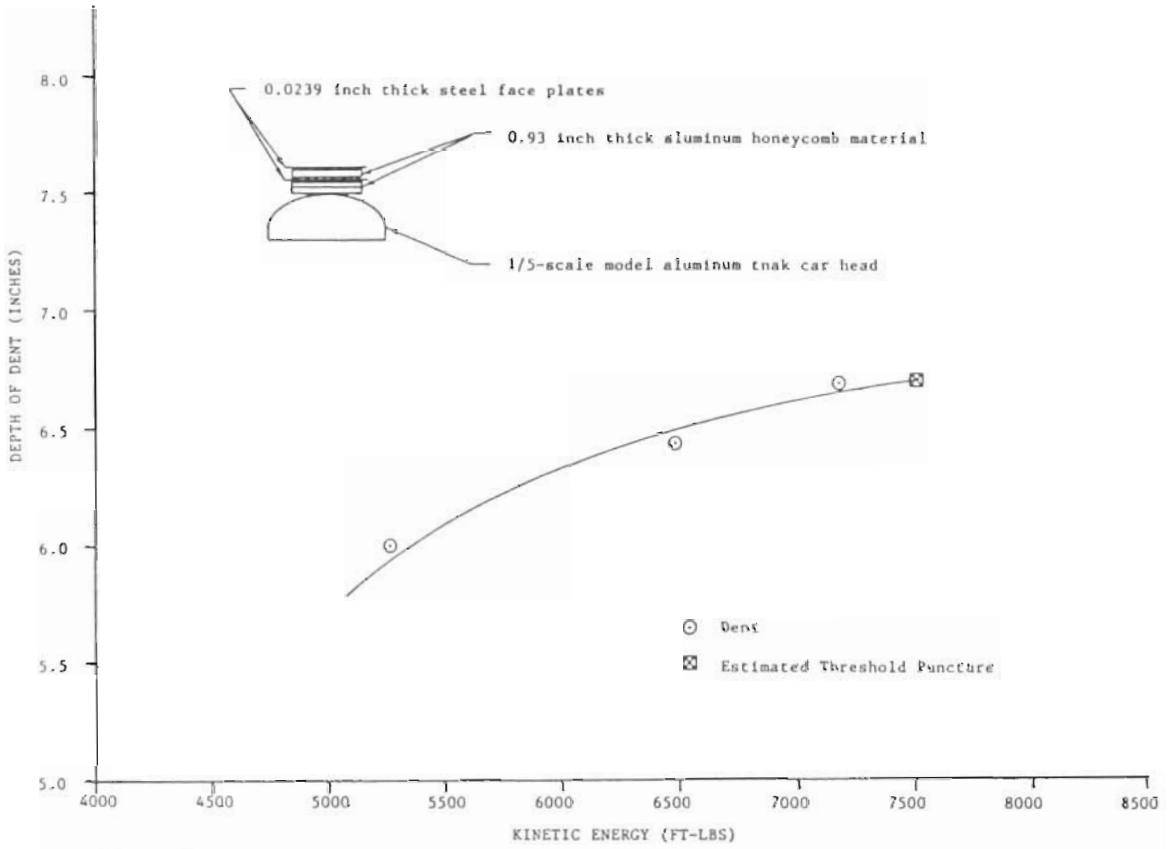

Figure A11. Dent depth vs. kinetic energy at impact of the 1/5-scale model aluminum tank car heads with steel face plate - aluminum honeycomb material in drop-weight impact tests.

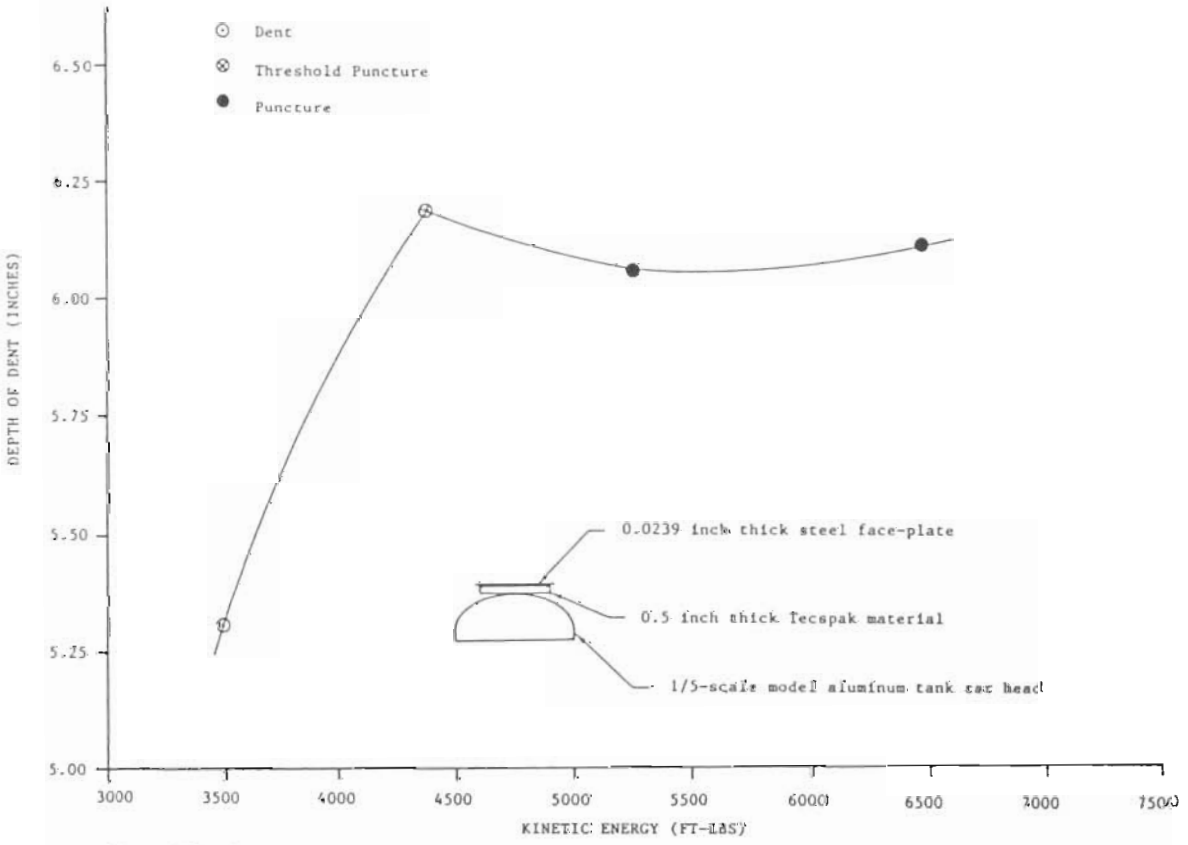

Figure A12. Dent depth vs. kinetic energy at impact of the 1/5-scale model aluminum tank car heads with steel face plate - Tecspak material in drop-weight impact tests.

A P P E N D I X B

Photographs of the 1/10- and 1/5-Scale Model Aluminum Impacted Tank Car Heads

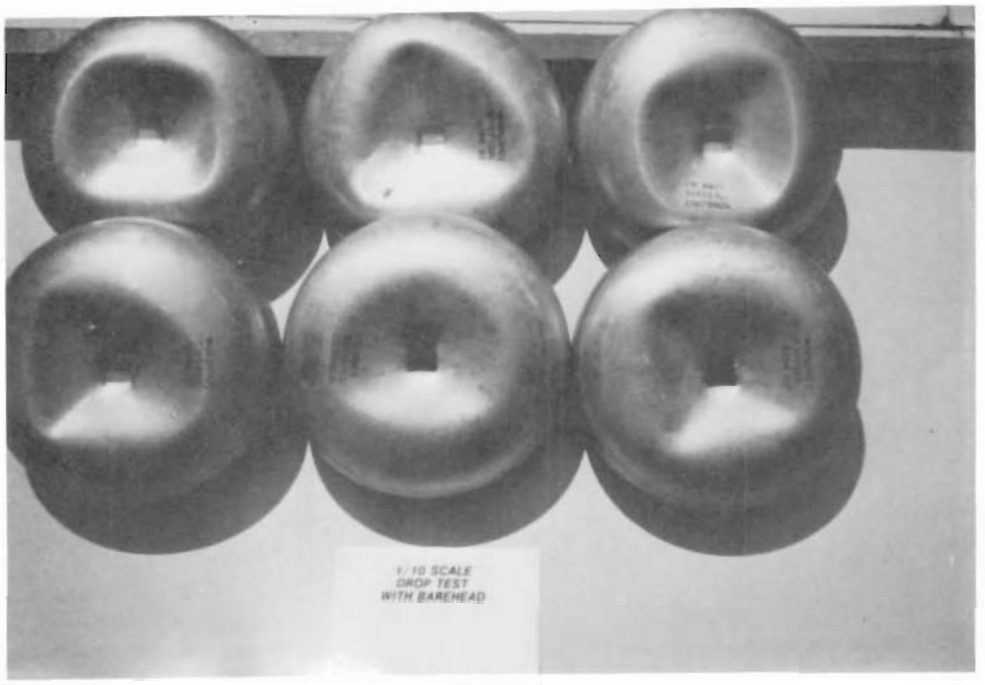

(a)

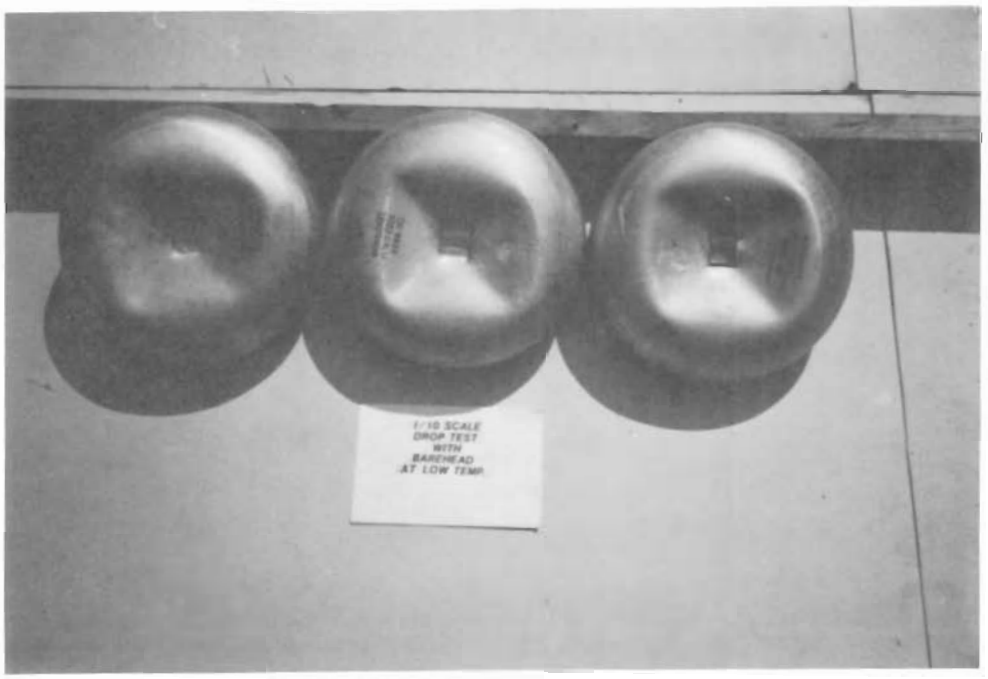

(b)

FIGURE B1. 1/10 - Scale Model Aluminum Tank Car Bareheads in Drop-Weight Impact Tests at (a) Room Temperature (b) Low Temperature

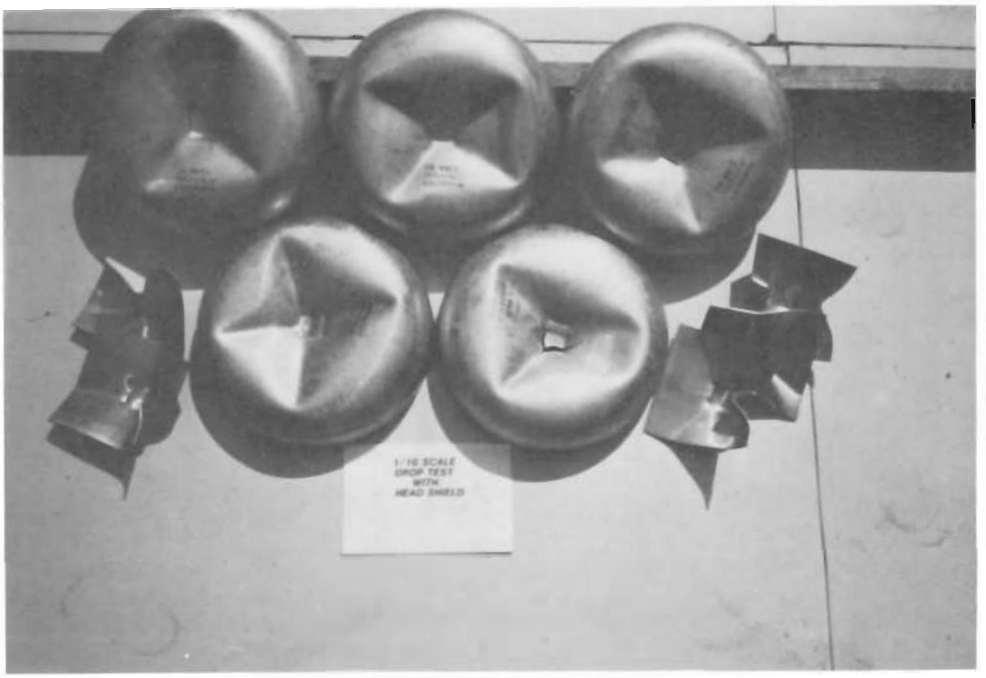

(a)

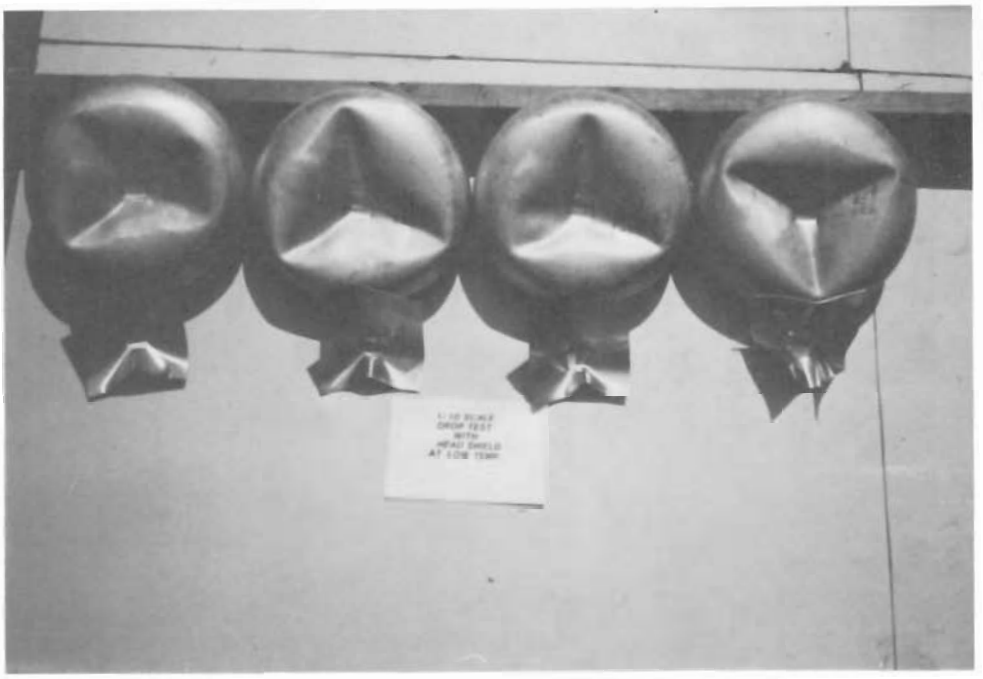

(b)

FIGURE B2. 1/10 - Scale Model Aluminum Tank Car Heads with Head Shields in Drop-Weight Impact Tests at (a) Room Temperature , (b) Low Temperature

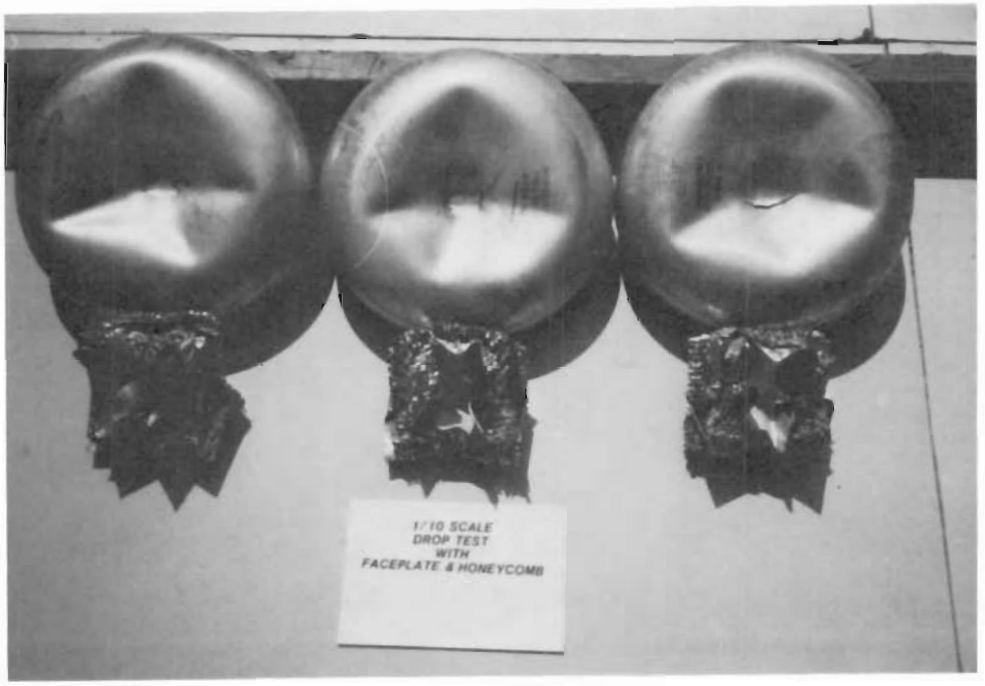

(a)

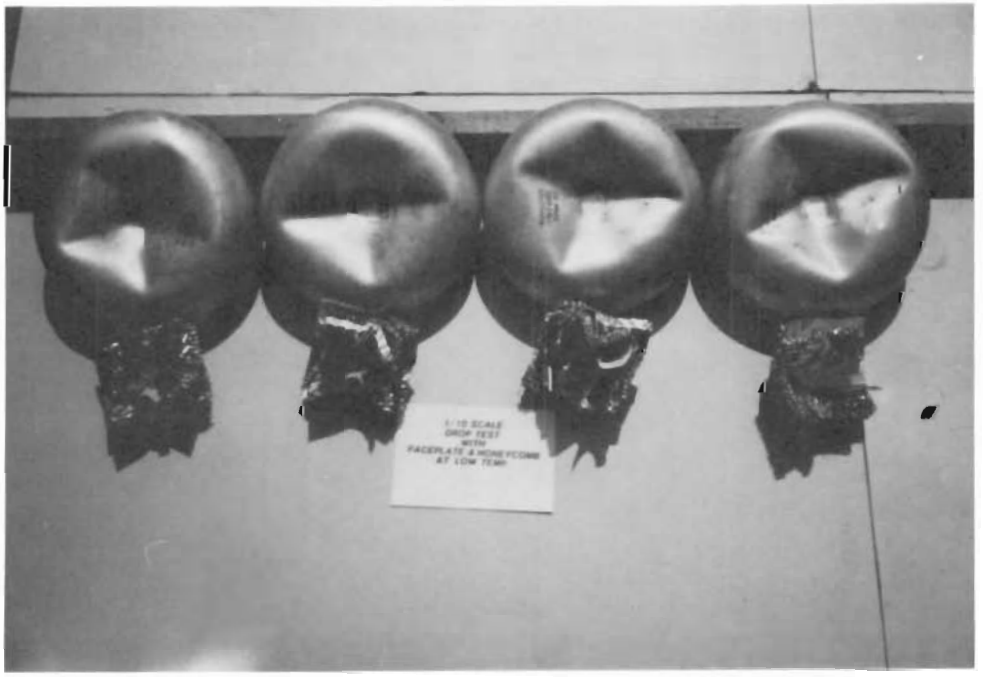

(b)

FIGURE B3. 1/10 - Scale Model Aluminum Tank Car Heads with Face Plate - Honeycomb Material in Drop-Weight Impact Tests at (a) Room Temperature, (b) Low Temperature

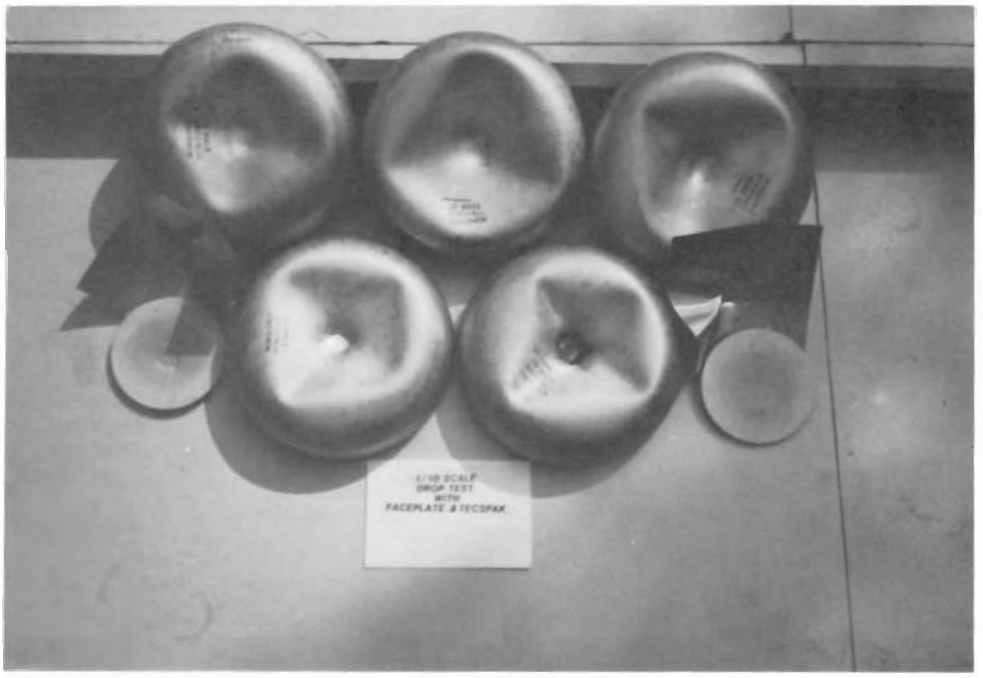

Figure B4. 1/10-Scale Model Aluminum Tank Car Heads with Faceplate and Tecspak Material in Drop-Weight Impact Tests

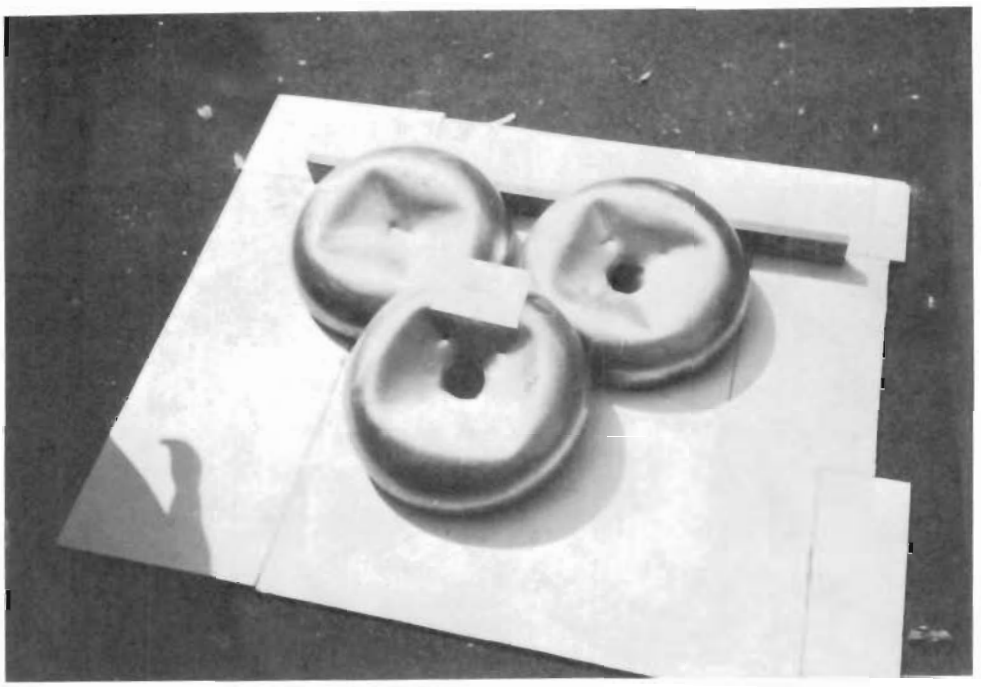

(a)

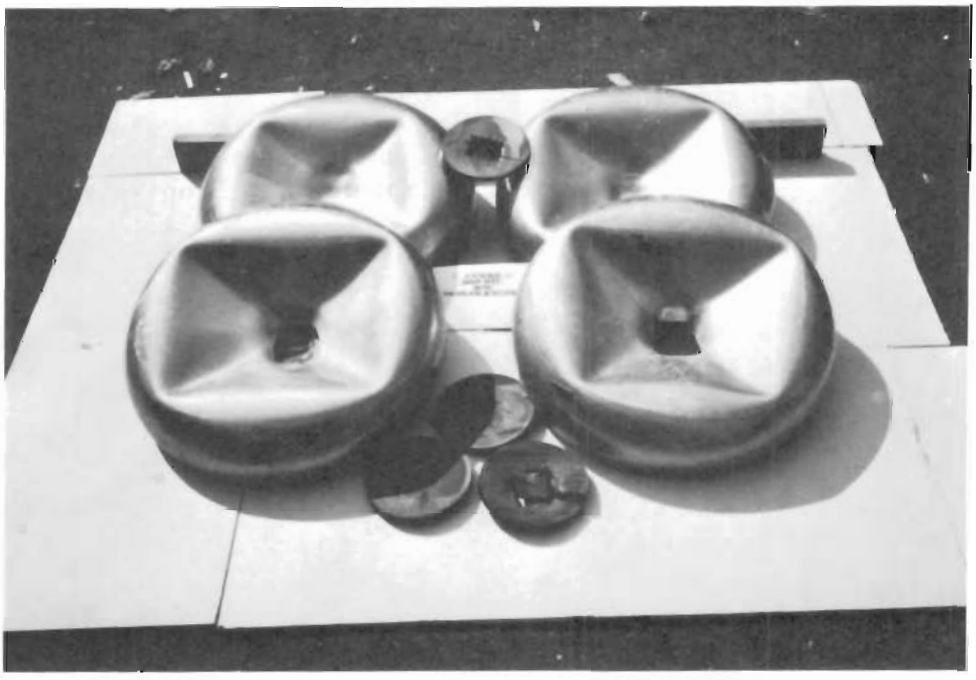

(b)

FIGURE B5. 1/5 - Scale Model Aluminum Tank Car Heads in Drop-Weight Impact Tests with (a) Bareheads (b) Steel Face Plate - Tecspak Material

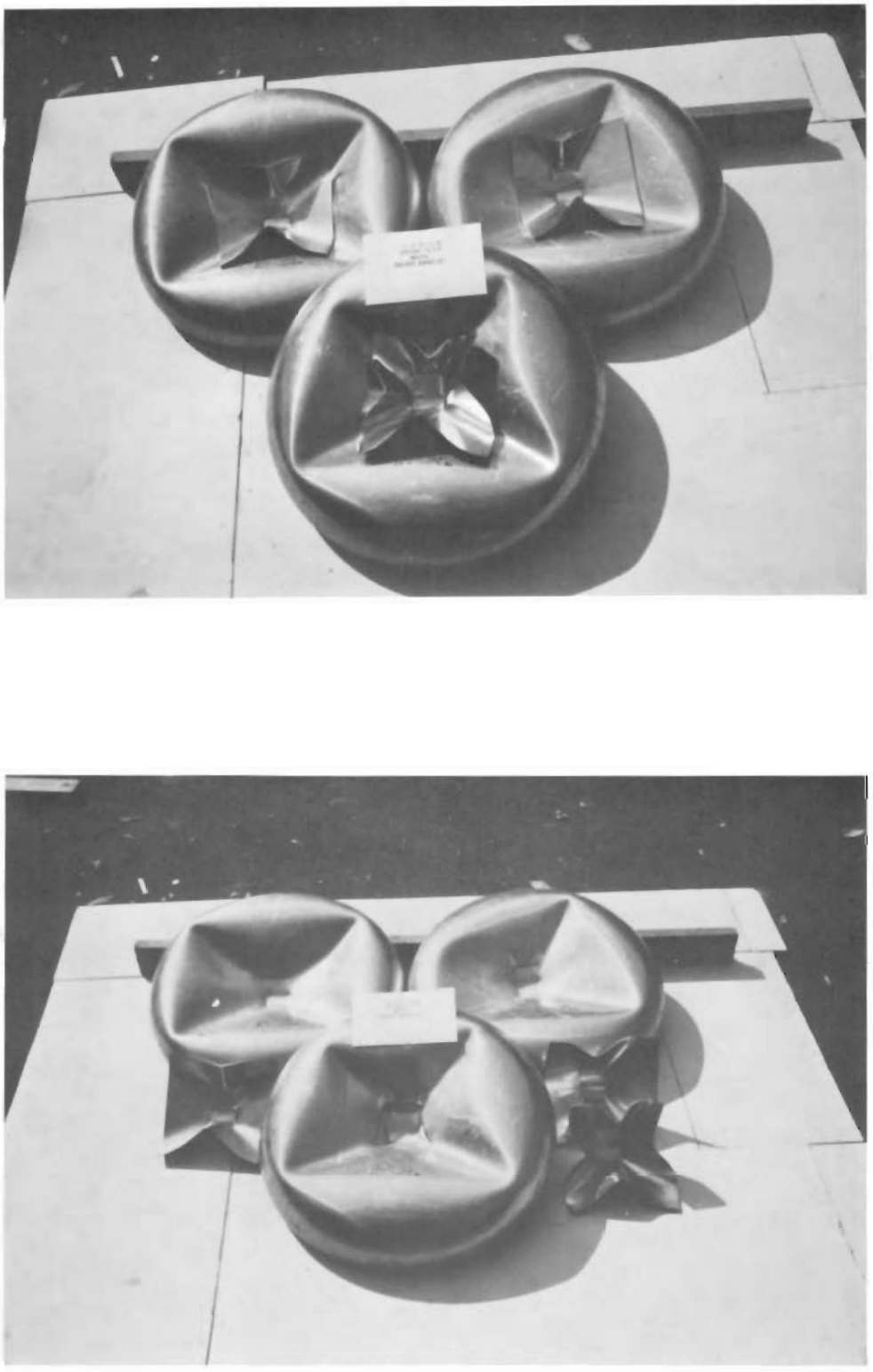

Figure B6. 1/5 scale model aluminum tank car heads with head shield in drop-weight impact tests.

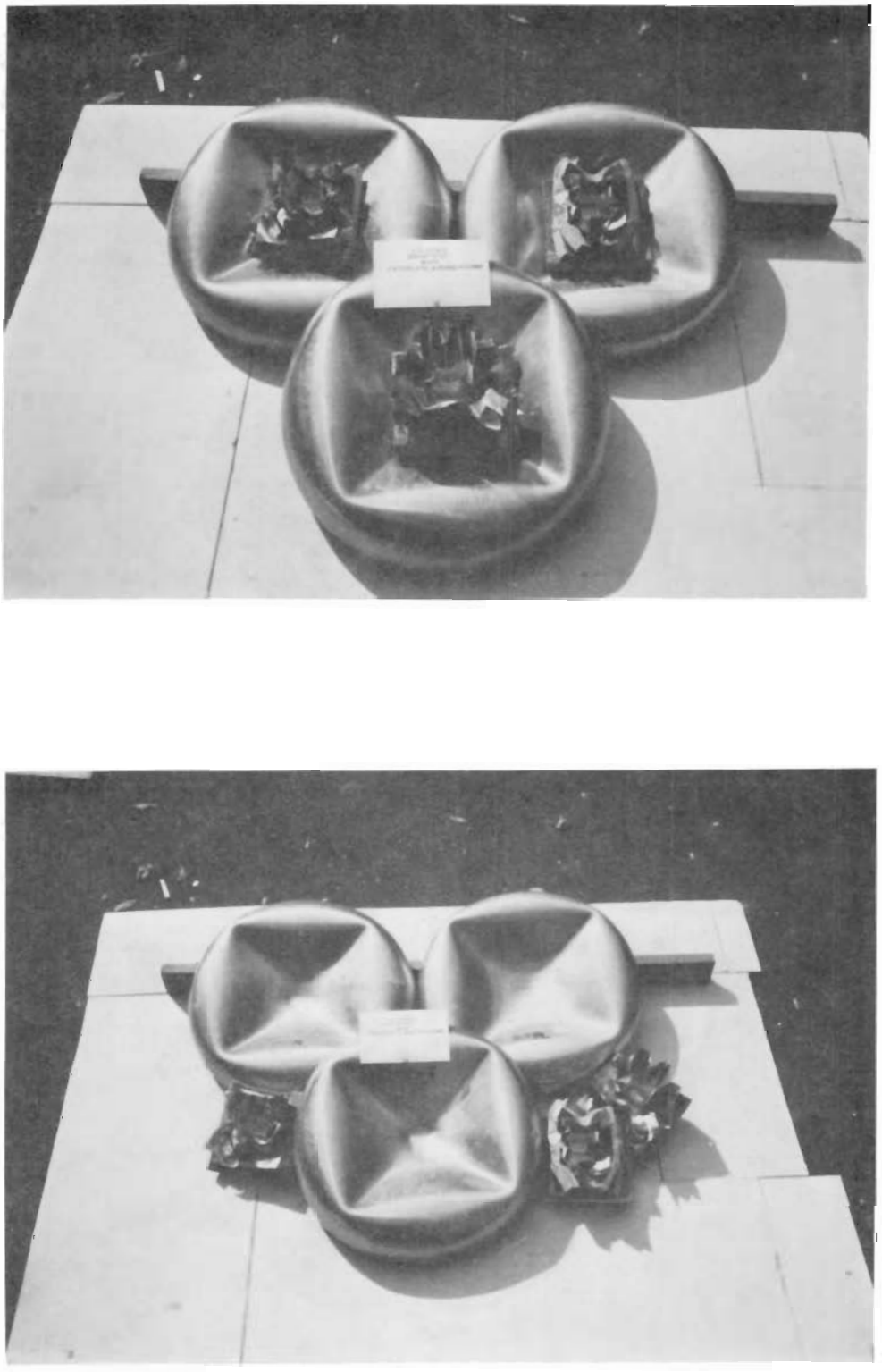

Figure B7. 1/5 scale model aluminum tank car heads with Faceplate and Honeycomb in drop-weight impact tests.

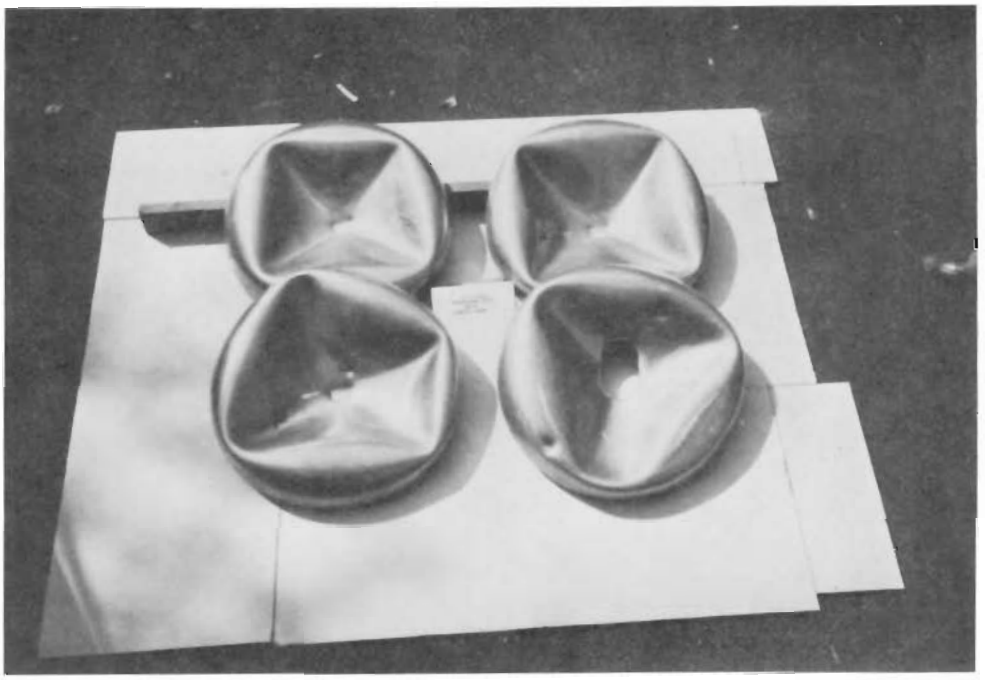

(a)

(b)

FIGURE B8. 1/5 - Scale Model Aluminum Tank Car Heads in Pendulum Impact Tests with (a) Empty Model Tank Car, (b) Model Tank Car Filled with Water

A P P E N D I X C

Deceleration Versus Time Curves for Selected Drop-Weight and Horizontal Impact Tests

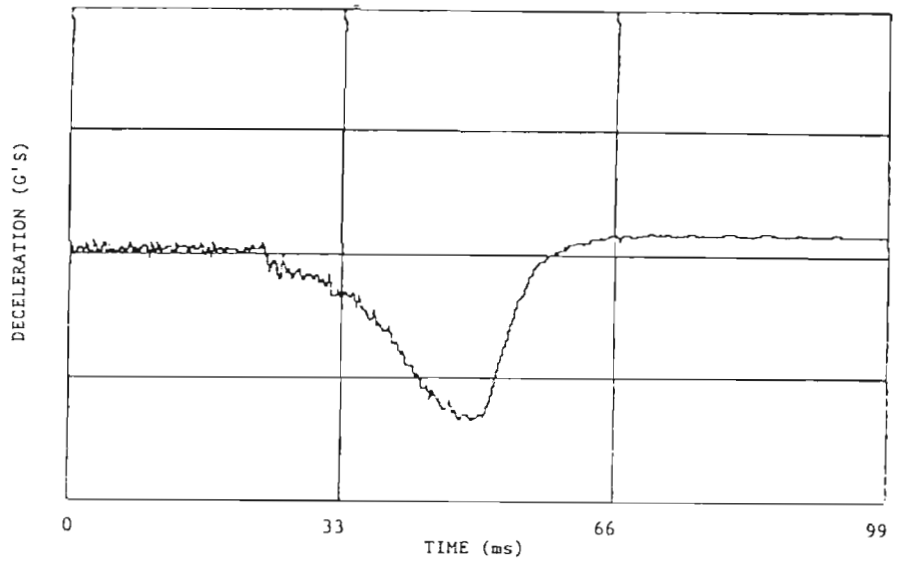

a. Impact Dent in Model (1-3)

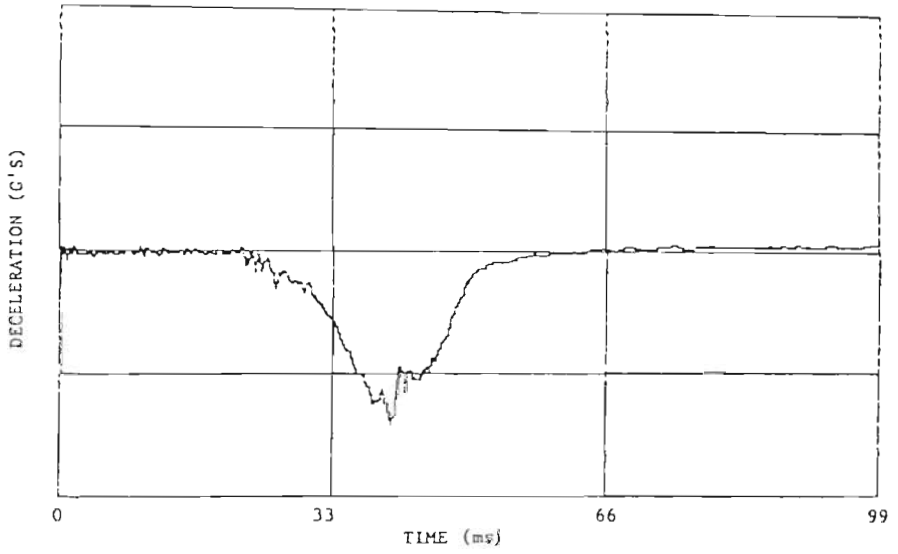

b. Impact Threshold Puncture in Model (4-17)

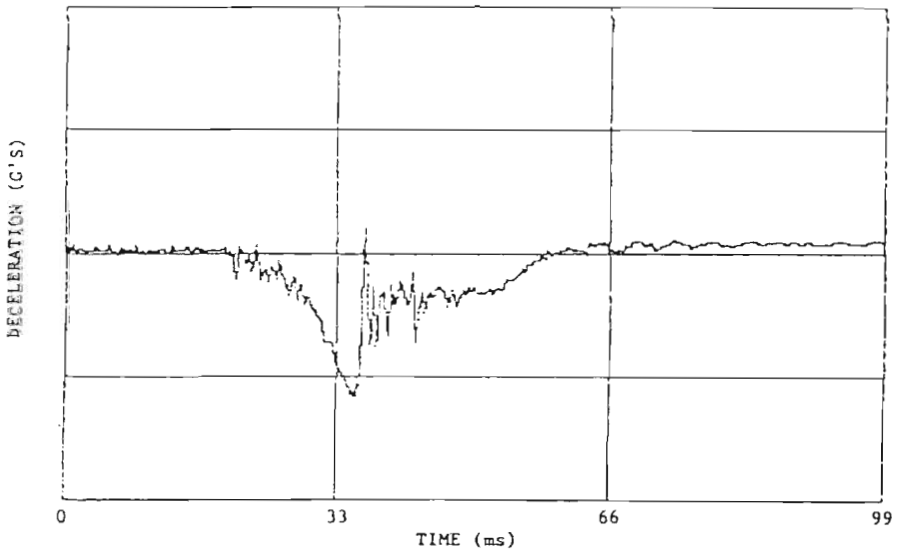

C. Impact Puncture in Model (5-12)

Figure C1. Deceleration versus Time Response in Drop-Weight Impact Tests for the 1/10-Scale Model Aluminum Tank Car Heads with Face Plate-Tecspak Material Protection

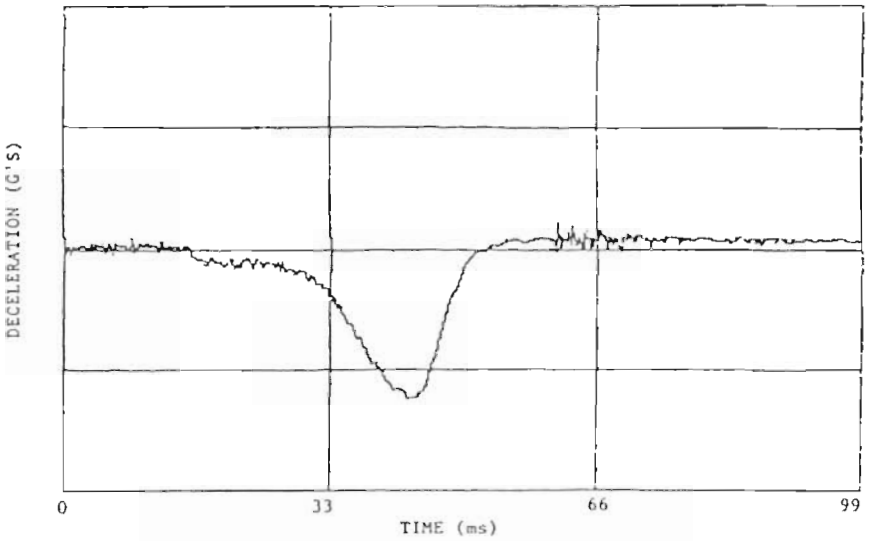

a. Impact Dent in Model (1-32)

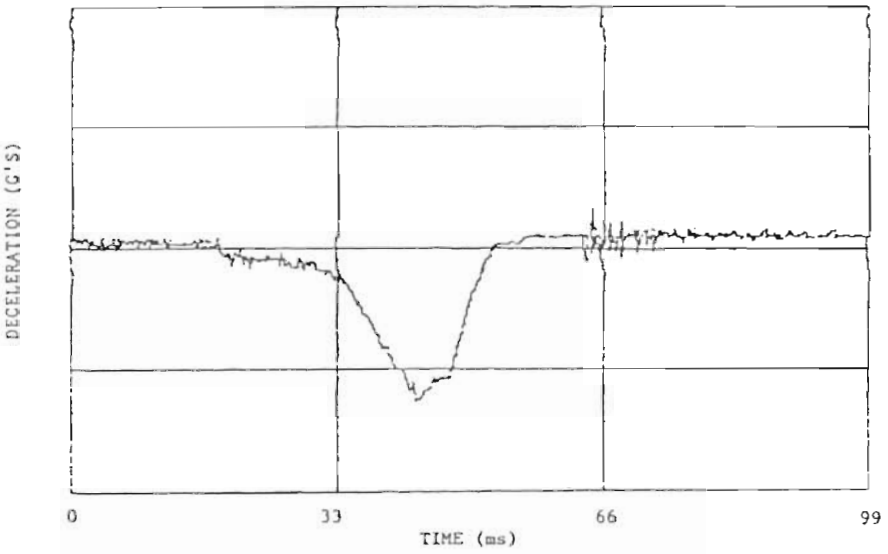

b. Impact Threshold Puncture in Model (2-39)

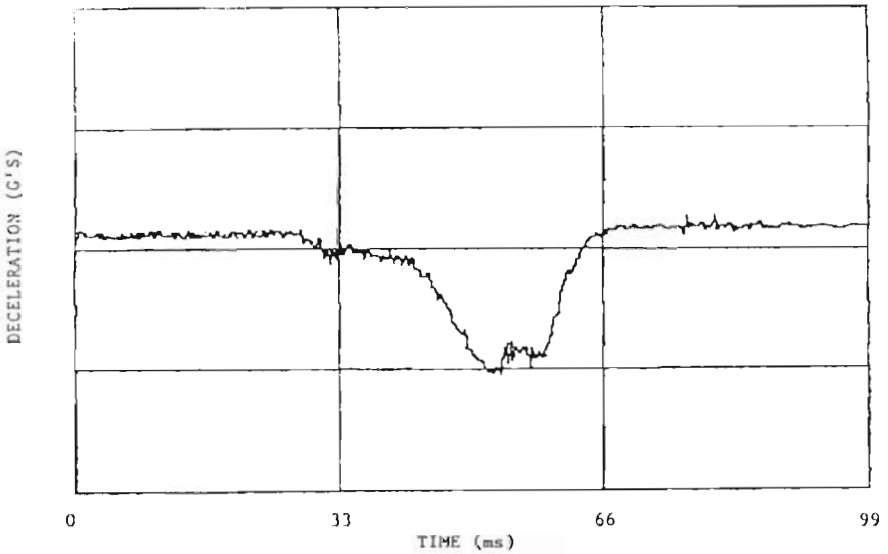

c. Impact Puncture in Model (3-33)

Figure C2. Deceleration versus Time Response in Drop-Weight Impact Tests for the 1/10-Scale Model Aluminum Tank Car Heads with Face Plate-Honeycomb Material Protection

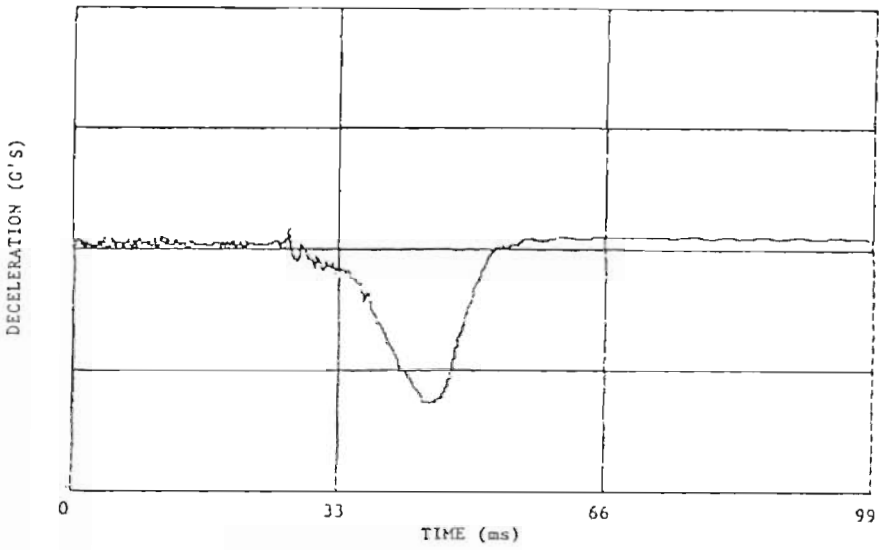

a. Impact Dent in Model (1-14)

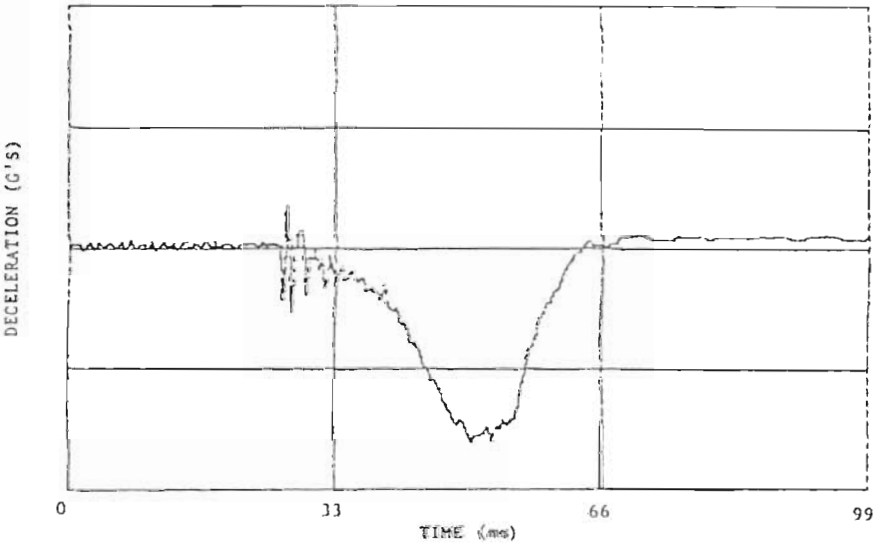

b. Impact Threshold Puncture in MOdel (3-13)

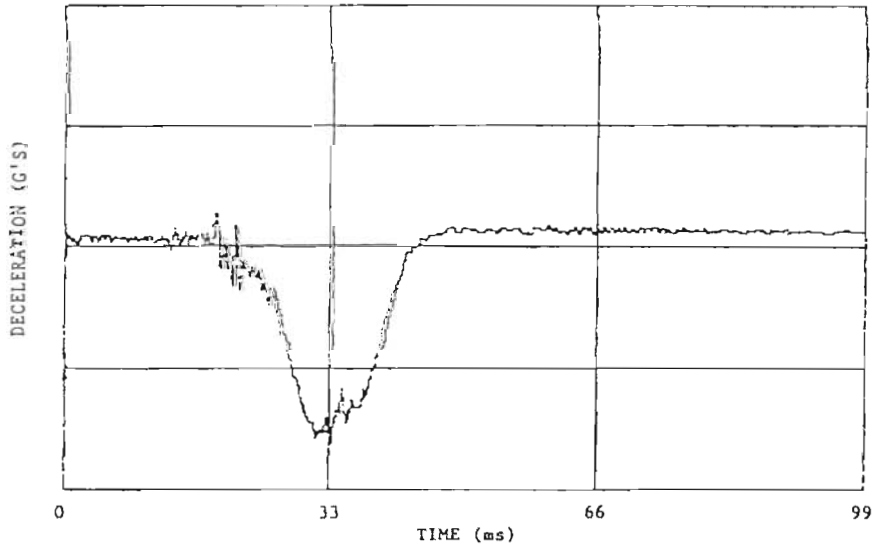

c. Impact Puncture in Model (5-16)

Figure C3. Deceleration versus Time Response in Drop-Weight Impact Tests for the 1/10-Scale Model Aluminum Tank Car Heads with Steel Head Shield Protection

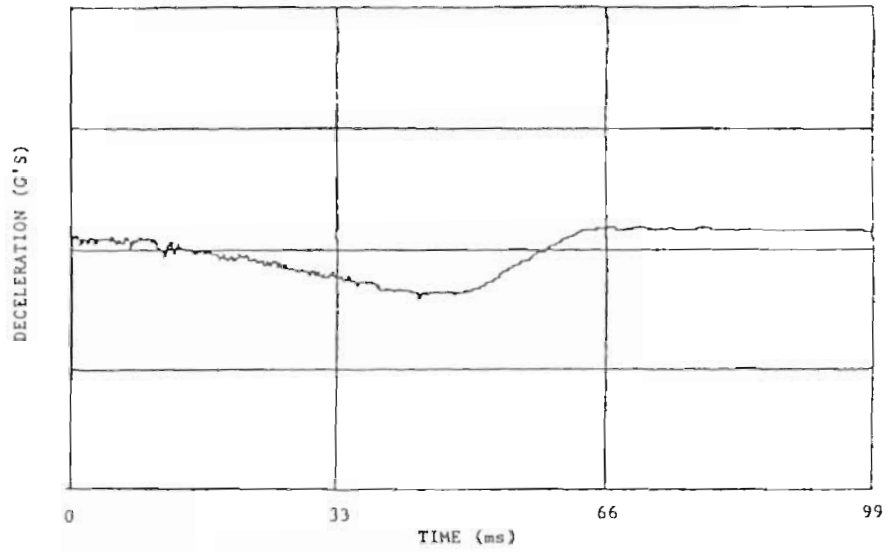

a. Impact Dent in Model (1-6)

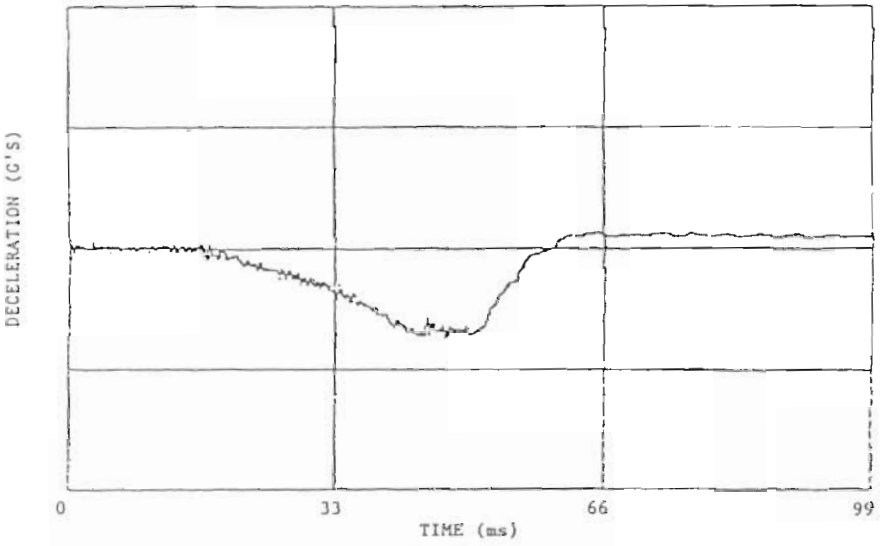

b. Impact Threshold Puncture in Model (3-4)

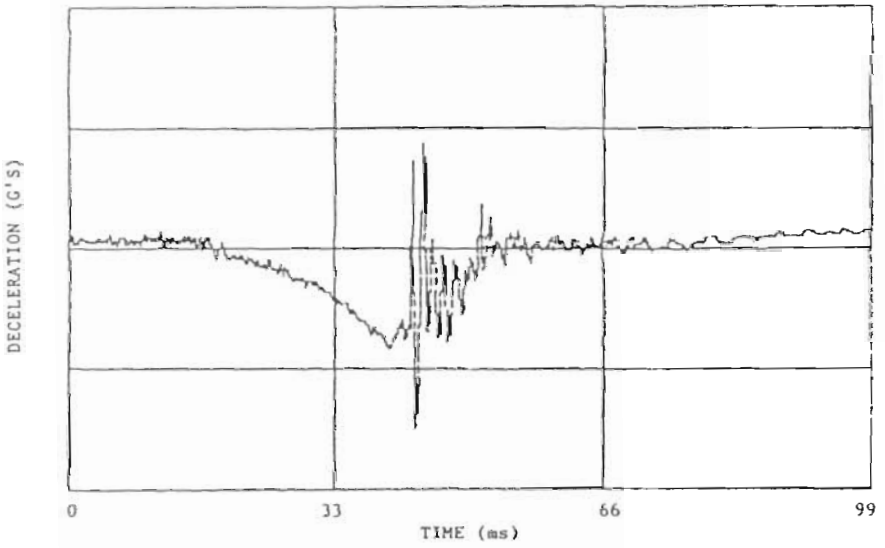

c. Impact Puncture in Model (6-2)

Figure C4. Deceleration versus Time Response in Drop-Weight Impact Tests for the 1/10-Scale Model Aluminum Tank Car Bareheads

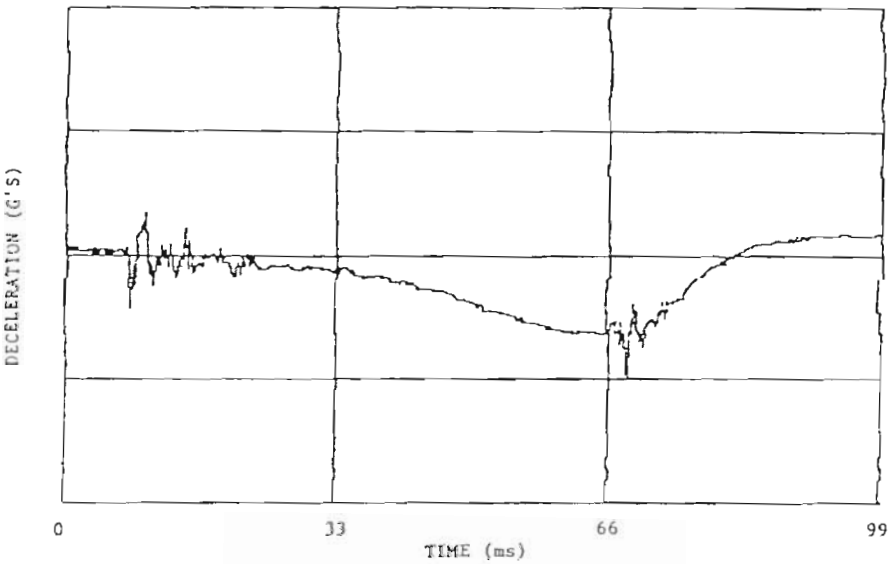

a. Impact Threshold Puncture in Model (2-62)

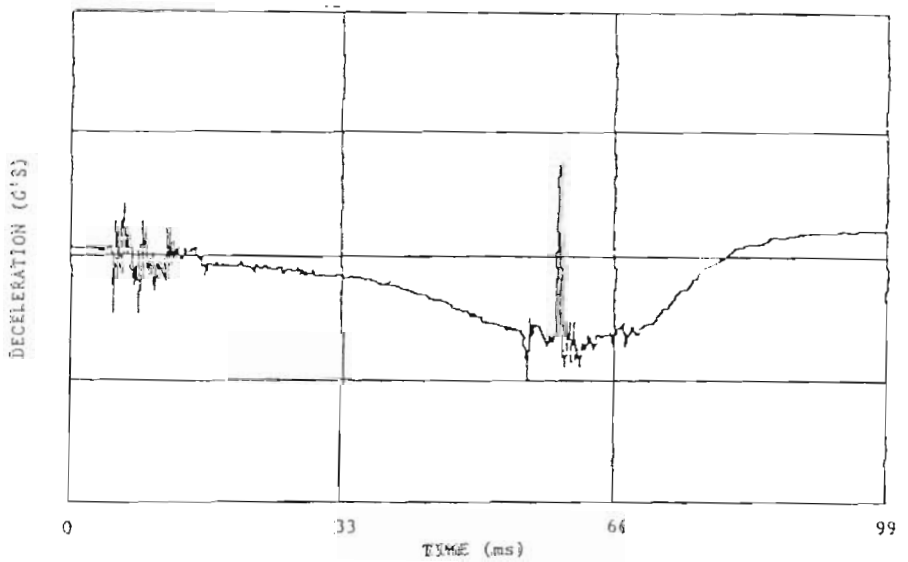

b. Impact Puncture in Model (3-61)

Figure C5. Deceleration versus Time Response in Drop-Weight Impact Tests for the 1/5-Scale Model Aluminum Tank car Heads with Face Plate-Tecspak Material Protection

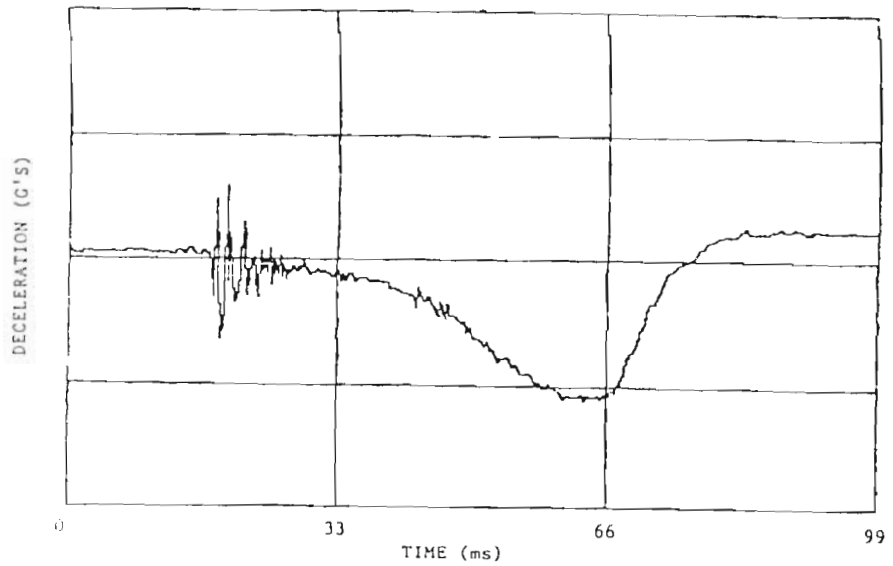

a. Impact Dent in MOdel (1-82)

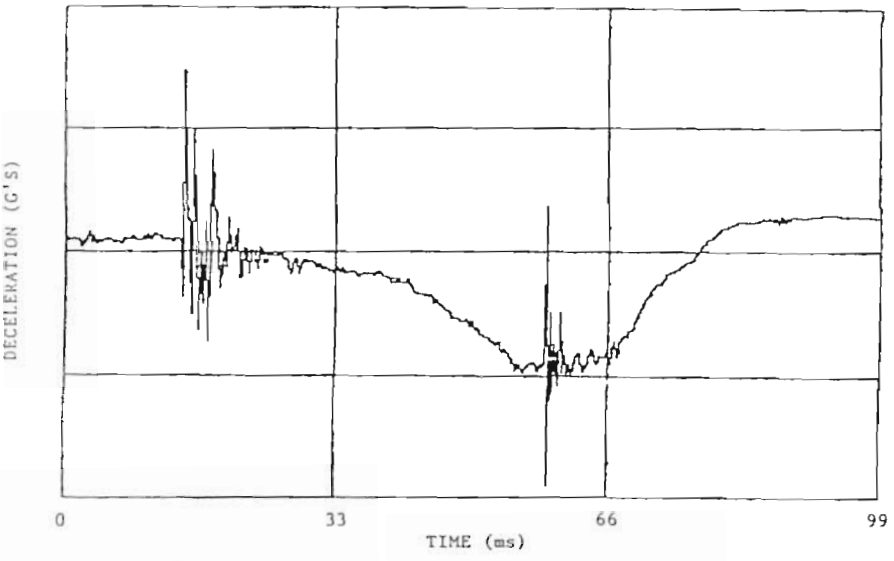

b. Impact Puncture in Model (2-80)

Figure C6. Deceleration versus Time Response in Drop-Weight Impact Tests for the 1/5-Scale Model Aluminum Tank Car Heads with Steel Head Shield Protection

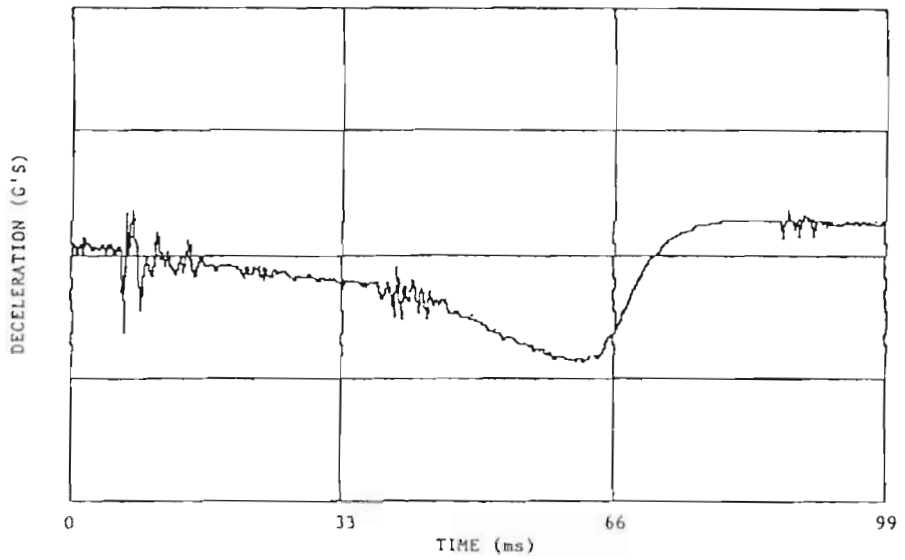

Figure C7. Deceleration versus Time Response in Drop-Weight Impact Tests for the 1/5-Scale Model Aluminum Tank Car Heads with Face Plate-Honeycomb Material Protection - Impact Dent in Model (3-59)

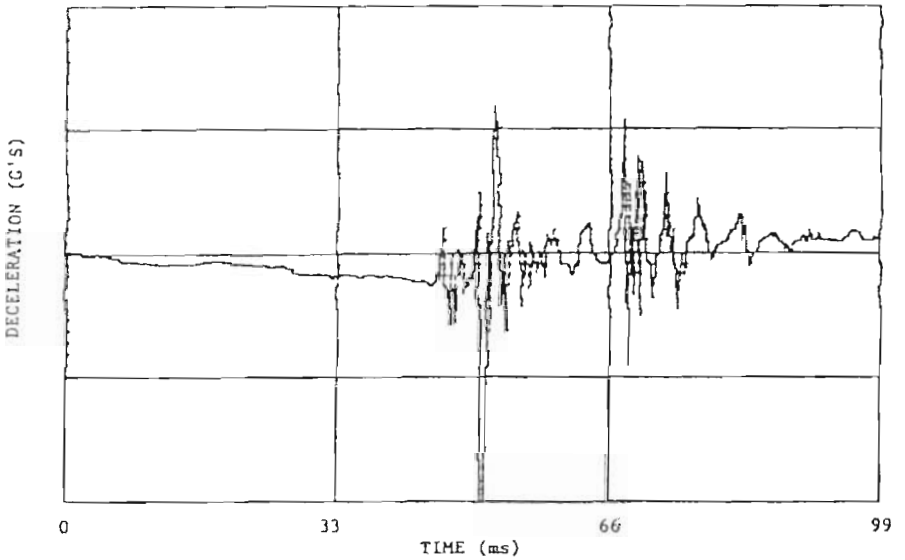

Figure C8. Deceleration versus Time Response in Drop-Weight Impact Tests for the 1/5-Scale Model Aluminum Tank Car Bareheads - Impact Puncture in Model (2-53)

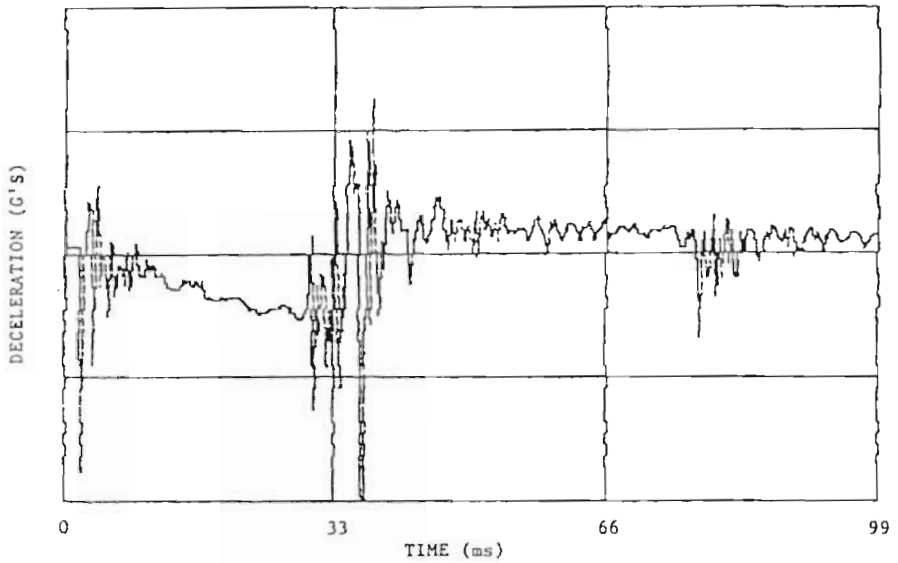

a. Impact Puncture in Model (6-49) with Model Tank Car Filled with Water

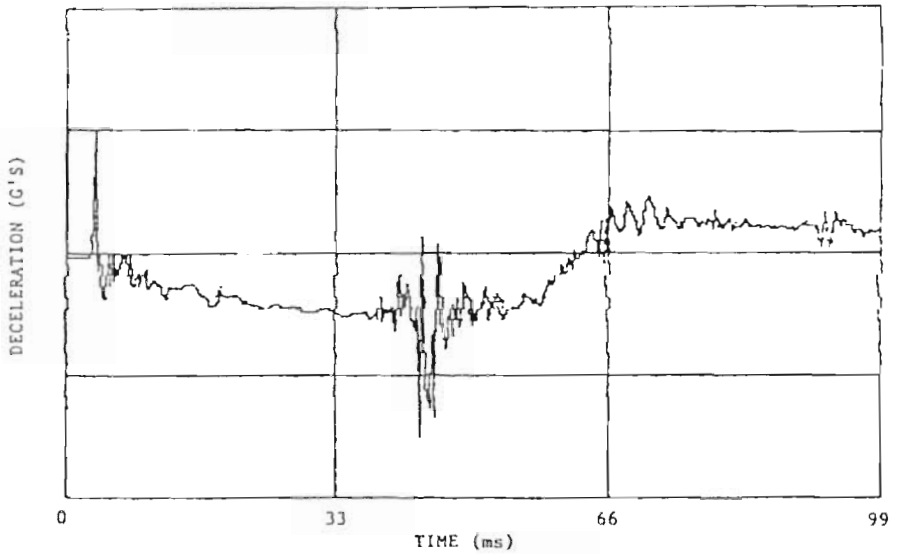

b. Impact Puncture in Model (3-48) with Empty Model Tank Car

Figure C9. Deceleration versus Time Response in Pendulum Impact Tests for the 1/5-Scale Model Aluminum Tank car Bareheads

APPENDIX D

The Dimensional Analysis Of The Scaling Laws

It was proposed in Reference 6 that fourteen (14) variables were used to describe the tank car head impact event. These variables are defined as follows:

D	tank head diameter	h	tank head thickness
R	tank head radius of curvature	m	mass of impacting body
d	indenter characteristic dimension	m'	mass of impacted body
V	initial velocity of impacting body	σ_y	head material yield stress
E_s	head material secant modulus	ρ_{fl}	density of fluid
P_o	internal pressure of impacted tank	ρ_{hd}	density of head material
$\dot{\epsilon}$	Strain rate associated with post impact deformation		
k_d	spring constant of impacting tank car draft gear		

The Buckingham π-theorem states that, given a list of variables, the total number of independent parameters which can be formed is equal to the total number of variables minus the number of primary units utilized. Since there are three primary units of mass, length, and time involved, eleven independent dimensionless parameters can be obtained from the initial list of fourteen variables. These parameters are defined as follows:

$$\pi_1 = \frac{\sqrt{m/k_d}}{D\sqrt{hd/E_s}}$$

The ratio of the time required for the impact force to reach a maximum to the time required for plastic waves to reach the edge of the head

$$\pi_2 = \frac{m}{m'}$$

The mass ratio of impacting body to impacted body.

$$\pi_3 = \frac{\sigma_y}{E_s}$$

Ratio of yield stress to secant modulus.

$$\pi_4 = \frac{h}{R}$$ Ratio of head thickness to radius of curvature.

$$\pi_5 = \frac{\sigma_y^2}{E_s \rho_{hd} \dot{\varepsilon}^2 h^2}$$ Ratio of strain energy to head kinetic energy of deformation

$$\pi_6 = \frac{mv^2 E_s}{\sigma_y^2 d^3}$$ Ratio of impact kinetic energy to strain energy.

$$\pi_7 = \frac{h}{D}$$ Ratio of head thickness to diameter.

$$\pi_8 = \frac{P_o R}{\sigma_y h}$$ Ratio of pressure-induced stress to material yield stress.

$$\pi_9 = \frac{\sigma_y^2}{E_s \rho_{fl} \dot{\varepsilon}^2 h^2}$$ Ratio of strain energy to energy absorbed by fluid.

$$\pi_{10} = \frac{d}{D}$$ Ratio of indenter characteristic length-to-head diameter.

$$\pi_{11} = \frac{\rho_{fl} D^2}{m}$$ Ratio of characteristic mass of fluid to mass of impacting body.

It is noted that these dimensionless parameters are intentionally formed by ratios of physically recognizable quantities such as impact kinetic energy, head deformation kinetic energy, and fluid kinetic energies, strain energy, etc.

The scaling laws in this study are formulated by matching each parameter for the scale model and full size case, i.e., $\pi_{im} = \pi_{if}$, for $i = 1,2,3,\ldots,11$, respectively. Moreover, the scaling laws also enforce that the geometric similarity is preserved. According to this argument, it is apparent, after reviewing the matching conditions for π_4, π_7, and π_8, that all of the length variables must be scaled by the same factor S as:

$$\frac{D_m}{D_f} = \frac{h_m}{h_f} = \frac{d_m}{d_f} = \frac{R_m}{R_f} = \frac{1}{S} \qquad (1)$$

The resulting matching relations for parameters can be simplified greatly if the same material is used for the model and the full scale, and the same fluid is also used to back up the model head and the full size tank head. Under these circumstances, $\sigma_{ym} = \sigma_{yf}$, $E_{sm} = E_{sf}$, $\rho_{hdm} = \rho_{hdf}$, $\rho_{flm} = \rho_{flf}$, and the following scaling relations are obtained:

$$\frac{m_m}{m_f} = \frac{m'_m}{m'_f} = \frac{1}{S^3} \qquad (2)$$

$$\frac{\dot{\varepsilon}_m}{\dot{\varepsilon}_f} = S \qquad (3)$$

$$P_{om} = P_{of} \qquad (4)$$

$$\frac{K_{dm}}{K_{df}} = \frac{1}{S} \qquad (5)$$

$$V_m = V_f \qquad (6)$$

The scale for strain is unity since strain is a nondimensional quantity and thus governed by similarity rules. If the stress-strain relationship is fixed, stress scale should also be unity. Time scale, based on $\dot{\varepsilon} = d\varepsilon/dt$. can be determined as $t_m/t_f = 1/S$. Since acceleration is defined by $a = dV/dt$, this yields acceleration scale as $a_m/a_f = S$. If F and A denote force and area, respectively, force scale can be obtained from $F = \sigma A$ as $F_m/F_f = 1/S^3$. Similarly, energy scale can also be obtained from E(energy) = FxS(distance) as $E_m/E_f = 1/S^3$.

A summary of scaling for important impact parameters is given as follows:

Energy	$E_m/E_f = 1/S^3$	(7)
Force	$F_m/F_f = 1/S^2$	(8)
Acceleration	$a_m/a_f = S$	(9)
Velocity	$V_m/V_f = 1$	(6)
Time	$t_m/t_f = 1/S$	(10)

The scaling laws required for the simulation of full scale behavior as

presented above evolve a contradictory point. In the simplification process of matching π-parameters for the model and the full scale, the material properties of both tank heads are assumed to be the same. But the scaling law for strain rate of Eq. (3), $\dot{\varepsilon}_m = S\dot{\varepsilon}_f$, which was derived based on the same material property assumption, calls for different stress-strain curves for the model and prototype. In other words, eq. (3) asks for different yield stress (σ_y) and material secant modulus (Es) for the model and prototype. As a result, the requirement from strain rate effect clearly contradicts with the earlier same material property assumption.

Based on this finding, the scaling laws listed above are, from very vigorous viewpoint, not quite valid. The degree of validity depends on the magnitude of error induced by strain rate effect. The magnitude of error, which is also related to the property of material employed, can be reduced by adopting a smaller s value.

To illustrate the effect of strain rate on the validity of scaling laws adopted in this study, mild steel, the material property of which is well known (References 12 and 13), is selected for demonstration. Two figures showing the effect of strain rate for mild steel reproduced from Reference 12. Figure D1 displays the variations of ultimate stress, yield stress, and total elongation with increasing strain rate. Figure D2 on the other hand, shows a series of stress-strain curves for various rates of strain.

It can be seen from Figure D1 that, with a strain rate of 10^{-3}/sec., the total elongation almost stays constant, while the ultimate stress increases with increased strain rate. The rate of increase is about 10 percent per decade for strain rates between 1/sec. and 10^{3}/sec. These observations along with the estimation of the area between two successive stress-strain curves in Figure D2 lead to the conclusion that an increase of one decade in strain rate can correspond to an increase of about 10 percent in the strain energy at failure. According to this argument, the strain rate scaling law, $\dot{\varepsilon}_m = S\dot{\varepsilon}_f$, demands that the strain energy in a model is proportionately larger than that of a full-scale tank car.

Now, we are ready to illustrate the effect of strain rate for mild steel on, for example, the velocity scaling. From the matching condition of 6 parameter,

$$\frac{m_m V_m^2 E_{sm}}{\sigma_{ym}^2 d_m^3} = \frac{m_f V_f^2 E_{sf}}{\sigma_{yf}^2 d^3} \qquad (11)$$

by applying Eqs. (1) and (2) to (11), this expression is reduced to

$$\frac{V_m^2}{V_f^2} = \frac{\sigma_{ym}^2/E_{sm}}{\sigma_{yf}^2/E_{sf}} \qquad (12)$$

The right hand side of this equation represents the ratio of strain energy of the model to that of the full scale. If S = 10, the above expression may yield $V_m/V_f = 1.1$ at the point of failure; or $V_m/V_f = 1.05$, which may be translated as threshold puncture velocity for the model, and that is about 5

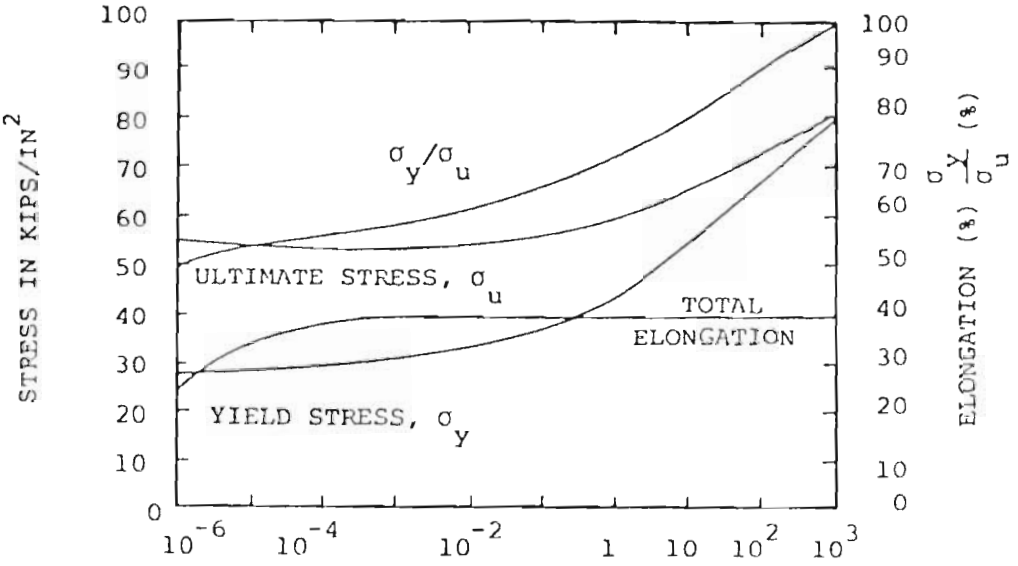

FIGURE D1. INFLUENCE OF RATE OF STRAIN ON TENSILE PROPERTIES OF OF MILD STEEL AT ROOM TEMPERATURE

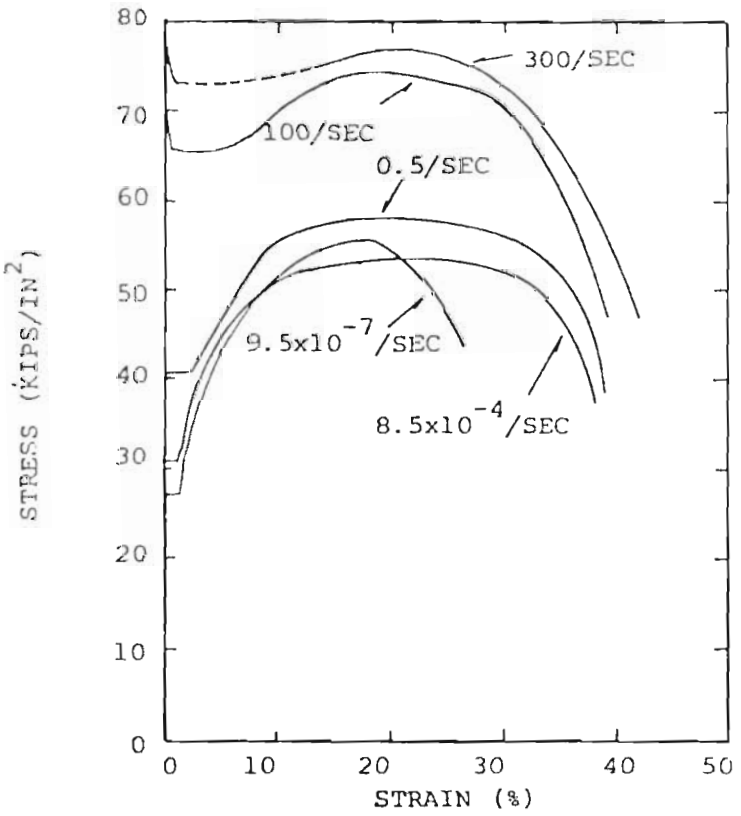

FIGURE D2. STRESS-STRAIN CURVES OF MILD STEEL AT ROOM TEMPERATURE FOR VARIOUS RATES OF STRAIN

percent higher than that for the prototype. This is in a direct contradiction to $V_m/V_f = 1$ of Eq. (6).

When the scaling is applied to the 1/5- and 1/10-scale models, a scaling factor of 2 will yield $V_m/V_f = 1.01$. With a difference of only 1 percent in the threshold puncture velocities between these two models, the strain rate effect can be neglected.

It may be concluded that the accuracy of the scaling laws adopated in this study depends on the error introduced by strain rate effect, the error involved is related to the magnitude of scale factor and the property of material used. The smaller the scaling factor and the less sensitive the material to the variation of the strain rate, the better the accuracy of the scaling laws adopated.